

**SPIN CALORITRONIC PHENOMENA DRIVEN BY  
SPIN-ORBIT COUPLING**



# **SPIN CALORITRONIC PHENOMENA DRIVEN BY SPIN-ORBIT COUPLING**

## **Proefschrift**

ter verkrijging van de graad van doctor  
aan de Technische Universiteit Delft,  
op gezag van de Rector Magnificus prof. ir. K. C. A. M. Luyben,  
voorzitter van het College voor Promoties,  
in het openbaar te verdedigen op maandag 2 juni 2014 om 15:00 uur

door

**Yan-Ting CHEN**

Master of Science in Electrophysics  
van National Chiao Tung University, Taiwan,  
geboren te Kaohsiung, Taiwan.

Dit concept-proefschrift is goedgekeurd door de promotor:

Prof. dr. ir. G. E. W. Bauer

Samenstelling promotiecommissie:

Rector Magnificus,	voorzitter
Prof. dr. ir. G. E. W. Bauer,	Technische Universiteit Delft, promotor
Prof. dr. ir. H. S. J. van der Zant	Technische Universiteit Delft
Prof. dr. ir. B. J. van Wees	Rijksuniversiteit Groningen
Prof. dr. E. Saitoh	Tohoku University
Prof. dr. B. J. Hickey	University of Leeds
Prof. dr. S. Takahashi	Tohoku University
Dr. M. Blaauboer	Technische Universiteit Delft
Prof. dr. Yu. V. Nazarov,	Technische Universiteit Delft, reservelid



Nederlandse Organisatie voor Wetenschappelijk Onderzoek

*Keywords:* Spintronics, spin caloritronics, spin-orbit coupling

*Printed by:* Gildeprint

*Front & Back:* Y.-W. Teng and P.-Y. Chao

Copyright © 2014 by Y.-T. Chen

Casimir PhD Series, Delft-Leiden 2014-14

ISBN 978-90-8593-189-8

An electronic version of this dissertation is available at

<http://repository.tudelft.nl/>.

*Bearth all things, believeth all things, hopeth all things, endureth all things.*

1 Corinthians 13



# PREFACE

Let me start by quoting Stendhal:

*One can acquire everything in solitude except character.*

For this I would like to express my gratitude to people who have shaped me so much in the past four years since I could not have done it myself.

The story went like this: at the beginning of 2010, I received an e-mail from *Prof. Bauer* in Delft, indicating there was a Ph.D. position in his group. I decided to apply and got the first chance in my life to visit Europe. During the interview, *Gerrit* must have observed my passion for Dutch weather and foods except theoretical physics in spin caloritronics. He offered me the job, and this was how I started my great adventure in Delft. I would like to thank *Gerrit* not only for advising me on my research, but also helping me develop the ability to handle science with sufficient concern. As a devil's advocate, *Gerrit* is a critical reader of my manuscripts. I got only twice "great!" in the four years: the first time was when I decided to go to his anniversary party, and the second time was when I managed to complete my committee of graduation. I hope you take this as a compliment, *Gerrit!*

*Yuli* always tells very inspiring stories and experiences which make our coffee more tasty. His questions in the group meetings are very appreciated but just a bit scary. For four years, I have shared the same birthday with *Yaroslav*, who seems to know almost everything and always keeps protecting the group by providing his knowledge. I was extremely impressed by *Jos'* teaching. He just manages to explain everything clearly in a very easy way such that you think everyone can do it, which is of course not the case. I have to thank *Miriam* for her positive words in my evaluations. She also shows us that a physicist does not have to be necessarily geeky but can have a very pleasant family life. Also our new faculty *Anton* and *Michael* have brought completely fresh air from the north, which will stimulate the group a lot for sure. I shall never forget our secretaries without them we are nothing. I miss the laughter of *Marjolein* who took care on many things when I started. *Erika*, in some sense quieter, somehow has gotten many new things for the group such as the fantastic coffee room.

It was *Stefan* who brought me to DUWO and C1000 as well as my apartment on Leeghwaterstraat. He has become a frequent visitor from Munich since 2012.

When I had to fix the tire of my bike for the first time, *Marnix*, as a recognized Dutch citizen, kindly introduced me how to do that. He even showed me how much pressure would lead to the explosion of the outer tire together with the inner one. Recently he also helped me with translation of my propositions and summary without exploding them. *Gio* always encourages me in very special ways. I remember on my first day he told me he's willing to help with everything. We have enjoyed dinners and drinks in Delft and the Hague, and he always shares his opinions and experiences sincerely. *Rakesh* is a guy who really enjoys his life. The parties hosted by him and *Nicole* were always lovely and cozy.

My officemate *Ciprian* is not only a talented physicist but also a brilliant chess player. Somehow he always manages to give nice words to people. He is a romanticist with huge passion about *Le Petit Prince*. *Hujun* and I had many interesting discussions about the culture and politics in Taiwan and China (hush!). There were a long period that only the two of us worked in our office (where were the other guys?). We also had many business trips together. *Dmitri* was not usually in Delft, but we had quite good discussions about future plans in academia. Like many Russians, he finished his Ph.D faster than people from rest of the world do. *Peng* is a very useful guy for Gerrit's students. From him we get a lot of knowledge in physics but also life in science. Besides being a physicist, *Yunshan* is also interested in art. After moving to Delft, she has developed very solid knowledge about nice restaurants in the Netherlands. I was very impressed by *Mariya*, who managed to finish her Ph.D in three years and publish a fiction at the same time, which was amazing.

*Chris V* knows a lot about how to be adapted to Dutch life. With excellent ability of observing people, he manages to help us with his knowledge and experiences. *Chris D* always can start conversations with various topics. The dinner on Thanksgiving was wonderful. I remember the turkey. *Marcin* has organized many meetings for people's graduation as well as just for fun. The most important memories I have in his house is the the very divergent liquor. It was simply too bad that I never had a chance to get drunk there.

*Alina* organized a very nice club for quantum transport study, and was always enthusiastic about everything related to the group. However, I must say I was very impressed by her mistaking Taiwan as Thailand. *Frans* was the last Dutch Ph.D in the group so far. He is a perfect superposition of a serious and a humorous state. *Olya* graduated from my home university in Taiwan and we had very pleasant discussions about Hsinchu. From her I had the chance to know *Dave*. At almost the same time, a long awaited reasonable and rational German *Paul* joined us.

I had the chance to talk to *Fateme M* in a summer school in Les Houches, and she shared many experiences as a foreigner in Europe. Her presentations were always carefully designed and beautiful. *Fateme J* has helped me many many times. I was so lucky to avoid many miseries because of her suggestions and ex-

periences. During some period I shared the same interest about vegetables with *Mireia*. Thanks to her information though I did not stick to being a vegetarian till the last moment. I would guess I see and talk to *Rodrigo* more often in gym rather than in the office. He has very special diet.

My relationship with *Akash* is much more complicated. As colleagues, roommates, and friends, we had no choice but just had to share many darkest secrets together. Below the blank is what I want but am not allowed to say in public:

From *Akash* I also got to know some nice friends such as *Roman*. I shall thank *Albert* for he and his flatmate *Eloi*'s nice jamóns and wine. He is the only guy from the theory group who ever suggested that I drink too much. *Sebastian* is a frequent visitor of gym in sports center with the hope to set up a boxing bag in our coffee room. It was a pity that *Jose* never really introduced us his girl friend even though he visits Leiden so often. *Rafel* is a passionate guitar player as well as a fan special liquor such as peanut flavored vodka. Our guest *Ville* keeps recommend me Linux after hearing that my laptop was broken. Considering the younger generatoin, actually we have quite some motivated Dutch master students such as *Alwin Wouter*, *Adriaan*, and *Jochen*. All of them are enthusiastic and helpful for the Ph.Ds who are mostly foreigners.

There have been many nice postdocs in the group as well. Thanks to *Mihajlo* for educating me how to use chipknip. I still remember the tapas in *Toni*'s farewell, and the singing of Tchaikovsky's violin concerto in *Francois*'s. *Berlinson* always appeared in the office in some unusual time. While *Mohammad* seems try to follow this tradition, the most fresh postdoc, *Tomohiro*, is trying to get his own way. I am grateful for discussions with senior guys who left the group years ago but are still in contact. Among them my special thanks to *Jiang* and *Xuhui*. Also my thanks to experimentalists downstairs who I have met randomly: *Kun*, *Diego*, *Erika*, and *Onder*.

I had the chances to know many people outside Delft. I would like to thank *Takahashi sensei*, *Saitoh sensei*, and *Mika san* for their kindness during the collaborations and my visits in Sendai. Also thanks to *Sebastian* in Garching for his useful comments in our papers. From *MACALO* I met and discuss with many people working in similar fields. Special thanks to *Prof. Arne Brataas*, *Andre*, *Erlend* from Trondheim; *Prof. van Wees*, *Fasil*, *Nynke*, *Juan* from Groningen; and *Prof. Kelly*, *Zhe*, *Yi*, *Rien* from Enschede.

In a country so far away from my hometown, I was lucky enough to have company of many Taiwanese people. My deepest gratitude to *Sin-Yun* for being my buddy in my last two years in Delft. She is excellent and seems be able to learn everything easily. I thank her for all the meals, tours, cycling, and infinite discussions

about almost everything. From her I met *Atreyo* and had the chance to enjoy delicious Surinamese foods! *Po-Ying* is a guy who observes the world and tells stories in a his unique way. He is the type of man who has the real sense of humor. We had so many funny chats with chips and beers. In summer we went to see pretty girls in Delftse Hout when *Ya-Wen* was not around. *Jui-Chi* has shown me not only her tremendous passion for foods, but more importantly, the strength which only exists in people who completely accept themselves. She's a knight always willing to help and everybody loves her. I've always been jealous of her. I thank *Ming-Hsuan* for bringing me cakes exactly when my birthdays came in these years and sharing so many happy and dark hours with me. She is an elegant connoisseur with many fine principles. Recently she has become a very brilliant dancer.

There was a period that I was passionate with chocolate cakes. Thanks to *Tsu-Han* who kindly offered her oven and all things needed in her place. The cakes we made together were really unbelievable! *Sheng-Chieh* was the master of almost everything and basically helped people on everything. He even helped me separate a cake into ten shares successfully. *Wei-Han* always manages to find interesting natural events in the mid of nowhere. He also knows (or probably creates) many fancy recipes which sometimes surprise us very much. *Yu-Ting* impressed me with her over optimistic attitude. Her desperate courage is just enough to make her laugh at horror films but unfortunately not enough for roller coasters. It was a pity that only till my last half year I met another Taiwanese alcoholic *Yi-Hsuan* with a lot of amazing stories. She is kind and never hesitates sharing anything with friends.

I was very pleased to have lunches with *Yu-Lung* and hear about her nice adventures. Sometimes *I-Rong* was there as well, which usually made the topics even more uncontrollable. *Jason* is always willing to discuss with me on quantum computation which is unfortunately not my expertise. He and his wife have hosted many nice dinner and movie nights. It was *Ju-Liang* who invited me to join his small jogging and biking tours. He was the last Taiwanese physicist I know in Delft till now. Besides being an enthusiastic baseball player, *Meng-Gang* is also very enthusiastic with Taiwanese politics. I remember the night-chats with beer and beer and more beer. I enjoyed to talk to *Hsiu-Chi*, who is sportive and had done many interesting trips. *Ju-Hsuan* has an ambition to open a store herself and always keeps going. I look forward visiting tau-gay-new's shop someday very soon. *Yu-Fang* always gives very positive and creative words to people. It is just too bad we have not had the chance to enjoy mushrooms together. *Yun-Hsuan* seems to know all the famous sightseeing spots as well as restaurants around the world, and I hope she can visit all nice places in Europe someday soon.

There are still a lot of people we had very pleasant time together: *Shi-Chi*, *Lun-Ni*, *Chang-Yu*, *Po-Chih*, *Hsing-Jui*, *Chen-Yi*, *Chao-Ping*, *Megan*, *Duncan*, *Yung-Cheng*, *Kai-Ting*, *Hui-Hsuan*, *Jyhi*, *Shannon*, *Jenny*, *Jill*, *Roy*, *Hung-Chu*, *Johana*,

*Chi-Yi, Takuji, Kuan-Ling, Ting-Yu, Joey, Shumeng, Shiau-Yan, Neo, Lavender, Tracy, and Chun-Wei.* I am sorry I just cannot manage to recall all the happy memories with you one by one, and I am even more sorry if someone is missed!

I am almost done with the acknowledgement, but I just want to say thank you all again and again. It was because of you a twixter has grown up finally. It was because of you I would like to call a small town 10000km from Taiwan *my home*. It was because of you I feel the bitterness when realizing the fact I have to go. Thank you for being such wonderful people, and I would love to call you *my friends*.

Lastly but most importantly, I have to thank my parents who spoil me with love. Papa, mama, this thesis is dedicated to you.

*Yan-Ting Chen  
Delft, May 2014*



# CONTENTS

<b>1</b>	<b>Introduction</b>	<b>1</b>
1.1	Electronic transport	1
1.2	Magnetic Order and Ferromagnetism	2
1.3	Transport in ferromagnets, GMR, and Spintronics	4
1.3.1	GMR	4
1.3.2	Spintronics	7
1.4	Spin-orbit coupling (SOC) and the Return of CIP	8
1.4.1	AMR	9
1.4.2	AHE	10
1.4.3	SHE	12
1.4.4	Return of CIP	13
1.5	Thermoelectric Effects and Spin Caloritronics	14
1.6	This thesis	16
	References	17
<b>2</b>	<b>Anomalous thermoelectric effects in ferromagnetic metals</b>	<b>23</b>
2.1	Introduction	24
2.2	Linear response and Onsager symmetry	27
2.3	Model	30
2.3.1	Boltzmann equation without spin-orbit interaction	31
2.3.2	Boltzmann equation with spin-orbit interaction	33
2.3.3	Collision terms in the presence of SOC	34
2.3.4	Modulation of velocity by side-jump scattering	37
2.4	Thermoelectric effects	39
2.4.1	AHE and its thermal analogues	39
2.4.2	AMR, PHE, and their thermal analogues	40
2.5	Conclusion	41
2.6	Appendix: Collision terms in the Boltzmann equation	41
2.6.1	First order terms without SOC	42
2.6.2	First order terms with SOC	44
2.6.3	Second order term with SOC	46
	References	46

<b>3</b>	<b>Theory of spin Hall magnetoresistance</b>	<b>51</b>
3.1	Introduction . . . . .	52
3.2	Transport theory in metals in contact with a magnetic insulator . . .	53
3.3	N F bilayers . . . . .	55
3.3.1	Limit of $G_i = \text{Im } G_{\uparrow\downarrow} \ll \text{Re } G_{\uparrow\downarrow} = G_r$ . . . . .	57
3.3.2	$G_r \gg \sigma / (2\lambda)$ . . . . .	59
3.3.3	$\lambda / d_N \gg 1$ . . . . .	59
3.3.4	Spin Hall AHE . . . . .	60
3.3.5	Comparison with experiments . . . . .	60
3.4	Spin valves . . . . .	63
3.4.1	Parallel Configuration ( $\hat{m} \cdot \hat{m}' = \pm 1$ ) . . . . .	63
3.4.2	Limit $\lambda / d_N \gg 1$ . . . . .	64
3.4.3	Perpendicular Configuration ( $\hat{m} \cdot \hat{m}' = 0$ ) . . . . .	65
3.4.4	Controlling the spin-transfer torque . . . . .	66
3.5	Summary . . . . .	67
	References . . . . .	68
<b>4</b>	<b>Size effect in the anisotropic magnetoresistance of ferromagnetic thin-films</b>	<b>71</b>
4.1	Introduction . . . . .	72
4.2	Theoretical Model . . . . .	73
4.2.1	Spin currents in ferromagnets . . . . .	74
4.2.2	Linear response . . . . .	75
4.2.3	Diffusion equations . . . . .	76
4.3	Results . . . . .	77
4.3.1	Floating Hall edges (open-circuit configuration) . . . . .	77
4.3.2	Short-circuit configuration . . . . .	79
4.4	Experimental tests . . . . .	80
4.5	Summary . . . . .	81
4.6	Appendix: Linear response matrix . . . . .	82
	References . . . . .	84
<b>5</b>	<b>Fuchs-Sondheimer theory of the spin Hall effect</b>	<b>89</b>
5.1	Introduction . . . . .	90
5.2	Relaxation time approximation . . . . .	91
5.2.1	Basics . . . . .	91
5.2.2	Boltzmann equations . . . . .	93
5.3	AHE . . . . .	94
5.3.1	Roughness effect on electric conductivity . . . . .	97

---

5.3.2 Spin current driven by spin-dependent roughness and AHE due to side-jump . . . . .	99
5.3.3 AHE due to skew scattering . . . . .	100
5.4 Correction due to roughness on the SMR . . . . .	101
5.5 Summary . . . . .	102
References . . . . .	103
<b>Summary</b>	<b>105</b>
<b>Samenvatting</b>	<b>107</b>
<b>Curriculum Vitæ</b>	<b>109</b>
<b>List of Publications</b>	<b>111</b>



# 1

## INTRODUCTION

### 1.1 ELECTRONIC TRANSPORT

Most of us live in a world surrounded by a lot of electronic devices. To sustain this modern world, the understanding and description of electronic transport of electrons and other carriers in conductors are of fundamental importance [1]. A very simple picture for this is that there are electrons which can flow freely in metals and contribute on the electric current. This free electron model was proposed by Drude and improved by Sommerfeld. From the view of quantum mechanics, a free electron is actually a plane wave expressed by the wavefunction at a certain position  $\vec{r}$

$$\psi_{\vec{k}}(\vec{r}) = \frac{1}{\sqrt{\Omega_r}} e^{i\vec{k}\cdot\vec{r}}, \quad (1.1)$$

where  $\vec{k}$  is the wave vector of the wave,  $\Omega_r$  is the volume occupied by the electron.

In solids, the condition is not that simple and the free electron model fails to explain many physical effects and features. The electrons in solid have to be described by the Bloch electrons

$$\psi_{\vec{k}}(\vec{r}) = e^{i\vec{k}\cdot\vec{r}} u_{\vec{k}}(\vec{r}), \quad (1.2)$$

where  $u$  is a periodic function with the same periodicity as the crystal, and  $\vec{k}$  here is the crystal wave vector. This description is Bloch's theorem, which was, however, only for perfect crystals. In real systems, there are defects, disorders, and impurities. The solution thus has to be a superposition of the Bloch waves and hopelessly

complicated. A solution for this trouble is to describe the electrons in a semiclassical way. Instead of the exact wavefunction, we express the electrons as a distribution function  $f_{\vec{k}}(\varepsilon, \vec{r})$ , which is the number of electrons at a certain position  $\vec{r}$  with a certain momentum  $\hbar\vec{k}$ . According to the uncertainty principle, we cannot know the position and momentum simultaneously, but we are allowed to do so when the scale of the system is well above the Fermi length  $1/k_F$ . The steady-state distribution function  $f_{\vec{k}}(\varepsilon, \vec{r})$  solves the Boltzmann equation

$$\vec{v}_{\vec{k}} \cdot \vec{\nabla} f_{\vec{k}} - \frac{\vec{F}}{\hbar} \cdot \vec{\nabla}_{\vec{k}} f_{\vec{k}} = \left( \frac{\partial f_{\vec{k}}}{\partial t} \right)_{\text{scatt.}}, \quad (1.3)$$

where  $\vec{v}_{\vec{k}}$  is the velocity,  $\vec{F}$  is the driving force, and the term on the right-hand-side called collision integral represents the scattering processes. The distribution function can be decomposed as an isotropic part  $f^0$  and an anisotropic part  $g_{\vec{k}}^a$  due to scattering and the driving force, and is directly related to physical quantities such as electric current

$$\vec{J}_c = e \sum_{\vec{k}} \vec{v}_{\vec{k}} f_{\vec{k}} = e \sum_{\vec{k}} \vec{v}_{\vec{k}} g_{\vec{k}}^a. \quad (1.4)$$

When disregarding the quantum coherence, this semiclassical description works pretty well and intuitively in many transport problems.

## 1.2 MAGNETIC ORDER AND FERROMAGNETISM

Technology involves not only the electric properties but also the magnetic properties of materials. Probably the first recorded use of magnetism and magnetic materials was compasses, which provides a tool to identify locations and directions. By systematical studies, we are now able to categorize materials according to their magnetic properties, i.e., the responses of materials subject to an external magnetic field as discussed below [2]. One should however note that the magnetic states (phases) can change when exceeding certain critical temperatures as well. Paramagnetic and diamagnetic materials do not have magnetic ordering and therefore no magnetization when there is no external magnetic field. In the presence of a magnetic field, a paramagnetic state exhibits a magnetization parallel to the field, while a diamagnetic state exhibits a magnetization antiparallel to the field. There are types of states have magnetic ordering spontaneously. In a ferromagnetic state, there are permanent magnetic moments align parallel a specific direction and exhibits a magnetization. In an antiferromagnetic state, there are equally amount magnetic moments align parallel and antiparallel to a specific direction; the magnetic moments cancel out each other, and the net magnetization is zero. There is similar cancelation in a ferrimagnetic state, but the cancelation is not complete, so there is a finite net magnetization.

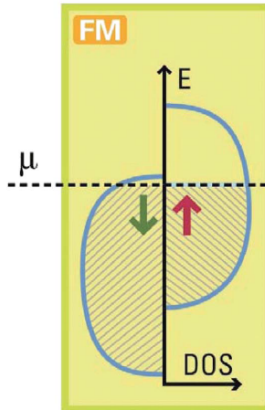


FIGURE 1.1: The simplest band structure of the ferromagnetic metals (from Ref. [71]).

The mechanism behind the spontaneous magnetic ordering are very complicated, but can be simplified by introducing an exchange field and exchange interaction. We take a ferromagnetic state as an example since it is of special importance in this thesis. The exchange interaction can be included by the Heisenberg Hamiltonian

$$H_{ex} = -J \sum_{i,j} \vec{s}_i \cdot \vec{s}_j, \quad (1.5)$$

where  $J$  is the strength of the exchange coupling,  $\vec{s}_i$  is the local magnetic moment labeled  $i$ . For  $J > 0$ , the magnetic moments tend to align parallel to each other in order to minimize the energy and a ferromagnetic state exhibit a *spontaneous magnetization* then appears. It requires a more complicated mean-field theory and take into account thermodynamics to fully describe the magnetic ordering, but the atomic model (Hund's rule) severely overestimates the orbital moments since in solids the orbital moments is largely quenched by bonding. This problem was solved through the development of band theory, which was first applied to magnetic systems by Mott, Slater, and Stoner, and the simplest band-like model of the ferromagnetic metals is called Stoner model [3, 4], which assumes the bonding interaction between the  $3d$  electrons causes a smearing of their energy into a band which can be described from physics and chemistry points of view. We consider the average finite energy width of the valence band states and we approximate the density of states (DOS) by a simple semicircle as shown in Fig. 1.1. In the presence of a Weiss field the centers of gravity of the states characterized by opposite

spins (which can be labeled as spin-up and spin-down) exhibit an energy separation, the exchange splitting  $\Delta$  when the spin-orbit coupling (see below) is not too strong. The bands are filled according to the Fermi statistics in which the temperature dependence is taken into account. The magnetization is then proportional to the number difference between electron with spin-up and spin-down following this simplified picture.

### 1.3 TRANSPORT IN FERROMAGNETS, GMR, AND SPINTRONICS

We can generate a charge current in a metal by driving the conduction electrons with an electric field or voltage. The linear response between the current and driving force is governed by Ohm's law. We also know that electrons carry both charge and spin. In normal metals, the spins of electrons are in random direction such that a charge current generated by an electric field is not associated with any transfer of angular momentum. It is not so in ferromagnetic metals. As we know, there is a spontaneous magnetization in a ferromagnet state, and we generate a current polarized along the magnetization if we apply an electric field on a ferromagnetic metal. Mott [5] figured out this fact and proposed the so-called two-current model to explain this effect in 1936. According to Mott, the conduction electrons in a ferromagnetic metal can either have a spin-polarization parallel or antiparallel to the magnetization of the ferromagnet, i.e., there are two channels for electrons: one is for spin-up and the other is for spin-down. This concept together with the bands described by the simple Stoner model, lead to the fact that the transport properties are spin-dependent in each channel, and the electric conductivity of one spin species is different from that of the other one, resulting in a net electric current which carries a non zero spin angular momentum. This can be seen from the simple band model illustrated in Fig. 1.1 as well. One finds that the DOS at the ground state chemical potential (which is the Fermi energy when  $T = 0$ ) is spin-dependent, so the electric conductivity of each spin species is spin-dependent, too. Therefore, the distribution of electrons is spin-dependent as well.

#### 1.3.1 GMR

With the development of experimental techniques such as molecular beam epitaxy, it became possible to fabricate multilayers made from very thin individual metallic layers, which led to the celebrated discovery of the giant magnetoresistance (GMR) with the geometry currents flow along the layer planes [CIP (current in-plane) configuration] [6, 7], in which a very large magnetoresistance was found between the parallel and antiparallel magnetic configurations as illustrated

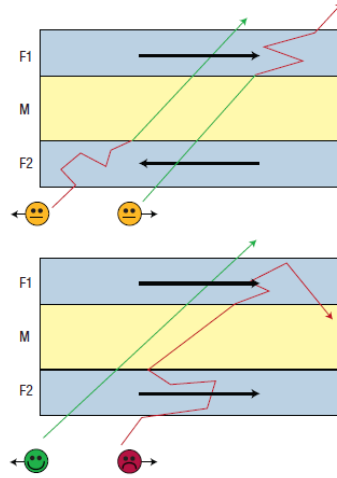


FIGURE 1.2: The illustrations for the CIP-GMR (from Ref. [8]).

in Fig. 1.2. This magnetoresistance can be understood as the following: in the parallel configuration, the electrons of one spin species can go through all the layers easily and the short circuit through this channel leads to a small resistance. On the other hand, in an antiparallel configuration, the electrons of both spin species are slowed down every second magnetic layer and the resistance is high [8, 9].

The first theory to analyze the CIP-GMR was proposed by Camley and Barnás by generalizing a Boltzmann approach developed by Fuchs and Sondheimer [10], which was originally used to analyze the thickness dependence of electric conductivity modulated by surface roughness in metallic thin films [11, 12]. The spin-dependent scattering at the interfaces in the multilayer is taken into account by a spin-dependent specularity parameter that interpolates between the limits of completely specular and completely diffusive scatterings. We set the electric field is applied along  $\hat{x}$ , and the metallic layers are grown along  $\hat{z}$ . After linearization, the spin-dependent Boltzmann equation in the relaxation time approximation reads [1]

$$v_z \frac{\partial g_{k\zeta}^a}{\partial z} + eE v_x \frac{\partial f^0}{\partial \varepsilon} = -\frac{g_{k\zeta}^a}{\tau}, \quad (1.6)$$

where  $\zeta = \uparrow / \downarrow$  denotes the spin,  $v_i$  is the  $i$  component of the velocity,  $\tau$  is the

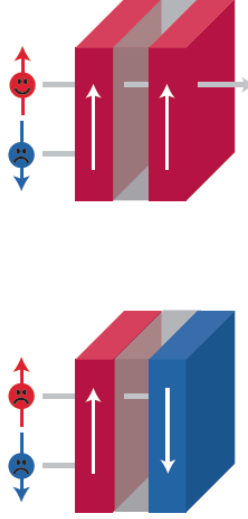


FIGURE 1.3: The illustrations for the CPP-GMR (from Ref. [14]).

momentum relaxation time of electrons. One can get the general solution

$$g_{\hat{k}\zeta}^{a(\pm)} = eEv_x\tau \left[ 1 + A_{\zeta}^{(\pm)} \exp\left(\frac{\mp z}{\tau|v_z|}\right) \right], \quad (1.7)$$

where we have used  $\pm$  to denote the case  $v_z > 0$  ( $v_z < 0$ ). The coefficient  $A_{\zeta}^{(\pm)}$  has to be fit by the boundary condition related to the spin-dependent roughness and depends on the magnetic configuration (which can be parallel or antiparallel). Thus one can calculate the distribution as well as the electric current which explains the CIP-GMR. Note that  $\tau|v_z| = \tau v |\cos\theta| = l |\cos\theta|$  where  $\theta$  is the angle between  $\hat{z}$  and  $\hat{k}$ .  $l = \tau v$  is the mean free path. Thus we see that the CIP-GMR is characterized by the length of the mean free path.

The latter discovered GMR in CPP (current perpendicular to plane, as illustrated in Fig. 1.3) configuration not only achieved higher magnetoresistance [15], but also arose the concept of spin accumulation since the length scale in the CPP-GMR is the spin diffusion length [16]. Valet and Fert applied the Boltzmann approach to explain the CPP-GMR. In addition to the anisotropic part  $g_{\hat{k}\zeta}^a$ , they introduced an isotropic term expressing the local variations of the chemical potential for spin  $\zeta$ ,  $\mu_{\zeta}$ , in order to account for spin accumulation. In this case, the transport

direction is normal to the plane (say, along  $\hat{x}$ ), and the Boltzmann equation reads

$$v_x \frac{\partial g_{\hat{k}\zeta}^a}{\partial x} - v_x \frac{\partial \bar{\mu}_\zeta}{\partial x} = -\frac{g_{\hat{k}\zeta}^a}{\tau} - \frac{\bar{\mu}_\zeta - \bar{\mu}_{-\zeta}}{\tau_{\text{sf}}} \quad (1.8)$$

where  $\bar{\mu}_\zeta = \bar{\mu}_\zeta - eVx$  is the electrochemical potential, and  $\tau_{\text{sf}}$  is the spin relaxation time which characterizes the spin flip process. In general,  $\tau_{\text{sf}} \gg \tau$ . The anisotropic part of distribution function can be expressed by a Legendre polynomial

$$g_{\hat{k}\zeta}^a = \sum_{n=1}^{\infty} g_{\zeta n}^a P_n(\cos\theta), \quad (1.9)$$

where now  $\theta$  is the angle between  $\hat{x}$  and  $\hat{k}$ .  $g_{\hat{k}\zeta}^a$  turns out to be related to  $\bar{\mu}_\zeta$  [16]. Averaging the Boltzmann equation Eq. (1.8) over all direction and using the recursive relation spelt out in Ref. [16], one gets the spin diffusion equation

$$\frac{\partial^2 (\bar{\mu}_\zeta - \bar{\mu}_{-\zeta})}{\partial x^2} = \frac{\bar{\mu}_\zeta - \bar{\mu}_{-\zeta}}{l_{\text{sf}}^2}, \quad (1.10)$$

where  $l_{\text{sf}}$  is the spin diffusion length.  $\bar{\mu}_\zeta$  then has to be fit by boundary conditions which depends on the magnetic configuration. Note that in this case the length scale is the spin diffusion length  $l_{\text{sf}}$ , which is in general much longer than the mean free path  $l$ .

### 1.3.2 SPINTRONICS

The GMR opened a new field named *spintronics* which studies the properties of electron spin with a view to improve the efficiency of electronic devices [13, 14]. For example, the GMR sensors of read heads had replaced the AMR (anisotropic magnetoresistance, see below) sensors. Following the concept that the transfer of a transverse spin current to a magnetic layer can be described by a *spin transfer torque* (STT) acting on the magnetic moment in the CPP-magnetic multilayers or spin valves introduced by Slonczewski [17] and Berger [18], huge amounts of theoretical and experimental works have been done due to the possible applications in technology such as the new generation of magnetic random access memory (MRAM) [19, 20]. The mechanism of the STT is illustrated in Fig. 3.7. An unpolarized from the bottom is filtered by the first ferromagnetic layer ( $M1$ ), resulting in a spin current. This spin then inserts a STT on the second magnetization on the second ferromagnetic layer ( $M2$ ).

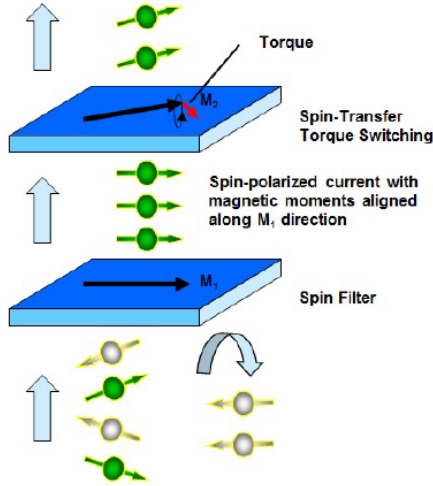


FIGURE 1.4: The illustrations for the STT (from Samsung Electronics).

## 1.4 SPIN-ORBIT COUPLING (SOC) AND THE RETURN OF CIP

The spin-orbit coupling (SOC, also called spin-orbit interaction) describes the coupling of the spin with the orbital angular momentum. From special relativity, the motion of an electron in an electric field results in a kinematic effect in which part of the electric field is seen as a magnetic field in the electron's rest frame. The interaction of the electron spin with the electric field (via the associated magnetic field in the electron's rest frame) is called the SOC, which has the form

$$H_{\text{so}} = \eta_{\text{so}} \boldsymbol{\sigma} \cdot \left[ \vec{\nabla} V \times \frac{1}{i} \vec{\nabla} \right], \quad (1.11)$$

where  $\eta_{\text{so}} = \hbar^2 / (4m_0^2 c^2)$  in terms of the bare electron mass  $m_0$  and velocity of light  $c$ ,  $\boldsymbol{\sigma}$  is the Pauli matrices,  $V$  is the potential, and  $(1/i)\vec{\nabla}$  is the momentum operator.

In the case of atoms, for example, the SOC refers to the interaction of the electron spin with the average Coulomb field of the nuclei and other electrons. Similarly, the SOC in solids is determined by the interaction of the electron spin with the average electric field corresponding to the periodic crystal potential. Other internal or external electric fields can produce additional SOC terms. The value of the SOC is about 1% to 10% when compared with the exchange interaction. However,

magnetism would not exist without the SOC, which also determines the magneto-crystalline anisotropy.

Except magnetic properties, the SOC is important for electronic transport as well. Since spin couples to the orbital momentum of electrons, the transport properties (which are related to orbital momentum) can be spin-dependent in the presence of the SOC. There are quite some important phenomena induced by the SOC in metallic ferromagnets such as the anisotropic magnetoresistance (AMR) [21] and the anomalous Hall effect (AHE) [22]. The spin Hall effect (SHE) [23] is an analogue of the AHE in normal metals.

### 1.4.1 AMR

The AMR is the phenomenon that the electric resistance in metallic ferromagnets depends on the relative orientation between the electric current and the magnetization [21]. It has been discovered a long time ago and was of considerable interest as a convenient tool to measure the magnetization direction electrically thereby serving as magnetic field sensor [24]. Although nowadays it is not used as magnetic sensors anymore, the AMR still keeps attracting some scientific attention nowadays [29]. The AMR in bulk ferromagnets is generally believed to have an extrinsic origin, caused by the SOC in the  $s$ - $d$  scattering in ferromagnets, *i.e.*, the conduction electrons are scattered into localized electrons by impurities [25–29]. The AMR in the magnetic Rashba two-dimensional electron gas is strongly enhanced by magnetic impurities [30]. An intrinsic mechanism was reported to contribute to the transverse component of magnetoresistance (the planar Hall effect) [31].

The AMR in a bulk ferromagnet  $\Delta\rho_b/\rho_F$  is defined as

$$\frac{\Delta\rho_b}{\rho_0} \equiv \frac{\rho_{\parallel} - \rho_{\perp}}{\rho_0}, \quad (1.12)$$

where  $\rho_{\parallel}$  ( $\rho_{\perp}$ ) is the resistivity for a magnetization parallel (transverse) to the applied current.  $\rho_0$  is an averaged value over directions. The latter has been defined differently in the literature, for example, as an average over the three principle directions as  $\rho_0 \equiv (\rho_{\parallel} + 2\rho_{\perp})/3$  in Ref.[24]. Defining  $\rho_{\parallel} = \rho_0 + \Delta\rho_b$  and  $\rho_{\perp} = \rho_0 - \Delta\rho_b$ , the dependence of the AMR on the magnetization direction with unit vector  $\hat{m}$  in an isotropic (or cubic) material and charge current bias along the  $\hat{x}$  direction reads:

$$\rho_{\text{long}} = \rho_0 + \Delta\rho_b m_x^2, \quad (1.13)$$

$$\rho_{\text{trans}} = \Delta\rho_b m_x m_y, \quad (1.14)$$

where  $\rho_{\text{long}}$  is the longitudinal component of electric resistivity (along  $\hat{x}$ ),  $\rho_{\text{trans}}$  is the transverse component along  $\hat{y}$ , and  $m_i$  is the  $\hat{i}$ -component of the magne-

tization direction unit vector.  $\Delta\rho_b$  can be derived microscopically from the  $s$ - $d$  model with a free  $s$ -electron conduction band and localized  $d$ -electrons with a strong exchange interaction and weaker SOC. Transport is carried by the conduction electrons with a contribution to the resistivity from scattering into the localized  $d$ -states by impurities that depends on the magnetization direction because of the SOC. The AMR ratio for strong ferromagnet then leads to [27]

$$\frac{\Delta\rho_b}{\rho_0} = \gamma \left( \frac{\rho_{s \rightarrow d\downarrow} - \rho_{s\uparrow}}{\rho_{s\uparrow}} \right) \quad (1.15)$$

where  $\gamma = (3/4)(\lambda/H_{\text{ex}})$  with  $\lambda = \hbar^2/(4m_0^2c^2)$  is the SOC constant and  $H_{\text{ex}}$  the exchange field of the  $d$ -states.  $\rho_{s\uparrow}$  is the resistivity of  $s$ -state electrons with majority spin ( $\uparrow$ ) and  $\rho_{s \rightarrow d\downarrow}$  a resistivity due to the  $s$ - $d$  scattering into minority-spin  $d$  states ( $\downarrow$ ). Eq. (4.4) has been refined by taking into account more scattering processes [28] but assuming  $\rho_{s\uparrow} = \rho_{s\downarrow}$  leading to a positive definite value

$$\frac{\Delta\rho_b}{\rho_0} = \frac{\gamma(\rho_{s \rightarrow d\downarrow} - \rho_{s \rightarrow d\uparrow})^2}{(\rho_s + \rho_{s \rightarrow d\downarrow})(\rho_s + \rho_{s \rightarrow d\uparrow})}. \quad (1.16)$$

Experimentally,  $\Delta\rho_b$  is indeed larger than zero for most ferromagnets, but exceptions have been observed [32, 33] and computed by a model that includes spin-dependent effective masses and number density of electrons in the conduction band [29]. In thin films  $\Delta\rho_b$  was found to be affected by surface roughness [34].

### 1.4.2 AHE

The Hall effect is the transverse voltage generated by a charge current/voltage bias in a perpendicular magnetic field [35]. The AHE, which was discovered at the same time, is caused by SOC potentials or magnetic orientational disorder (which again requires the SOC) and have been the subject of research for several decades [22]. There are still controversies about its microscopic mechanism, i.e., whether it is *intrinsic* (caused by the band structure of material as affected by the SOC), or *extrinsic* (caused by impurities with a significant spin-orbit scattering amplitude). Presumably there is no global truth, but the answer depends on the specific material in question. The intrinsic AHE originates from the SOC inherent to the material band structure, which gives rise to an anomalous velocity that can be included into semiclassical transport methods such as the Boltzmann equation [36]. For ballistic systems the AHE can be computed by first principles calculations, often in good agreement with experiments that have been carried out in diffuse samples [22, 37–39]. The purely extrinsic mechanisms are classified as *side-jump* and *skew scattering*, which can be distinguished by characteristic dependence on the electric resistivity. The side-jump mechanism can be pictured in

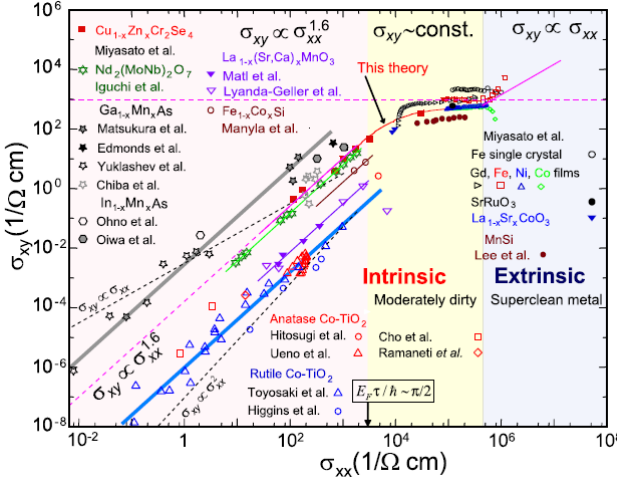


FIGURE 1.5: The scaling of the anomalous Hall conductivity as a function of the longitudinal conductivity  $\sigma_{xx}$  in different regimes (from Ref. [45]).

terms of incoming and outgoing trajectories of the electron upon scattering from an impurity that are displaced in a side-step (in a direction that depends on the spin polarization) but without associated directional deflection [40]. Recently this contribution to the anomalous Hall conductivity has been extracted directly from the electronic structure of a perfect crystal [41, 42]. Skew scattering relies on the spin dependence of the scattering angle of the electrons reflecting from a given impurity [43]. Recently *ab initio* calculations for the extrinsic AHE are carried out. A unified theory that takes account of both the intrinsic and extrinsic effects [44] found that the AHE is dominated by skew scattering in the clean (high conductivity) limit, where the Hall conductivity is linear to the longitudinal conductivity. The intrinsic contribution becomes dominant at intermediate impurity densities, where the Hall conductivity does not depend on resistivity. In dirty systems the AHE depends on conductivity according to a power law [45, 46]. The whole scenario of the scaling of the AHE as a function of electric conductivity is given in Fig. 1.5. A first-principles approach applicable to both pure and disordered systems leads to the conclusion that the skew scattering term dominates the side-jump contribution in the dilute regime [47].

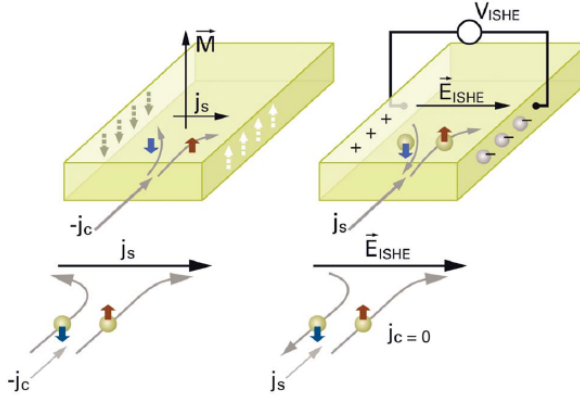


FIGURE 1.6: The illustrations for the SHE and the ISHE (from Ref. [71]).

### 1.4.3 SHE

Predicted theoretically by Dyakonov and Perel in 1971 [48], the SHE is the transverse spin current/accumulation generated by a charge current with spin polarization perpendicular to the plane of the two currents (see Fig. 1.6) [23]. The SHE is closely related to the AHE, but does not require an external magnetic field and/or ferromagnetism, meaning that the SHE does not require broken time reversal symmetry. The SHE was scarcely noticed until Hirsch [49] and Zhang [50] rediscovered it and brought it to the attention of the spintronics community around the the end of the second millennium since the SHE can be a promising way to generate spin currents. Despite some experiments already revealed features of the SHE [51] and its inverse effect, the inverse spin Hall effect (ISHE) [52, 53] in the last century, the first observation of the SHE was in a semiconductor system in 2004 [54], while the first direct electronic measurement on a metallic system was achieved in 2006 [55].

Similar to the AHE, there are different physical mechanisms causing the SHE, which are strongly dependent on specific materials and systems. The extrinsic mechanisms of the SHE was formulated by the Boltzmann approach [56]. The side-jump mechanism was taken into account by the modification of the velocity operator by the SOC term in the Hamiltonian as discussed in Ref. [57]. Due to the SOC at the impurity scattering,

$$\vec{v}_{\vec{k}_c} = \frac{\hbar \vec{k}}{m} + \omega_{\vec{k}_c}, \quad (1.17)$$

where

$$\omega_{\vec{k}\zeta} = \alpha_{\text{H}}^{\text{SJ}} \left( \boldsymbol{\sigma}_{\zeta\zeta} \times \frac{\hbar \vec{k}}{m} \right) \quad (1.18)$$

is the so-called anomalous velocity with  $\boldsymbol{\sigma}_{\zeta\zeta}$  points the direction of spin polarization. The side-jump parameter is defined as  $\alpha_{\text{H}}^{\text{SJ}} = \eta_{\text{so}}^- / (k_{\text{F}} l)$ , where  $\eta_{\text{so}}^- = \eta_{\text{so}} k_{\text{F}}^2$  is the dimensionless spin orbit parameter,  $k_{\text{F}}$  is the Fermi wave vector, and  $l$  is the mean free path. On the other hand, the skew scattering can be taken into account by including extra terms in the collision integral of the Boltzmann equation, which leads to the solution

$$\mathbf{g}_{\vec{k}\zeta}^a = \tau \frac{\partial f^0}{\partial \epsilon} (\vec{v}_{\vec{k}} - \alpha_{\text{H}}^{\text{SS}} \boldsymbol{\sigma}_{\zeta\zeta} \times \vec{v}_{\vec{k}}) \cdot \vec{\nabla} \bar{\mu}_{\zeta}, \quad (1.19)$$

where

$$\alpha_{\text{H}}^{\text{SS}} = \frac{2\pi}{3} \eta_{\text{so}}^- N(0) V_{\text{imp}} \quad (1.20)$$

in the second term is the skew scattering parameter with  $N(0)$  the DOS at energy zero and  $V_{\text{imp}}$  the averaged strength of the impurities. When one sets the applied fields along  $\hat{x}$  and focuses on electrons with spin polarization  $\boldsymbol{\sigma}_{\zeta\zeta} = \pm \hat{z}$ , one can calculate a  $\hat{z}$ -polarized spin Hall current flowing along  $\hat{y}$  by the expression of the spin current (with the same unit as the electric current)

$$\vec{j}_s = e \sum_{\zeta} \sum_{\vec{k}} \zeta \vec{v}_{\vec{k}\zeta} \mathbf{g}_{\vec{k}\zeta}^a. \quad (1.21)$$

The intrinsic mechanism associated with the spin dependent band structure of the material is not spelt out here, but can be in principle renormalized in the anomalous velocity since it does not dependent on the scattering process itself. A scenario similar to Fig. 1.5 which verifies which mechanism dominates at which regime, i.e., the evolution of the SHE as a function of mobility has been predicted [58].

#### 1.4.4 RETURN OF CIP

It is shown that most interest is in the CPP structures after the discovery of the CPP-GMR since the spin transfer effects are more relevant. Recently, however, the SOC has brought the attention of the spintronics community back to the CIP studies on layered systems made of thin-films consist of ferromagnet and heavy normal metal such as platinum. The strong SOC in the heavy metal results in the observed torques at the interface between normal metal and ferromagnet in the CIP measurements, which can even achieve the magnetization switching, thereby providing a promising scenario for new types of magnetic storage devices [60, 61]. These current-induced torques can be generated by the SHE in the

normal metal [61] or by the spin-orbit torque from the broken inversion symmetry at the interface [60, 62]. Also the spin orbit torque from the Dzyaloshinskii-Moriya interaction in a ferromagnet with a non uniform magnetization such as domain walls has been discussed extensively. In a typical bilayer system, except using a metallic ferromagnet, it was discovered that ferromagnetic insulators such as yttrium iron garnet (YIG) can be useful as well since YIG boasts very low magnetization damping [63]. Moreover, in systems made of a normal metal and a ferromagnetic insulator, the electric current only flows in the metal, which importantly simplifies the complexity of a transport theory [64]. Two of the chapters in this thesis are focused on SOC generated effects in bilayer made from a normal metal and a ferromagnetic insulator.

## 1.5 THERMOELECTRIC EFFECTS AND SPIN CALORITRONICS

Ohm's law tell us that an electric current can be generated in a metal by applying a electric voltage. Analogously, applying a temperature field generates a thermal current, i.e., a flow of thermal energy, which is formulated by [1]

$$\vec{Q} = \sum_{\vec{k}} (\varepsilon - \mu_0) \vec{v}_{\vec{k}} g_{\vec{k}}^a. \quad (1.22)$$

Note that the anisotropic part of distribution function in the presence of an electric field and temperature gradient is (dropping the spin indices)

$$g_{\vec{k}}^a = \tau \frac{\partial f^0}{\partial \varepsilon} \vec{v}_{\vec{k}} \cdot \left( \vec{\nabla} \bar{\mu} + \frac{\varepsilon - \mu_0}{T} \vec{\nabla} T \right). \quad (1.23)$$

Together with the expression of charge current, the linear response between the (electric and heat) currents and the (electric and thermal) forces can be written as

$$\begin{pmatrix} \vec{J} \\ \vec{Q} \end{pmatrix} = \sigma \begin{pmatrix} 1 & ST \\ \Pi & \kappa T / \sigma \end{pmatrix} \begin{pmatrix} \frac{1}{e} \vec{\nabla} \mu \\ -\frac{1}{T} \vec{\nabla} T \end{pmatrix}, \quad (1.24)$$

where currents are generated by the gradients of the electrochemical potential  $\bar{\mu}$  and temperature  $T$ .  $\sigma$  is the (Drude) electric conductivity, and  $\kappa$  is the heat conductivity [1]. The off-diagonal terms are non-zero due to the electron-hole asymmetry at the Fermi energy, such that an electric current can be generated by applying a temperature gradient in a metal except an electric field. This is called the Seebeck effect, and  $S$  is the Seebeck coefficient. The inverse effect of the Seebeck effect is given the name Peltier, which describes the cooling and heating at the

reservoirs or junctions by an electric current. Time reversal symmetry of quantum mechanics is reflected by Onsager's reciprocity relations (since the sum of the products of currents times driving forces equals the dissipation) [65] that lead to Kelvin-Onsager relation between the Seebeck and Peltier coefficients  $\Pi = ST$ . In the Sommerfeld approximation,

$$S = -e\mathcal{L}_0 T \frac{\partial}{\partial \varepsilon} \ln \sigma(\varepsilon)|_{\mu_0}, \quad (1.25)$$

where the electronic charge is  $-e$ , and  $\mu_0$  is the ground state chemical potential. In this limit the Wiedemann-Franz law  $\kappa = \sigma \mathcal{L}_0 T$  holds. All response matrix elements are functions of the state of the system, depending upon variables such as composition and temperature.

Except being coupled to charge, heat also interacts with spin [66–68], which opened a field concerned with non equilibrium phenomena related to spin, charge, entropy and energy transport called spin caloritronics [69–71]. Historically, Johnson discussed the non equilibrium thermodynamics of charge, spin, and heat in metallic heterostructures with collinear configurations [66], while only the thermal analogue of the CIP-GMR was studied experimentally [67]. Experimental and theoretical works in magnetic multilayers nanowires have been done by the Lausanne group systematically [68]. From the latter half of the first decade of this century, spin caloritronics started getting more attention from the magnetism/spintronics society because of the growing technological concerns such as the breakdown of the Moore's law due to the thermodynamics bottleneck as well as several important predictions/discoveries of new effects. Spin caloritronic phenomena are roughly classified into (i) independent electron, (ii) collective, and (iii) relativistic effects [70], which are briefly discussed as the following.

The independent electron effects are the generalization of collinear magnetoelectronic effect such as the GMR. In analogy with the giant magnetoresistance, magneto-Seebeck and magneto-Peltier effects arise in heterostructures [66, 68, 72]. The spin-dependent Seebeck [73] and Peltier [74] effects have been demonstrated in lateral spin valves as well as the observation of the spin heat accumulation [75], i.e., an imbalance between temperatures of the majority and minority spins [76]. The thermal analogue of the tunneling magnetoresistance in magnetic tunnel junctions are observed as well.

The collective effects are generated by the collective dynamics of the magnetic order parameter that couples to single particle spins via the STT and spin pumping. The thermal spin transfer torque was predicted [77] and confirmed experimentally in nanowire spin valves [78]. Another important discovery is the pure spin current generated by a temperature gradient in a ferromagnet, i.e., the spin Seebeck effect (SEE) [79], which introduced an alternative way to generate

spin currents except the spin Hall effect even in ferromagnetic insulators [80], and therefore allows thermal injection of spin currents from the ferromagnet into an attached nonmagnetic metal over a macroscopic scale of several millimeters. The SEE cannot be explained by the independent electron transport, but has to be explained in terms of phonon-magnon and phonon-electron drag effects mediated through the substrate [81]. Its Onsager reciprocal, the spin Peltier effect, which is a magnon heat current generated by a spin current through the interface with the metal contact has been observed [82].

The relativistic effects are the generalization of the corrections due to relativistic SOC such as the anisotropic magnetoresistance, the anomalous Hall effect, and the spin Hall effect. In the presence of an external magnetic field, the thermoelectric analogues exist and can be classified into three groups: the Nernst effect stands for the Hall voltage induced by a heat current, while the name Ettingshausen stands for the reciprocal effect, *viz.* a heat current induced transverse to an applied charge current. The transverse heat current driven by a temperature bias (thermal Hall effect) is associated with the names Righi-Leduc. In normal label, we add 'spin' to each effect just as what we did to the SHE, and we have the spin Nernst effect and so on. In metallic ferromagnet, we distinguish the configuration in which the magnetization is normal to both currents (anomalous Hall effect (AHE), anomalous Nernst effect (ANE), *etc.*) from the configuration with in-plane magnetization (planar Hall effect (PHE), planar Nernst effect (PNE), *etc.*).

## 1.6 THIS THESIS

This thesis covers several important issues in spin caloritronics and spintronics induced by the SOC. In chapter 2, we studied the relativistic spin caloritronic effects by developing a semiclassical theory for anomalous thermoelectric effects in ferromagnetic metals due to spin-orbit scattering at impurities, such as the anomalous Nernst and Ettingshausen effect, the planar thermal Hall effects, and thermoelectric anisotropic magnetoresistance. While some work has been done with emphasis on the intrinsic SOC [45, 83, 84], our extrinsic theory systemizes the competing effects/mechanisms from a microscopic point of view and identifies the parameters needed to describe experiments.

In Chapter 3, We present a theory of the spin Hall magnetoresistance (SMR) in multilayers made from an insulating ferromagnet F, such as yttrium iron garnet (YIG), and a normal metal N with spin-orbit interactions, such as platinum (Pt). The SMR is induced by the simultaneous action of spin Hall and inverse spin Hall effects and therefore a non-equilibrium proximity phenomenon. We compute the SMR in F|N and F|N|F layered systems, treating N by spin-diffusion theory with quantum mechanical boundary conditions at the interfaces in terms of the spin-

mixing conductance. Our results explain the experimentally observed spin Hall magnetoresistance in N|F bilayers. For F|N|F spin valves we predict an enhanced SMR amplitude when magnetizations are collinear. The SMR and the spin-transfer torques in these trilayers can be controlled by the magnetic configuration.

In Chapter 4, we relax the limitation in Chapter 2 that transport normal to the boundaries due to the AHE is not relevant. We predict a new contribution of anisotropic magnetoresistance in metallic ferromagnets as simultaneous action of the anomalous Hall effect and its inverse. By diffusion theory, we compare this contribution with the conventional AMR, demonstrating that they can be distinguished experimentally by studying its dependence on the film thickness.

We present a Boltzmann analysis to quantify how the surface/interface scattering affect the spin Hall physics in Chapter 5. We propose due to spin-dependent scattering at the N|YIG interface, a spin polarized current is generated when applying an electric field parallel to the interface. When the magnetization is out-of-plane, this spin-polarized current contributes a transverse charge current via the inverse spin Hall effect. Furthermore, the results reveal that the conventional SMR theory developed in Chapter 3 has to be corrected in the thin-film limit.

## REFERENCES

- [1] N. W. Ashcroft and N. D. Mermin, *Solid State Physics* (Saunders, Philadelphia, 1976).
- [2] J. Stöhr and H. C. Siegmann, *Magnetism* (Springer, Berlin Heidelberg, 2006).
- [3] E. C. Stoner, *Proc. Roy. Soc.* **154**, 656 (1936).
- [4] E. C. Stoner, *Proc. Roy. Soc.* **165**, 372 (1938).
- [5] N. Mott and H. Wills, *Proc. R. Soc.* **153**, 699 (1936).
- [6] M. N. Baibich, J. M. Broto, A. Fert, F. Nguyen Van Dau, F. Petroff, P. Etienne, G. Creuzet, A. Friederich, and J. Chazelas, *Phys. Rev. Lett.* **61**, 2472 (1988).
- [7] G. Binash, P. Grünberg, F. Saurenbach, and W. Zinn, *Phys. Rev. B* **39**, 4828 (1989).
- [8] C. Chappert, A. Fert, and F. Nguyen Van Dau, *Nature Mater.* **6**, 813 (2007).
- [9] A. Fert, *Rev. Mod. Phys.* **80**, 1517 (2008).
- [10] R. E. Camley and J. Barnaś, *Phys. Rev. Lett.* **63**, 664 (1989).
- [11] K. Fuchs, *Proc. Cambridge Philos. Soc.* **34**, 100 (1938).

- [12] E. H. Sondheimer, *Adv. Phys.* **1**, 1 (1952).
- [13] S. D. Bader and S. S. P. Parkin, *Ann. Rev. Cond. Matt. Phys.* **1**, 71 (2010).
- [14] J. Sinova and I Žutić, *Nature Mater.* **11**, 368 (2012).
- [15] L. Piraux, J. M. George, J. F. Despres, C. Leroy, E. Ferain, R. Legras, K. Ounadjela, and A. Fert, *Appl. Phys. Lett.* **65**, 2784 (1994).
- [16] T. Valet and A. Fert, *Phys. Rev. B* **48**, 7099 (1993).
- [17] J. C. Slonczewski, *J. Magn. Magn. Mater.* **159**, L1 (1996).
- [18] L. Berger, *Phys. Rev. B* **54**, 9353 (1996).
- [19] S. S. P. Parkin, M. Hayashi, and L. Thomas, *Science* **320**, 190 (2008).
- [20] N. Locatelli, V. Cros, and J. Grollier, *Nature Mater.* **13**, 11 (2013).
- [21] W. Thomson, *Proc. R. Soc. London* **8**, 546 (1857).
- [22] For a review, see, N. Nagaosa, J. Sinova, S. Onoda, A. H. MacDonald, and N. P. Ong, *Rev. Mod. Phys.* **82**, 1539 (2010).
- [23] For a review see: T. Jungwirth, J. Wunderlich, and K. Olejník, *Nature Mater.* **11**, 382 (2012).
- [24] T. R. McGuire and R. I. Potter, *IEEE Trans. Magn.* **11**, 1018 (1975).
- [25] J. Smit, *Physica* **16**, 612 (1951).
- [26] L. Berger, *Physica* **30**, 1141 (1964).
- [27] I. A. Campbell, A. Fert, and O. Jaoul, *J. Phys. C* **3**, S95 (1975).
- [28] A. P. Malozemoff, *Phys. Rev. B* **32**, 6080 (1985); *Phys. Rev. B* **34**, 1853 (1986).
- [29] S. Kokado, M. Tsunoda, K. Harigaya, and A. Sakuma, *J. Phys. Soc. Jpn.* **81**, 024705 (2012).
- [30] A. A. Kovalev, Y. Tserkovnyak, K. Výborný, and J. Sinova, *Phys. Rev. B* **79**, 195129 (2009).
- [31] K.-J. Friedland, M. Bowen, J. Herfort, H. P. Schönherr, and K. H. Ploog, *J. Phys. Condens. Matter* **18**, 2641 (2006).
- [32] T. R. McGuire, J. A. Aboaf, and E. Kloholm, *IEEE Trans. Magn.* **20**, 972 (1984).

- [33] M. Tsunoda, Y. Komasaki, S. Kokado, S. Isogami, C.-C. Chen, and M. Takahashi, *Appl. Phys. Express* **2**, 083001 (2009).
- [34] Th. G. S. M. Rijks, R. Coehoorn, M. J. M. de Jong, and W. J. M. de Jonge, *Phys. Rev. B* **51**, 283 (1995).
- [35] E. H. Hall, *Am. J. Math.* **2**, 287 (1879).
- [36] R. Karplus and J. M. Luttinger, *Phys. Rev.* **95**, 1154 (1954).
- [37] Y. Yao, L. Kleinman, A. H. MacDonald, J. Sinova, T. Jungwirth, D. S. Wang, E. Wang, and Q. Niu, *Phys. Rev. Lett.* **92**, 037204 (2004).
- [38] X. Wang, J. R. Yates, I. Souza, and D. Vanderbilt, *Phys. Rev. B* **74**, 195118 (2006).
- [39] X. Wang, D. Vanderbilt, J. R. Yates, and I. Souza, *Phys. Rev. B* **76**, 195109 (2007).
- [40] L. Berger *Phys. Rev. B* **2**, 4559 (1970).
- [41] A. A. Kovalev, J. Sinova, and Y. Tserkovnyak, *Phys. Rev. Lett.* **105**, 036601 (2010).
- [42] J. Weischenberg, F. Freimuth, J. Sinova, Stefan Blügel, and Yuriy Mokrousov, *Phys. Rev. Lett.* **107**, 106601 (2011).
- [43] J. Smit, *Physica* **21**, 877 (1955).
- [44] S. Onoda, N. Sugimoto, N. Nagaosa, *Phys. Rev. Lett.* **97**, 126602 (2006).
- [45] S. Onoda, N. Sugimoto, N. Nagaosa, *Phys. Rev. B* **77**, 165103 (2008), and references therein.
- [46] T. Miyasato, N. Abe, T. Fujii, A. Asamitsu, S. Onoda, Y. Onose, N. Nagaosa, and Y. Tokura, *Phys. Rev. Lett.* **99**, 086602 (2007).
- [47] S. Lowitzer, D. Ködderitzsch, and H. Ebert, *Phys. Rev. Lett.* **105**, 266604 (2010).
- [48] M. I. Dyakonov and V. I. Perel, *Phys. Lett. A* **35**, 459 (1971); M. I. Dyakonov and V. I. Perel, *Zh. Eksp. Ter. Fiz.* **13**, 657 (1971).
- [49] J. E. Hirsch, *Phys. Rev. Lett.* **83**, 1834 (1999).
- [50] S. Zhang, *Phys. Rev. Lett.* **85**, 393 (2000).
- [51] A. Fert, A. Frièderich, and A. Hamzic, *J. Magn. Magn. Mater.* **24**, 231 (1981).
- [52] A. A. Bakun, B. P. Zakharchenya, A. A. Rogachev, M. N. Tkachuk, and V. G. Fleisher, *Sov. Phys. JEST Lett.* **40**, 1293 (1984).

- [53] M. N. Tkachuk, B. P. Zakharchenya, and V. G. Fleisher, *Sov. Phys. JEST Lett.* **44**, 59 (1986).
- [54] Y. K. Kato, R. C. Myers, A. C. Gossard, and D. D. Awschalom, *Science* **306**, 1910 (2004).
- [55] S. O. Valenzuela and M. Tinkham, *Nature* **442**, 176 (2006).
- [56] S. Takahashi, H. Imamura, and S. Maekawa, in *Concepts in Spin Electronics*, edited by S. Maekawa (Oxford University Press, U.K., 2006), pp. 343-370.
- [57] S. K. Lyo and T. Holstein, *Phys. Rev. Lett.* **7**, 423 (1972).
- [58] G. Vignale, *J. Supercond. Nov. Magn.* **23**, 3 (2009).
- [59] *Spin Current*, edited by S. Maekawa (Oxford University Press, U.K., 2012).
- [60] I. M. Miron, K. Garello, G. Gaudin, P.-J. Zermatten, M. V. Costache, S. Auffret, S. Bandiera, B. Rodmacq, A. Schuhl, and P. Gambardella, *Nature* **476**, 189 (2011).
- [61] L. Liu, C. F. Pai, Y. Li, H. W. Tseng, D. C. Ralph, and R. A. Buhrman, *Science* **336**, 555 (2012).
- [62] V. M. Edelstein, *Solid State Commun.* **73**, 233 (1990).
- [63] Y. Kajiwara, K. Harii, S. Takahashi, J. Ohe, K. Uchida, M. Mizuguchi, H. Umezawa, H. Kawai, K. Ando, K. Takanashi, S. Maekawa, and E. Saitoh, *Nature* **464**, 262 (2010).
- [64] A. Brataas, Yu. V. Nazarov, and G. E. W. Bauer, *Phys. Rev. Lett.* **84**, 2481 (2000); *Eur. Phys. J. B* **22**, 99 (2001).
- [65] L. Onsager, *Phys. Rev.* **37**, 405 (1931).
- [66] M. Johnson and R. H. Silsbee, *Phys. Rev. B* **35**, 4959 (1987).
- [67] J. Shi, K. Pettit, E. Kita, S. S. P. Parkin, R. Nakatani, and M. B. Salamon, *Phys. Rev. B* **54**, 15273 (1996).
- [68] L. Gravier, S. S.-Guisan, F. Reuse, and J.-Ph. Ansermet, *Phys. Rev. B* **73**, 024419 (2006); **73**, 052410 (2006).
- [69] G. E. W. Bauer, A. H. MacDonald, and S. Maekawa, *Solid State Commun.* **150**, 459 (2010).
- [70] G. E. W. Bauer, E. Saitoh, and B. J. van Wees, *Nature Mater.* **11**, 391 (2012).

- [71] S. R. Boona, R. C. Myers, and J. P. Heremans, *Energy Environ. Sci.* **7**, 885 (2014).
- [72] M. Hatami, and G. E. W. Bauer, Q. Zhang, and P. J. Kelly, *Phys. Rev. B* **79**, 174426 (2009).
- [73] A. Slachter, F. L. Bakker, J. P. Adam, and B. J. van Wees, *Nature Phys.* **6**, 879 (2010).
- [74] J. Flipse, F. L. Bakker, A. Slachter, F. K. Dejene, and B. J. van Wees, *Nature Nanotech.* **7**, 166 (2012).
- [75] F. K. Dejene, J. Flipse, G. E. W. Bauer, and B. J. van Wees, *Nature Phys.* **9**, 636 (2013).
- [76] T. T. Heikkilä, M. Hatami, G. E. W. Bauer, *Solid State Commun.* **150**, 475 (2010).
- [77] M. Hatami, G. E. W. Bauer, Q. Zhang, and P. J. Kelly, *Phys. Rev. Lett.* **99**, 066603 (2007).
- [78] H. Yu, S. Granville, D. P. Yu, and J.-Ph. Ansermet, *Phys. Rev. Lett.* **104**, 146601 (2010).
- [79] K. Uchida, S. Takahashi, K. Harii, J. Ieda, W. Koshibae, K. Ando, S. Maekawa, and E. Saitoh, *Nature* **455**, 778 (2008).
- [80] K. Uchida, J. Xiao, H. Adachi, J. Ohe, S. Takahashi, J. Ieda, T. Ota, Y. Kajiwara, H. Umezawa, H. Kawai, G. E. W. Bauer, S. Maekawa, and E. Saitoh, *Nature Mater.* **9**, 894 (2010).
- [81] H. Adachi, K. Uchida, E. Saitoh, and S. Maekawa, *J. Phys. Soc. Jpn.* **76**, 036501 (2013).
- [82] J. Flipse, F. K. Dejene, D. Wagenaar, G. E. W. Bauer, J. Ben Youssef, and B. J. van Wees, arXiv:1311.4772 (cond-mat.mes-hall).
- [83] Z. Ma, *Solid State Commun.* **150**, 510 (2010).
- [84] X. Liu and X. C. Xie, *Solid State Commun.* **150**, 471 (2010).



# 2

## ANOMALOUS THERMOELECTRIC EFFECTS IN FERROMAGNETIC METALS

**Yan-Ting CHEN**

*We present a semiclassical theory for anomalous thermoelectric effects in ferromagnetic metals due to spin-orbit scattering at impurities, such as the anomalous Nernst and Ettingshausen effect, the planar thermal Hall effects, and thermoelectric anisotropic magnetoresistance. Our theory systemizes the competing effects/mechanisms from a microscopic point of view and identifies the parameters needed to describe experiments.*

---

Parts of this chapter have been collaborated with Saburo Takahashi and Gerrit E. W. Bauer

## 2.1 INTRODUCTION

Spintronics deals with the coupling between the electron spin and charge degrees of freedom in the properties of materials and devices [1]. Recently, the sub-field called spin caloritronics, which seeks to exploit the coupling among electronic charge, spin and entropy/energy transport in solid state structures, has attracted some attention [2]. Utilizing the spin degree of freedom in conducting nano-scale structures to control charge and heat currents on the same footing can provide new functionalities for electronic devices and heat engines. An important class of spintronic materials are metallic ferromagnets, especially transition metals and its alloys. Here we present a study of the thermoelectric response of thin films made from metallic ferromagnets.

The coupling between charge and heat currents is referred to as thermoelectricity. In ferromagnets, the Seebeck and Peltier coefficients are spin-dependent. In analogy with the giant magnetoresistance, magneto-Seebeck and magneto-Peltier effects arise in heterostructures [3–5]. The spin-dependent Seebeck [6] and Peltier [7] effects have been demonstrated in lateral spin valves as well as the observation of the spin heat accumulation [8], *i.e.*, an imbalance between temperatures of the majority and minority spins [9]. The spin Seebeck effect [10] is now believed to not be related to conventional spin-dependent thermoelectrics [11].

The Hall effect [12], *i.e.*, the transverse voltage generated by a charge current/voltage bias in a perpendicular magnetic field, has thermoelectric equivalents, *viz.* the Nernst, Ettingshausen, and Righi-LeDuc effects [13]. The Nernst effect stands for the Hall voltage induced by a heat current, while the name Ettingshausen stands for the reciprocal effect, *viz.* a heat current induced transverse to an applied charge current. The transverse heat current driven by a temperature bias (thermal Hall effect) is associated with the names Righi-Leduc. In ferromagnets, a transverse Hall response exists even without applied magnetic fields and is referred to as “anomalous” (or “extraordinary”) [12]. We distinguish the configuration in which the magnetization is normal to both currents (anomalous Hall effect (AHE), anomalous Nernst effect (ANE), *etc.*) from the configuration with in-plane magnetization (planar Hall effect (PHE), planar Nernst effect (PNE), *etc.*). All these effects might provide new functionalities for heat management in magnetoelectronic nano-structures.

The anomalous Hall effect is caused by spin-orbit coupling (SOC) potentials or magnetic orientational disorder (which again requires the SOC) and have been the subject of research for several decades [14]. There are still controversies about its microscopic mechanism, *i.e.* whether it is *intrinsic* (caused by the band structure of material as affected by the SOC), or *extrinsic* (caused by impurities with a significant spin-orbit scattering amplitude). Presumably there is no global truth, but the answer depends on the specific material in question. The intrinsic AHE orig-

inates from the SOC inherent to the material band structure, which gives rise to an anomalous velocity that can be included into semiclassical transport methods such as the Boltzmann equation [15]. For ballistic systems the AHE can be computed by first principles calculations, often in good agreement with experiments that have been carried out in diffuse samples [14, 16–18]. In this paper, we pursue the purely extrinsic mechanism, which are classified as *side-jump* and *skew scattering*, which can be distinguished by characteristic dependence on the electric resistivity. The side-jump mechanism can be pictured in terms of incoming and outgoing trajectories of the electron upon scattering from an impurity that are displaced in a side-step (in a direction that depends on the spin polarization) but without associated directional deflection [19]. Recently this contribution to the anomalous Hall conductivity has been extracted directly from the electronic structure of a perfect crystal [20, 21]. Skew scattering relies on the spin dependence of the scattering angle of the electrons reflecting from a given impurity [22]. Recently *ab initio* calculations for the extrinsic AHE are carried out. A unified theory that takes account of both the intrinsic and extrinsic effects [23] found that the AHE is dominated by skew scattering in the clean (high conductivity) limit, where the Hall conductivity is linear to the longitudinal conductivity. The intrinsic contribution becomes dominant at intermediate impurity densities, where the Hall conductivity does not depend on resistivity. In dirty systems the AHE depends on conductivity according to a power law [24, 25]. A first-principles approach applicable to both pure and disordered systems leads to the conclusion that the skew-scattering term dominates the side-jump contribution in the dilute regime [27].

The planar Hall effect (PHE) is closely related with the dependence of the electric resistance on the magnetization direction or anisotropic magnetoresistance (AMR) since both are even functions of the magnetization direction [28–31]. A giant PHE has been observed in magnetic semiconductors [32], which is a convenient measure for the magnetization direction. The AMR/PHE is believed also originated from anisotropic scattering due to the SOC. Theories have been developed by taking into account a resistivity due to the *s-d* scattering [31, 33–35]. There are also semiclassical calculations for alloys [36] diluted magnetic semiconductors [37, 38] by the Boltzmann approach and for two dimensional electron gas with Rashba SOC by Kubo formalism [39].

Recently several observations and theories of the anomalous Nernst effect in various material/systems have been reported. Measurements of the anomalous Hall and Nernst effects were performed in metallic ferromagnets [25, 26], ferromagnetic semiconductors [40, 41], spinel ferromagnet [42], and non-local spin valves [43]. Seki *et al* [44] invoked an anomalous Nernst effect to explain observed Hall voltages in FePt/Au lateral heterostructures, although a spin Nernst effect in the gold contacts could cause similar effects. Recently the ANE has been demon-

strated in lateral spin valves and analyzed by a finite-element model (see below) [45]. Weiler *et al.* found recently an anomalous Nernst signal that was created by a local temperature gradient created by a scannable laser beam [46]. The Ettingshausen coefficient has been implied from measurements of Nernst, thermopower, and Hall experiments and Onsager's reciprocity relations [42]. The thermal analogues of the AMR and PHE, an anisotropic longitudinal thermopower and planar Nernst effect (PNE) have been demonstrated in dilute magnetic semiconductors [47] and metallic ferromagnet [34, 48, 49]. The PNE measured in ferromagnetic thin-film [48] together with measurements of the ANE, is a useful tool to extract the intrinsic (transverse) spin Seebeck effect [50, 51]. Systematic measurements of anomalous Hall/Nernst effect and planar Hall/Nernst effect for a general magnetization have been recently performed in FePt alloy [52]. We are not aware of an experimental observation of the anomalous Ettingshausen and/or Righi-Leduc effect in metals.

The ANE can be quantified in terms of the transverse (Hall) thermoelectric conductivity  $\alpha_{xy}$ , which is related to the spectral anomalous Hall conductivity  $\sigma_{xy}(\varepsilon)$  *via* the generalized Mott formula [53]

$$\alpha_{xy} = -\frac{1}{e} \int d\varepsilon \frac{\partial f(\varepsilon)}{\partial \mu} \sigma_{xy}(\varepsilon) \frac{\varepsilon - \mu}{kT}, \quad (2.1)$$

where  $-e$  is the electronic charge,  $T$  the temperature, and  $\mu$  the chemical potential. For a small temperature bias the Sommerfeld expansion of the Dirac distribution function  $f$  leads to "Mott's Law", according to which the Seebeck coefficient (thermopower) is proportional to the energy derivative of the electrical conductivity at the chemical potential. First-principles calculations for  $\alpha_{xy}$  based on a defect-free electronic structure [54] agree with the experiments in Ref. [42]. First principles calculations were also carried out for the scattering-independent (including intrinsic and side-jump) ANE in ferromagnetic metals and alloys [55]. Onoda *et al.* obtained thermoelectric coefficients including both intrinsic and extrinsic contributions from the anomalous Hall conductivity by applying Mott's Law and the generalized Wiedemann-Franz law  $\kappa_{ij} = \sigma_{ij} \mathcal{L}_0 T$ , where  $\mathcal{L}_0 = (\pi k_B)^2 / 3e^2$  is the Lorenz constant [23, 24]. An anomalous magnon thermal Hall effect has been predicted [56–58] that in metals should provide an additional contribution to the ANE. The anomalous and planar Righi-Leduc effects was analyzed phenomenologically in ferromagnets [59].

From the above literature survey we conclude that general theoretical analysis of thermal Hall phenomena in metals is still limited, although there are recent first principle calculations includes all thermal Hall effects in ferromagnetic alloys [60]. Here we report a pragmatic rather than first-principles approach that includes phenomenologically all (longitudinal and transverse, anomalous and planar) thermoelectric effects in ferromagnetic metal films. It is based on a semiclassical linear

response for a ferromagnetic metal with impurities that carry a significant SOC (or equivalently, directional magnetic disorder) that holds for arbitrary magnetization direction. We thus provide a theoretical model that includes the multitude of possible thermoelectric effects and the number of required independent parameters. Our method generalizes the Boltzmann analysis for the spin Hall effect in Ref. [61] by including a thermal driving force [62] and ferromagnetism [63]. We do engage into the importance of the intrinsic contribution due to Berry phase and other effects in the presence of the SOC in the host metal. The intrinsic/extrinsic problem should be answered by microscopic theory for the transport parameters as a function of doping and temperature. Since the contribution of anomalous Hall conductivity due to side-jump mechanism is scattering-independent [19–21, 55], an intrinsic contribution simply renormalizes the phenomenological side-jump parameter in our model.

This paper is organized as follows. In Sec. 2.2 we sketch the basic physics of linear response theory and Onsager reciprocity. In Sec. 2.3 we present the semi-classical theory based on a microscopic model of short-range impurity scattering and discuss the extrinsic mechanisms, including side-jump and skew scattering. Thermoelectric effects are summarized as a normal and a Hall response matrix with relevant parameters in Sec. 2.4. The last section summarizes the conclusions and provides an outlook.

## 2.2 LINEAR RESPONSE AND ONSAGER SYMMETRY

Thermoelectricity is about the coupling of heat and charge currents. A heat current  $\mathbf{Q}$  can drag charges and generate a thermopower voltage in open circuits or charge current  $\mathbf{J}$  in closed circuits. *Vice versa* a charge current may generate a heat current. In the small bias limit the thermoelectric response becomes linear and can be described by a response matrix between driving forces and currents

$$\begin{pmatrix} \mathbf{J} \\ \mathbf{Q} \end{pmatrix} = \sigma \begin{pmatrix} 1 & ST \\ \Pi & \kappa T/\sigma \end{pmatrix} \begin{pmatrix} \frac{1}{e} \nabla \mu \\ -\frac{1}{T} \nabla T \end{pmatrix}, \quad (2.2)$$

where currents are generated by the gradients of the electrochemical potential  $\mu$  and temperature  $T$ .  $\sigma$  is the electric conductivity,  $S$  is the Seebeck coefficient, and  $\kappa$  is the heat conductivity [64]. Time reversal symmetry of quantum mechanics is reflected by Onsager's reciprocity relations [65] that lead to Kelvin-Onsager relation between the Seebeck and Peltier coefficients  $\Pi = ST$ .

In the independent electron approximation thermoelectric phenomena in metals are generated by electron-hole asymmetry at the Fermi level. In the Sommerfeld approximation,

$$S = -e \mathcal{L}_0 T \frac{\partial}{\partial \varepsilon} \ln \sigma(\varepsilon) |_{\mu_0}, \quad (2.3)$$

where the electronic charge is  $-e$ , and  $\mu_0$  is the ground state chemical potential. In this limit the Wiedemann-Franz law

$$\kappa = \sigma \mathcal{L}_0 T \quad (2.4)$$

holds. All response matrix elements are functions of the state of the system, depending upon variables as composition, temperature. In the following we will be mainly interested by the thermoelectric response in bulk ferromagnetic films with magnetization  $\mathbf{M}$ .

The spin dependence of the thermoelectric properties in isotropic and monodomain metallic ferromagnets can be expressed in the two-current model of majority and minority spins as a  $12 \times 12$  matrix equation:

$$\begin{pmatrix} \mathbf{J} \\ \mathbf{J}_s \\ \mathbf{Q} \\ \mathbf{Q}_s \end{pmatrix} = \mathbf{G} \begin{pmatrix} \frac{1}{e} \nabla \mu \\ \frac{1}{e} \nabla \mu_s / 2 \\ -\frac{1}{T_0} \nabla T \\ -\frac{1}{T_0} \nabla T_s / 2 \end{pmatrix}, \quad (2.5)$$

where

$$\mathbf{J} = \mathbf{J}_\uparrow + \mathbf{J}_\downarrow, \quad (2.6)$$

$$\mathbf{J}_s = \mathbf{J}_\uparrow - \mathbf{J}_\downarrow, \quad (2.7)$$

$$\mathbf{Q} = \mathbf{Q}_\uparrow + \mathbf{Q}_\downarrow, \quad (2.8)$$

$$\mathbf{Q}_s = \mathbf{Q}_\uparrow - \mathbf{Q}_\downarrow. \quad (2.9)$$

are the charge, spin, particle-heat and spin-heat currents.  $\mu = (\mu_\uparrow + \mu_\downarrow)/2$  is the charge electrochemical potential,  $\mu_s = \mu_\uparrow - \mu_\downarrow$  is the difference between chemical potentials of the two spin species, *i.e.*, the spin accumulation,  $T = (T_\uparrow + T_\downarrow)/2$  is the average temperature, and  $T_s = T_\uparrow - T_\downarrow$  is the spin heat accumulation [8, 66]. In ferromagnetic bulk films at room temperature inter-spin and electron-phonon scattering are effective and  $T_\uparrow = T_\downarrow = T$ , which implies that the spin heat current  $\mathbf{Q}_s$ , though existing, drops out of the coupled equations. The matrix dimension is then reduced to  $9 \times 9$ .

The response matrix  $\mathbf{G}$  as a function of the magnetization direction can be written as

$$\mathbf{G}(\hat{\mathbf{M}}) = \mathbf{G}_0 \mathbf{1} + \mathbf{G}_1 \hat{\mathbf{M}} \times + \mathbf{G}_2 (\hat{\mathbf{M}} \hat{\mathbf{M}} \cdot - \mathbf{1}), \quad (2.10)$$

where  $\mathbf{G}_0$ ,  $\mathbf{G}_1$ , and  $\mathbf{G}_2$  are  $3 \times 3$  matrices correspond to the normal response without the SOC, the responses to the first and second order in SOC, respectively.  $\mathbf{1}$  is a three-dimension identity matrix which preserves the direction of driving forces,

while  $\hat{\mathbf{M}} \times$  and  $\hat{\mathbf{M}} \cdot$  denote the cross and dot products between the magnetization  $\mathbf{M}$  and the driving forces.

For a set of irreversible processes, Onsager's theorem states that the elements of the response matrix satisfies reciprocity, *i.e.*  $\mathbf{G}_{ij}(\hat{\mathbf{M}}) = \epsilon_{ij} \mathbf{G}_{ji}(-\hat{\mathbf{M}})$ , where the magnetization  $\hat{\mathbf{M}}$  breaks time reversal symmetry. In Eq. (4.8),  $\epsilon_{ij} = 1$  for the normal and second order SOC response, while  $\epsilon_{ij} = -1$  for the first order SOC response [38, 65]. For convenience, we assume an isotropic system. Without loss of generality, we take all external driving forces along the  $\hat{\mathbf{x}}$  direction:

$$\begin{pmatrix} \frac{1}{e} \nabla \mu \\ \frac{1}{e} \nabla \mu_s / 2 \\ -\frac{1}{T_0} \nabla T \end{pmatrix} = \hat{\mathbf{x}} \begin{pmatrix} \frac{1}{e} \partial_x \mu \\ \frac{1}{e} \partial_x \mu_s / 2 \\ -\frac{1}{T_0} \partial_x T \end{pmatrix}, \quad (2.11)$$

and consider the thin film longitudinal and Hall transport in the  $\hat{\mathbf{x}}\text{-}\hat{\mathbf{y}}$  plane. The linear response relation are then reduced to  $6 \times 6$ .

Arbitrary angles between current and magnetization can be treated by separating contributions from magnetizations either perpendicular to or in the plane of the film. When the magnetization is out-of-plane  $\hat{\mathbf{M}} = \hat{\mathbf{z}}$

$$\begin{pmatrix} \mathbf{J} \\ \mathbf{J}_s \\ \mathbf{Q} \end{pmatrix} = [\hat{\mathbf{x}}(\mathbf{G}_0 - \mathbf{G}_2) + \hat{\mathbf{y}}\mathbf{G}_1] \begin{pmatrix} \frac{1}{e} \partial_x \mu \\ \frac{1}{e} \partial_x \mu_s / 2 \\ -\frac{1}{T_0} \partial_x T \end{pmatrix}. \quad (2.12)$$

We see that now the normal response  $\mathbf{G}_0$  is corrected by  $\mathbf{G}_2$  along the longitudinal direction  $\hat{\mathbf{x}}$ , while the response to the first order of SOC,  $\mathbf{G}_1$ , contributes the AHE and its thermal analogues in the  $\hat{\mathbf{y}}$  direction.

When we let the magnetization rotate in the  $\hat{\mathbf{x}}\text{-}\hat{\mathbf{y}}$  plane, *i.e.*,  $\hat{\mathbf{M}} = \hat{\mathbf{x}} \cos \phi + \hat{\mathbf{y}} \sin \phi$  with  $\phi$  the angle between transport and magnetization directions, the in-plane current response reads

$$\begin{pmatrix} \mathbf{J} \\ \mathbf{J}_s \\ \mathbf{Q} \end{pmatrix} = \{\hat{\mathbf{x}}[(\mathbf{G}_0 - \mathbf{G}_2) + \mathbf{G}_2 \cos^2 \phi] + \hat{\mathbf{y}}\mathbf{G}_2 \cos \phi \sin \phi\} \begin{pmatrix} \frac{1}{e} \partial_x \mu \\ \frac{1}{e} \partial_x \mu_s / 2 \\ -\frac{1}{T_0} \partial_x T \end{pmatrix}. \quad (2.13)$$

We see that  $\mathbf{G}_2$  due to second order SOC contributes the AMR, PHE, and their thermal analogues when the magnetization is rotating in-plane.  $\mathbf{G}_1$  only contributes to current flow in the  $\hat{\mathbf{z}}$  direction, which is not relevant for our analysis here. However, the charge and/or spin accumulate at the edges along  $\hat{\mathbf{z}}$  due to  $\mathbf{G}_1$  may contribute relevantly in the limit of thin-films [68].

## 2.3 MODEL

We wish to formulate experimental observables in terms of parameters that are based on a generic microscopic model. We assume here that the host is a weakly disordered good metal. The SOC is significant only in short-range impurity scattering potentials, noting that very similar effects can be obtained by frozen directional magnetic disorder. We do not claim that this model contains all the physics, since there is ample evidence for SOC effects stemming from the band structure. Nevertheless, phenomenologically it is not so easy to distinguish intrinsic and extrinsic effects in transport studies on macroscopic samples [67]. The final parameters derived here should therefore be interpreted as effective ones that depend on the band structure and disorder in yet unspecified and temperature-dependent manner. We follow here Ref. [61], which is modified to include ferromagnetism and temperature effects [62, 63].

We discuss (a) an out-of-plane magnetization  $\hat{\mathbf{M}} = \hat{\mathbf{z}}$ , and (b) a rotating in-plane magnetization  $\hat{\mathbf{M}} = \hat{\mathbf{x}} \cos \phi + \hat{\mathbf{y}} \sin \phi$  separately. We consider a ferromagnet in which the exchange field is of the order of the Fermi energy, implying that electron flows with polarization not collinear with the magnetization direction  $\hat{\mathbf{M}}$  are absorbed immediately and exert a spin transfer torque on the magnetic texture. The spin polarizations of particle currents are then locked to  $\pm \hat{\mathbf{M}}$ . We consider here only sufficiently weak currents such that current-induced magnetization dynamics can be disregarded.

The Hamiltonian reads

$$H = H_0 + U(\mathbf{r}), \quad (2.14)$$

where  $H_0$  leads to the time-independent Schrödinger equation for electron states with spin  $\zeta = \pm 1$

$$H_0 |\mathbf{k}\zeta\rangle = \varepsilon_{k\zeta} |\mathbf{k}\zeta\rangle. \quad (2.15)$$

For a ferromagnetic metal in the Stoner model and spin quantization axis along the magnetization:

$$\varepsilon_{k\zeta} = \frac{\hbar^2 k^2}{2m_\zeta} + \zeta \Delta - \mu_0, \quad (2.16)$$

in which the band structure is parameterized by a spin-dependent effective mass  $m_\zeta$ , the ferromagnetic exchange splitting  $\zeta \Delta$  and the ground state chemical potential  $\mu_0$  is the energy zero.

The material is sprinkled with short-range impurities with scattering potential

$$U(\mathbf{r}) = V_{\text{imp}}(\mathbf{r}) + V_{\text{so}}, \quad (2.17)$$

where the short-range potential scatterers  $V_{\text{imp}}$  are distributed randomly over positions  $\mathbf{r}_i$  with concentration  $n_{\text{imp}}$  :

$$V_{\text{imp}}(\mathbf{r}) = \sum_i (1V_i + J\boldsymbol{\sigma} \cdot \mathbf{S}_i) \delta(\mathbf{r} - \mathbf{r}_i). \quad (2.18)$$

Here  $J\boldsymbol{\sigma} \cdot \mathbf{S}_i$  ( $V_i$ ) are spin (in)dependent short range scattering potentials at position  $\mathbf{r}_i$  where  $J$  is the exchange potential,  $\boldsymbol{\sigma}$  is the vector of the Pauli spin matrices, and  $\mathbf{S}_i$  the magnetic moment of the impurities labeled by subscript  $i$ . The SOC term  $V_{\text{so}} = \eta_{\text{so}}\boldsymbol{\sigma} \cdot [\nabla V_{\text{imp}}(\mathbf{r}) \times \frac{1}{i}\nabla]$  is characterized by the SOC constant  $\eta_{\text{so}} = \hbar^2 / (4m_0^2 c^2)$  in terms of the bare electron mass  $m_0$  and velocity of light  $c$ , but in condensed matter the parameter can be renormalized.

In the semiclassical two-current model,[69] the charge ( $\mathbf{J}_\zeta$ ) and heat currents ( $\dot{\mathbf{Q}}_\zeta$ ) in spin channel  $\zeta$  are a consequence of a non-equilibrium electronic distribution  $f_{\hat{\mathbf{k}}\zeta}(\varepsilon, \mathbf{r})$ , which is a function of wave vector direction  $\hat{\mathbf{k}}$  and spin index  $\zeta = \pm 1 \equiv (\uparrow, \downarrow)$ . The energy zero is again at  $\mu_0$ . Introducing the expectation value for the group velocity  $\langle \mathbf{v}_{\mathbf{k}\zeta} \rangle$ ,

$$\mathbf{J}_\zeta = -e \sum_{\mathbf{k}} \langle \mathbf{v}_{\mathbf{k}\zeta} \rangle f_{\hat{\mathbf{k}}\zeta}, \quad (2.19)$$

$$\dot{\mathbf{Q}}_\zeta = \sum_{\mathbf{k}} \varepsilon_{\mathbf{k}\zeta} \langle \mathbf{v}_{\mathbf{k}\zeta} \rangle f_{\hat{\mathbf{k}}\zeta}. \quad (2.20)$$

### 2.3.1 BOLTZMANN EQUATION WITHOUT SPIN-ORBIT INTERACTION

Let us first obtain, the currents Eqs. (2.19-2.20) as functions of voltage and temperature bias without SOC for reference. In this limit the distribution function is the solution of the Boltzmann equation, which in the steady state reads

$$\left( \mathbf{v}_{\mathbf{k}\zeta} \cdot \nabla_{\mathbf{r}} + \frac{\mathbf{F}_\zeta}{\hbar} \cdot \nabla_{\mathbf{k}} \right) f_{\hat{\mathbf{k}}\zeta} = \left( \frac{\partial f_{\hat{\mathbf{k}}\zeta}}{\partial t} \right)_{\text{scatt.}}. \quad (2.21)$$

The group velocity  $\mathbf{v}_{\mathbf{k}\zeta} = \nabla_{\mathbf{k}} \varepsilon_{\mathbf{k}\zeta}$  by Eq. (2.16), while  $\mathbf{F}_\zeta = e\nabla\phi - \zeta(\partial\Delta/\partial T)\nabla T$  originates from the gradient of the electric potential  $\phi$  and exchange splitting  $\Delta$ . Inelastic scattering has been assumed to be strong such that the isotropic part of the distribution function in momentum space is locally thermalized to the Fermi-Dirac form at temperature  $T(\mathbf{r})$  and spin-dependent chemical potential shift  $\mu_\zeta(\mathbf{r})$ :

$$f_\zeta^0(\varepsilon, \mathbf{r}) = \left[ \exp \frac{\varepsilon - \varepsilon_F - \mu_\zeta(\mathbf{r})}{k_B T(\mathbf{r})} + 1 \right]^{-1}. \quad (2.22)$$

The spin-conserving and spin-flip elastic impurity scatterings give rise to the collision terms on the right-hand side of Eq. (2.21), which are derived in Appendix 2.6.

To the lowest order approximation without the SOC scattering,

$$\left( \frac{\partial f_{\mathbf{k}\zeta}}{\partial t} \right)_{\text{scatt.}} = -\frac{g_{\mathbf{k}\zeta}^a}{\tau_{0,\zeta}} - \frac{f_{\zeta}^0 - f_{-\zeta}^0}{\tau_{\text{sf}0,\zeta}}, \quad (2.23)$$

where  $g_{\mathbf{k}\zeta}^a = f_{\mathbf{k}\zeta} - f_{\zeta}^0$  is the anisotropic part of distribution function and  $\tau_{0,\zeta}$  is the transport relaxation time

$$\tau_{0,\zeta}^{-1}(\varepsilon) \equiv \tau_{\text{sc}0,\zeta}^{-1}(\varepsilon) + \tau_{\text{sf}0,\zeta}^{-1}(\varepsilon) \quad (2.24)$$

which contains spin-conserving and spin-flip contributions

$$\tau_{\text{sc}0,\zeta}^{-1}(\varepsilon) = \frac{2\pi}{\hbar} n_{\text{imp}} N_{\zeta}(\varepsilon) \left( \overline{V^2} + J^2 \frac{\overline{S^2}}{3} \right), \quad (2.25)$$

$$\tau_{\text{sf}0,\zeta}^{-1}(\varepsilon) = \frac{2\pi}{\hbar} n_{\text{imp}} N_{-\zeta}(\varepsilon) J^2 \frac{2\overline{S^2}}{3}, \quad (2.26)$$

where  $\overline{X}$  denotes the configurational (ensemble) average over randomly distributed impurities  $\overline{X} = \mathcal{V}^{-N_{\text{imp}}} \int d\mathbf{r}_1 \cdots d\mathbf{r}_{N_{\text{imp}}} X(\mathbf{r}_1, \cdots, \mathbf{r}_{N_{\text{imp}}})$  with  $N_{\text{imp}}$  the total number of impurities,  $n_{\text{imp}} = N_{\text{imp}}/\mathcal{V}$  is the density of scatterers, and  $N_{\zeta}(\varepsilon) = \sum_{\mathbf{k}} \delta(\varepsilon_{\mathbf{k}\zeta} - \varepsilon)/\mathcal{V}$  is the spin-dependent electronic density of states per unit of volume. The spin-flip relaxation time here is caused by the disorder in the direction of the impurity magnetic moments and lumped together with the spin-flip scattering induced by the spin-orbit interaction discussed below. We can therefore disregard it here.

Linearizing the drift terms on the left-hand side of Eq. (2.21),

$$\mathbf{v}_{\mathbf{k}\zeta} \cdot \left( -\frac{\partial f^0}{\partial \varepsilon} \nabla \left( \bar{\mu}_{\zeta} + \frac{\varepsilon - \mu_0}{T_0} T \right) + \nabla g_{\mathbf{k}\zeta}^a \right) = -\frac{g_{\mathbf{k}\zeta}^a}{\tau_{\text{sc}0,\zeta}}, \quad (2.27)$$

where  $\bar{\mu}_{\zeta} \equiv \mu_{\zeta} - e\phi$  is the spin-dependent electrochemical potential. The anisotropic part of the distribution function now reads to lowest order:

$$g_{\mathbf{k}\zeta}^a(\varepsilon, \mathbf{r}) = \tau_{\text{sc}0,\zeta} \frac{\partial f^0(\varepsilon)}{\partial \varepsilon} \mathbf{v}_{\mathbf{k}\zeta} \cdot \left( \nabla \bar{\mu}_{\zeta}(\mathbf{r}) + \frac{\varepsilon - \mu_0}{T_0} \nabla T(\mathbf{r}) \right), \quad (2.28)$$

Substituting the velocity and distribution function into Eqs. (2.19-2.20) to obtain the thermoelectric response in spin-channel  $\zeta$ :

$$\begin{pmatrix} \mathbf{J}_{\zeta} \\ \dot{\mathbf{Q}}_{\zeta} \end{pmatrix} = \sigma_{\zeta} \begin{pmatrix} 1 & S_{\zeta} T \\ \Pi_{\zeta} & \kappa_{\zeta} T / \sigma_{\zeta} \end{pmatrix} \begin{pmatrix} \frac{1}{e} \nabla \bar{\mu}_{\zeta} \\ -\frac{1}{T} \nabla T \end{pmatrix}, \quad (2.29)$$

where we introduced the electric conductivity  $\sigma_\zeta(\varepsilon) = e^2 N_\zeta(\varepsilon) D_\zeta(\varepsilon)$  with spin-dependent density of states  $N_\zeta$  and diffusion constant  $D_\zeta = v_{k_\zeta}^2 \tau_{\text{sc}0,\zeta}/3$ , the Seebeck coefficient (thermopower)  $S_\zeta = -e \mathcal{L}_0 T \partial_\varepsilon \ln \sigma_\zeta|_{\mu_0}$ , the Peltier coefficient  $\Pi_\zeta = S_\zeta T$ , and the heat conductivity  $\kappa_\zeta = \sigma_\zeta \mathcal{L}_0 T$ . Note that we invoked the Sommerfeld approximation to simplify  $S_\zeta$ , but it can be calculated by the Mott formula in a general condition, e.g., in a system with temperature not so low [53].

$$\begin{aligned} \begin{pmatrix} \mathbf{J}_c^0 \\ \mathbf{J}_s^0 \\ \mathbf{Q}^0 \end{pmatrix} &= \sigma \begin{pmatrix} 1 & P & ST_0 \\ P & 1 & P'ST_0 \\ ST_0 & P'ST_0 & \mathcal{L}_0 T_0^2 \end{pmatrix} \begin{pmatrix} \frac{1}{e} \partial_x \mu_c \\ \frac{1}{e} \partial_x \mu_s / 2 \\ -\frac{1}{T_0} \partial_x T \end{pmatrix} \hat{\mathbf{x}} \\ &\equiv \hat{\mathbf{x}} \mathbf{G}_0 \begin{pmatrix} \frac{1}{e} \partial_x \mu_c \\ \frac{1}{e} \partial_x \mu_s / 2 \\ -\frac{1}{T_0} \partial_x T \end{pmatrix}, \end{aligned} \quad (2.30)$$

where we introduced the *normal* response matrix

$$\mathbf{G}_0 = \sigma \begin{pmatrix} 1 & P & ST_0 \\ P & 1 & P'ST_0 \\ ST_0 & P'ST_0 & \mathcal{L}_0 T_0^2 \end{pmatrix}. \quad (2.31)$$

Here  $\sigma = \sigma_\uparrow + \sigma_\downarrow$  is the electrical conductivity,  $S = -e \mathcal{L}_0 T_0 \partial_\varepsilon \log \sigma|_{\varepsilon_F}$  the thermopower,  $P \equiv (\sigma_\uparrow - \sigma_\downarrow) / (\sigma_\uparrow + \sigma_\downarrow)$  the polarization of the electric conductivity, and  $P' \equiv (\sigma'_\uparrow - \sigma'_\downarrow) / (\sigma'_\uparrow + \sigma'_\downarrow)$  the polarization of the derivative of the conductivity.  $|P| \leq 1$ , but  $P'$  can take any value in principle.

### 2.3.2 BOLTZMANN EQUATION WITH SPIN-ORBIT INTERACTION

The SOC has several effects on the transport properties. SOC enhances both the spin-conserved scattering and the scattering between the majority and minority spin channels that causes spin-flip scattering and magnetization dependence of the collision terms of the Boltzmann equation that cause the anisotropic magnetoresistance (AMR). Preferential scattering of up-spin (majority) electrons and down-spin (minority) electrons in opposite transverse directions results in an anomalous Hall current perpendicular to both the driving electric field and the magnetization directions. The spin-asymmetric scattering can be described by two mechanisms. First, the two trajectories are asymmetrically bent during scattering at an impurity, thereby affecting the anisotropic part of distribution function. This “skew scattering” can be taken into account by modifying the collision terms [61]. Secondly, there is an abrupt spin-dependent “side-jump” scattering that can be captured by the modification of the velocity operator by the SOC term in the Hamiltonian [70]. These effects will be separately discussed below.

### 2.3.3 COLLISION TERMS IN THE PRESENCE OF SOC

Including SOC-induced spin-conserved and spin-spin scatterings, the collision terms can still be written

$$\left(\frac{\partial f_{\mathbf{k}\zeta}}{\partial t}\right)_{\text{scatt.}} \approx -\frac{g_{\mathbf{k}\zeta}^a}{\tau_{\zeta}} - \frac{f_{\zeta}^0 - f_{-\zeta}^0}{\tau_{\text{sf},\zeta}}, \quad (2.32)$$

but  $\tau_{\zeta}^{-1} = \tau_{\text{sc}0,\zeta}^{-1} + \tau_{\text{sc}1,\zeta}^{-1} + \tau_{\text{sf}0,\zeta}^{-1} + \tau_{\text{sf}1,\zeta}^{-1}$  and  $\tau_{\text{sf},\zeta}^{-1} = \tau_{\text{sf}0,\zeta}^{-1} + \tau_{\text{sf}1,\zeta}^{-1}$  with additional momentum and magnetization direction-dependent relaxation rates which lead to the AMR/PHE and its thermoelectric analogues (see below)

$$\tau_{\text{sc}1,\zeta}^{-1}(\varepsilon, \hat{\mathbf{k}}) = \frac{2\pi}{\hbar} n_{\text{imp}} N_{\zeta}(\varepsilon) \left( \overline{V^2} + \frac{1}{3} J^2 S^2 \right) (\tilde{\eta}_{\text{so},\zeta}(\varepsilon))^2 \frac{|\hat{\mathbf{M}} \times \hat{\mathbf{k}}|^2}{3}, \quad (2.33)$$

$$\tau_{\text{sf}1,\zeta}^{-1}(\varepsilon, \hat{\mathbf{k}}) = \frac{2\pi}{\hbar} n_{\text{imp}} N_{-\zeta}(\varepsilon) \left( \overline{V^2} + \frac{2}{3} J^2 S^2 \right) (\tilde{\eta}_{\text{so}}^{\text{sf}}(\varepsilon))^2 \frac{2 - |\hat{\mathbf{M}} \times \hat{\mathbf{k}}|^2}{3}, \quad (2.34)$$

where

$$(\tilde{\eta}_{\text{so},\zeta}(\varepsilon))^2 \equiv \left[ \eta_{\text{so}} \frac{2m_{\zeta}(\varepsilon - \zeta\Delta)}{\hbar^2} \right]^2, \quad (2.35)$$

$$(\tilde{\eta}_{\text{so}}^{\text{sf}}(\varepsilon))^2 \equiv \eta_{\text{so}}^2 \left[ \frac{2m_{\zeta}(\varepsilon - \zeta\Delta)}{\hbar^2} \right] \left[ \frac{2m_{-\zeta}(\varepsilon + \zeta\Delta)}{\hbar^2} \right], \quad (2.36)$$

are the renormalized SOC parameters. The total scattering rate is the sum of the impurity scattering and SOC scattering rates (Matthiessen's rule [64]).

In order to capture the distribution functions in the presence of skew scattering we have to include higher order contributions in the scattering potential to the collision terms (see the Appendix)

$$\left(\frac{\partial f_{\mathbf{k}\zeta}}{\partial t}\right)_{\text{scatt.}} \approx -\frac{g_{\mathbf{k}\zeta}^a}{\tau_{\zeta}} - \frac{f_{\zeta}^0 - f_{-\zeta}^0}{\tau_{\text{sf},\zeta}} + \sum_{\mathbf{k}'} P_{\mathbf{k}\mathbf{k}'}^{\zeta\zeta'(2)} g_{\mathbf{k}'\zeta'}^a,$$

where

$$P_{\mathbf{k}\mathbf{k}'}^{\zeta\zeta'(2)} = \frac{4\pi}{\hbar} \eta_{\text{so}} [(\mathbf{k}' \times \mathbf{k}) \cdot \hat{\mathbf{M}}] n_{\text{imp}} N_{\zeta}(\varepsilon) \overline{V^3} \delta_{\zeta\zeta'} \delta(\varepsilon_{k\zeta} - \varepsilon_{k'\zeta'}). \quad (2.37)$$

The Boltzmann equation then becomes

$$\begin{aligned} & \mathbf{v}_{\mathbf{k}\zeta} \cdot \left( -\frac{\partial f^0}{\partial \varepsilon} \nabla \left( \bar{\mu}_{\zeta} + \frac{\varepsilon - \mu_0}{T_0} T \right) + \nabla g_{\mathbf{k}\zeta}^a \right) \\ &= -g_{\mathbf{k}\zeta}^a \left( \frac{1}{\tau_{\zeta}^{(i)}} + \frac{(\hat{\mathbf{M}} \cdot \hat{\mathbf{k}})^2}{\tau_{\zeta}^{(a)}} \right) - (f_{\zeta}^0 - f_{-\zeta}^0) \left( \frac{1}{\tau_{\text{sf},\zeta}^{(i)}} + \frac{(\hat{\mathbf{M}} \cdot \hat{\mathbf{k}})^2}{\tau_{\text{sf},\zeta}^{(a)}} \right) + \sum_{\mathbf{k}'} P_{\mathbf{k}\mathbf{k}'}^{\zeta\zeta(2)} g_{\mathbf{k}'\zeta'}^a, \end{aligned} \quad (2.38)$$

where we have decomposed  $\tau_\zeta^{-1}$  (and analogously  $\tau_{sf,\zeta}^{-1}$ ) into isotropic ( $i$ ) and anisotropic ( $a$ ) parts:

$$\frac{1}{\tau_\zeta^{(a)}} = \frac{2\pi}{\hbar} n_{\text{imp}} \left[ -N_\zeta \left( \overline{V^2} + \frac{1}{3} J^2 \overline{S^2} \right) (\tilde{\eta}_{so,\zeta})^2 + N_{-\zeta} \left( \overline{V^2} + \frac{2}{3} J^2 \overline{S^2} \right) (\tilde{\eta}_{so}^{sf})^2 \right], \quad (2.39)$$

$$\frac{1}{\tau_\zeta^{(i)}} = \frac{1}{\tau_\zeta} - \frac{1}{\tau_\zeta^{(a)}} \frac{(\hat{\mathbf{M}} \cdot \hat{\mathbf{k}})^2}{3}. \quad (2.40)$$

With the ansatz for transport in the film plane

$$\mathbf{g}_{\mathbf{k}\zeta}^a = \mathbf{g}_{k\zeta}^{(x)} \mathbf{k}_x + \mathbf{g}_{k\zeta}^{(y)} \mathbf{k}_y, \quad (2.41)$$

using  $\int \mathbf{k}_x \mathbf{k}_y d\Omega_{\hat{\mathbf{k}}} = 0$  and  $\hat{\mathbf{M}} = (m_x, m_y, m_z)$ ,

$$\begin{aligned} -v_{k\zeta} \frac{\partial f^0}{\partial \varepsilon} \partial_x \left( \bar{\mu}_\zeta + \frac{\varepsilon - \mu_0}{T_0} T \right) = & - \left( \frac{1}{\tau_\zeta^{(i)}} + \frac{3m_x^2 + m_y^2 + m_z^2}{5\tau_\zeta^{(a)}} \right) \mathbf{g}_{k\zeta}^{(x)} - \frac{2m_x m_y}{5\tau_\zeta^{(a)}} \mathbf{g}_{k\zeta}^{(y)} \\ & + \frac{3}{4\pi} \int d\Omega_{\hat{\mathbf{k}}} \left( \sum_{\mathbf{k}'} P_{\hat{\mathbf{k}}\hat{\mathbf{k}}'}^{\zeta\zeta(2)} \mathbf{g}_{\mathbf{k}'\zeta}^a \mathbf{k}_x \right), \end{aligned} \quad (2.42)$$

$$\begin{aligned} 0 = & - \frac{2m_x m_y}{5\tau_\zeta^{(a)}} \mathbf{g}_{k\zeta}^{(x)} - \left( \frac{1}{\tau_\zeta^{(i)}} + \frac{m_x^2 + 3m_y^2 + m_z^2}{5\tau_\zeta^{(a)}} \right) \mathbf{g}_{k\zeta}^{(y)} \\ & + \frac{3}{4\pi} \int d\Omega_{\hat{\mathbf{k}}} \left( \sum_{\mathbf{k}'} P_{\hat{\mathbf{k}}\hat{\mathbf{k}}'}^{\zeta\zeta(2)} \mathbf{g}_{\mathbf{k}'\zeta}^a \mathbf{k}_y \right). \end{aligned} \quad (2.43)$$

We can obtain the anisotropic distribution from Eqs. (2.42-2.43) for any magnetization direction. Below we separately derive the anisotropic distribution for magnetization out-of-plane ( $\hat{\mathbf{M}} = \hat{\mathbf{z}}$ ) and in-plane ( $\hat{\mathbf{M}} = \hat{\mathbf{x}} \cos \phi + \hat{\mathbf{y}} \sin \phi$ ).

For  $\hat{\mathbf{M}} = \hat{\mathbf{z}}$ :

$$-v_{k\zeta} \frac{\partial f^0}{\partial \varepsilon} \partial_x \left( \bar{\mu}_\zeta + \frac{\varepsilon - \mu_0}{T_0} T \right) = - \left( \frac{1}{\tau_\zeta^{(i)}} + \frac{1}{5\tau_\zeta^{(a)}} \right) \mathbf{g}_{k\zeta}^{(x)} + \frac{3}{4\pi} \int d\Omega_{\hat{\mathbf{k}}} \left( \sum_{\mathbf{k}'} P_{\hat{\mathbf{k}}\hat{\mathbf{k}}'}^{\zeta\zeta(2)} \mathbf{g}_{\mathbf{k}'\zeta}^a \mathbf{k}_x \right), \quad (2.44)$$

$$0 = - \left( \frac{1}{\tau_\zeta^{(i)}} + \frac{1}{5\tau_\zeta^{(a)}} \right) \mathbf{g}_{k\zeta}^{(y)} + \frac{3}{4\pi} \int d\Omega_{\hat{\mathbf{k}}} \left( \sum_{\mathbf{k}'} P_{\hat{\mathbf{k}}\hat{\mathbf{k}}'}^{\zeta\zeta(2)} \mathbf{g}_{\mathbf{k}'\zeta}^a \mathbf{k}_y \right). \quad (2.45)$$

Using

$$\begin{aligned}
\sum_{\mathbf{k}'} P_{\mathbf{k}\mathbf{k}'}^{\zeta\zeta(2)} g_{\mathbf{k}'\zeta}^a &= \frac{4\pi}{\hbar} \eta_{so} n_{\text{imp}} N_{\zeta}(\varepsilon) \overline{V_{\zeta}^3} \sum_{\mathbf{k}'} [(\mathbf{k}' \times \mathbf{k}) \cdot \boldsymbol{\sigma}_{\zeta\zeta}] \delta(\varepsilon_{k\zeta} - \varepsilon_{k'\zeta'}) \sum_{\alpha=x,y,z} g_{k\zeta}^{(\alpha)} \mathbf{k}'_{\alpha} \\
&= \frac{4\pi}{\hbar} \eta_{so} n_{\text{imp}} N_{\zeta}(\varepsilon) \overline{V_{\zeta}^3} (\mathbf{k} \times \boldsymbol{\sigma}_{\zeta\zeta}) \cdot \sum_{\alpha=x,y,z} g_{k\zeta}^{(\alpha)} \sum_{\mathbf{k}'} \mathbf{k}' \mathbf{k}'_{\alpha} \delta(\varepsilon_{k\zeta} - \varepsilon_{k'\zeta'}) \\
&= \zeta \frac{4\pi}{3\hbar} \eta_{so} n_{\text{imp}} N_{\zeta}^2(\varepsilon) \overline{V_{\zeta}^3} k (\mathbf{k} \times \hat{\mathbf{z}}) \cdot \sum_{\alpha=x,y} g_{k\zeta}^{(\alpha)} \hat{\alpha} \\
&= \zeta \frac{4\pi}{3\hbar} \tilde{\eta}_{so,\zeta} n_{\text{imp}} N_{\zeta}^2(\varepsilon) \overline{V_{\zeta}^3} \sum_{\alpha=x,y,z} g_{k\zeta}^{(\alpha)} (\mathbf{k}_{\beta} m_{\gamma} - \mathbf{k}_{\gamma} m_{\beta}), \tag{2.46}
\end{aligned}$$

and defining a hybrid relaxation time

$$\tilde{\tau}_{\zeta} = \left( \frac{1}{\tau_{\zeta}^{(i)}} + \frac{1}{5\tau_{\zeta}^{(a)}} \right)^{-1}, \tag{2.47}$$

the solution is

$$g_{k\zeta}^{(x)} = \tilde{\tau}_{\zeta} v_{k\zeta} \frac{\partial f^0}{\partial \varepsilon} \partial_x \left( \bar{\mu}_{\zeta} + \frac{\varepsilon - \mu_0}{T_0} T \right), \tag{2.48}$$

$$g_{k\zeta}^{(y)} = \zeta \frac{4\pi}{3\hbar} \tilde{\tau}_{\zeta} \tilde{\eta}_{so,\zeta} n_{\text{imp}} N_{\zeta}^2 \overline{V_{\zeta}^3} g_{k\zeta}^{(x)} \equiv \alpha_{\text{H},\zeta}^{\text{SS}} g_{k\zeta}^{(x)}, \tag{2.49}$$

where

$$\alpha_{\text{H},\zeta}^{\text{SS}}(\varepsilon) = \zeta \frac{4\pi^2}{3\hbar} \tilde{\tau}_{\zeta} \tilde{\eta}_{so,\zeta} n_{\text{imp}} N_{\zeta}^2 \overline{V_{\zeta}^3} \tag{2.50}$$

parameterizes the skew scattering contribution to the anomalous Hall effect [61].

When the magnetization is in-plane

$$-v_{k\zeta} \frac{\partial f^0}{\partial \varepsilon} \partial_x \left( \bar{\mu}_{\zeta} + \frac{\varepsilon - \mu_0}{T_0} T \right) = - \left( \frac{1}{\tau_{\zeta}^{(i)}} + \frac{1 + 2 \cos^2 \phi}{5\tau_{\zeta}^{(a)}} \right) g_{k\zeta}^{(x)} - \frac{2 \cos \phi \sin \phi}{5\tau_{\zeta}^{(a)}} g_{k\zeta}^{(y)}, \tag{2.51}$$

$$0 = - \frac{2 \cos \phi \sin \phi}{5\tau_{\zeta}^{(a)}} g_{k\zeta}^{(x)} - \left( \frac{1}{\tau_{\zeta}^{(i)}} + \frac{1 + 2 \sin^2 \phi}{5\tau_{\zeta}^{(a)}} \right) g_{k\zeta}^{(y)}, \tag{2.52}$$

which leads to the components

$$g_{k\zeta}^{(x)} \approx \left[ 1 - \frac{2\tau_{\zeta}^{(i)}}{5\tau_{\zeta}^{(a)}} \cos^2 \phi \right] \tilde{\tau}_{\zeta} v_{k\zeta} \frac{\partial f^0}{\partial \varepsilon} \partial_x \left( \bar{\mu}_{\zeta} + \frac{\varepsilon - \mu_0}{T_0} T \right), \tag{2.53}$$

$$g_{k\zeta}^{(y)} \approx \left[ -\frac{2\tau_{\zeta}^{(i)}}{5\tau_{\zeta}^{(a)}} \cos \phi \sin \phi \right] \tilde{\tau}_{\zeta} v_{k\zeta} \frac{\partial f^0}{\partial \varepsilon} \partial_x \left( \bar{\mu}_{\zeta} + \frac{\varepsilon - \mu_0}{T_0} T \right). \tag{2.54}$$

Eqs. (2.53-2.54) lead to the AMR, the PHE, and their thermal analogues, as verified below in Sec. 2.4.2.

### 2.3.4 MODULATION OF VELOCITY BY SIDE-JUMP SCATTERING

The canonical electron velocity operator  $\mathbf{v}$  is defined by the Heisenberg relation

$$\mathbf{v} = \dot{\mathbf{r}} = \frac{1}{i\hbar} [\mathbf{r}, H], \quad (2.55)$$

where  $\mathbf{r}$  is the position operator and  $H$  is the single electron Hamiltonian described above. Since the position operator does not commute with the spin orbit interaction,

$$\mathbf{v} = -i \frac{\hbar}{m} \nabla + \boldsymbol{\sigma} \times \frac{\eta_{so}}{\hbar} \sum_i (\mathbf{1} V_i + J \boldsymbol{\sigma} \cdot \mathbf{S}_i) \vec{\nabla} \delta(\mathbf{r} - \mathbf{r}_i) \equiv \mathbf{v}_0 + \mathbf{v}_{so}. \quad (2.56)$$

The expectation value of the electron velocity for a state  $\mathbf{k}\zeta$  in the first order Born approximation, which reads

$$\begin{aligned} |\mathbf{k}\zeta\rangle^{(1)} &\rightarrow |\mathbf{k}\zeta\rangle + \frac{1}{\mathcal{V}} \sum_{\mathbf{k}'} |\mathbf{k}'\zeta\rangle \frac{\sum_i (V_i + \boldsymbol{\sigma}_{\zeta\zeta} \cdot \mathbf{S}_i) e^{i(\mathbf{k}-\mathbf{k}') \cdot \mathbf{r}_i}}{\epsilon_{k\zeta} - \epsilon_{k'\zeta} + i\delta} \\ &+ \frac{1}{\mathcal{V}} \sum_{\mathbf{k}'} |\mathbf{k}'-\zeta\rangle \frac{\sum_i (\boldsymbol{\sigma}_{\zeta-\zeta} \cdot \mathbf{S}_i) e^{i(\mathbf{k}-\mathbf{k}') \cdot \mathbf{r}_i}}{\epsilon_{k\zeta} - \epsilon_{k'-\zeta} + i\delta} \\ &\approx |\mathbf{k}\zeta\rangle + \frac{1}{\mathcal{V}} \sum_{\mathbf{k}'} |\mathbf{k}'\zeta'\rangle \frac{\sum_i (V_i + \boldsymbol{\sigma}_{\zeta\zeta'} \cdot \mathbf{S}_i) e^{i(\mathbf{k}-\mathbf{k}') \cdot \mathbf{r}_i}}{\epsilon_{k\zeta} - \epsilon_{k'\zeta'} + i\delta} \end{aligned} \quad (2.57)$$

where we assumed the spin-flip due to the magnetic disorders is weak such that can be disregarded.

We know that  ${}^{(1)}\langle \mathbf{k}\zeta | \mathbf{v}_0 | \mathbf{k}\zeta \rangle^{(1)} \approx \hbar \mathbf{k} / m_\zeta$  is the normal velocity, while the anoma-

lous velocity comes from  $^{(1)}\langle \mathbf{k}_\zeta | \mathbf{v}_{so} | \mathbf{k}'_\zeta \rangle^{(1)}$ . The matrix can be calculated as

$$\begin{aligned}
& \langle \mathbf{k}_\zeta | \mathbf{v}_{so} | \mathbf{k}'_\zeta \rangle \\
&= \langle \mathbf{k}_\zeta | \boldsymbol{\sigma} \times \frac{\eta_{so}}{\hbar} \sum_i (\mathbf{1}V_i + J\boldsymbol{\sigma} \cdot \mathbf{S}_i) \vec{\delta}'(\mathbf{r} - \mathbf{r}_i) | \mathbf{k}'_\zeta \rangle \\
&= \frac{\eta_{so}}{\mathcal{V}\hbar} \left[ \boldsymbol{\sigma} \times \sum_i (\mathbf{1}V_i + J\boldsymbol{\sigma} \cdot \mathbf{S}_i) \right]_{\zeta\zeta} \int d\mathbf{r} \left[ \vec{\delta}'(\mathbf{r} - \mathbf{r}_i) e^{-i(\mathbf{k}-\mathbf{k}') \cdot \mathbf{r}} \right] \\
&= \frac{\eta_{so}}{\mathcal{V}\hbar} \left[ \boldsymbol{\sigma} \times \sum_i (\mathbf{1}V_i + J\boldsymbol{\sigma} \cdot \mathbf{S}_i) \right]_{\zeta\zeta} \left[ \delta(\mathbf{r} - \mathbf{r}_i) e^{-i(\mathbf{k}-\mathbf{k}') \cdot \mathbf{r}} \Big|_{-\infty}^{\infty} - \int d\mathbf{r} \delta(\mathbf{r} - \mathbf{r}_i) \nabla e^{-i(\mathbf{k}-\mathbf{k}') \cdot \mathbf{r}} \right] \\
&= \frac{\eta_{so}}{\mathcal{V}\hbar} \left[ \boldsymbol{\sigma} \times \sum_i (\mathbf{1}V_i + J\boldsymbol{\sigma} \cdot \mathbf{S}_i) \right]_{\zeta\zeta} \left[ -\nabla e^{-i(\mathbf{k}-\mathbf{k}') \cdot \vec{r}} \Big|_{\mathbf{r}=\mathbf{r}_i} \right] \\
&= i \frac{\eta_{so}}{\mathcal{V}\hbar} \left[ \boldsymbol{\sigma} \times \sum_i (\mathbf{1}V_i + J\boldsymbol{\sigma} \cdot \mathbf{S}_i) \right]_{\zeta\zeta} (\mathbf{k} - \mathbf{k}') e^{-i(\mathbf{k}-\mathbf{k}') \cdot \mathbf{r}_i}. \tag{2.58}
\end{aligned}$$

Thus the anomalous term by the spin-orbit interaction in the impurity scattering potentials in the expectation value reads

$$\begin{aligned}
\omega_{\mathbf{k}\zeta} &\equiv \overline{^{(1)}\langle \mathbf{k}_\zeta | \mathbf{v}_{so} | \mathbf{k}_\zeta \rangle^{(1)}} \\
&\approx \frac{2}{\mathcal{V}} \text{Re} \sum_{\mathbf{k}'} \frac{\langle \zeta \mathbf{k} | \mathbf{v}_{so} | \mathbf{k}'_\zeta \rangle \sum_i (V_i + \boldsymbol{\sigma}_{\zeta\zeta} \cdot \mathbf{S}_i) e^{i(\mathbf{k}-\mathbf{k}') \cdot \mathbf{r}_i}}{\varepsilon_{\mathbf{k}\zeta} - \varepsilon_{\mathbf{k}'\zeta} + i\delta} \\
&= \frac{2\pi\eta_{so}}{\hbar\mathcal{V}^2} \sum_{\mathbf{k}'} [\boldsymbol{\sigma}_{\zeta\zeta} \times (\mathbf{k} - \mathbf{k}')] \overline{\sum_j (V_j + \boldsymbol{\sigma}_{\zeta\zeta} \cdot \mathbf{S}_j) e^{-i(\mathbf{k}-\mathbf{k}') \cdot \mathbf{r}_j} \sum_i (V_i + \boldsymbol{\sigma}_{\zeta\zeta} \cdot \mathbf{S}_i) e^{i(\mathbf{k}-\mathbf{k}') \cdot \mathbf{r}_i} \delta(\varepsilon_{\mathbf{k}\zeta} - \varepsilon_{\mathbf{k}'\zeta})} \\
&\approx \frac{\eta_{so}m_\zeta}{\hbar\tau_{sc0,\zeta}} \left( \boldsymbol{\sigma}_{\zeta\zeta} \times \frac{\hbar\mathbf{k}}{m_\zeta} \right) \equiv \alpha_{H,\zeta}^{\text{SJ}}(\varepsilon) \left( \boldsymbol{\sigma}_{\zeta\zeta} \times \frac{\hbar\mathbf{k}}{m_\zeta} \right), \tag{2.59}
\end{aligned}$$

where we introduced the Hall angle due to side-jump reads

$$\alpha_{H,\zeta}^{\text{SJ}}(\varepsilon) = \frac{\eta_{so}m_\zeta}{\hbar\tau_{sc0,\zeta}}, \tag{2.60}$$

and  $\tau_{sc0,\zeta}$  is the spin-conserved scattering time without the SOC.  $\omega_{\mathbf{k}\zeta}$  is normal to both the group velocity  $\hbar\mathbf{k}/m_\zeta$  and the polarization  $\boldsymbol{\sigma}_{\zeta\zeta} = \zeta\mathbf{M}$ . Thus only the  $z$ -component of  $\mathbf{M}$  contributes when transport in the film ( $x$ - $y$  plane) is considered, so it does not contribute anything when the magnetization is in-plane, i.e., it does not contribute on the AMR/PHE effects.  $\alpha_{H,\zeta}^{\text{SJ}}$  scales is linear to  $\eta_{so}$  and the inverse of  $\tau_{sc0,\zeta}$ . Each impurity contributes a small "side-jump" contribution that adds up to the total Hall current normal to the applied electric field and magnetization direction.

## 2.4 THERMOELECTRIC EFFECTS

In this section, we derive the currents and response matrices for the in-plane magnetization ( $\hat{\mathbf{M}} = \hat{\mathbf{z}}$ ) and the out-of-plane magnetization ( $\hat{\mathbf{M}} = \hat{\mathbf{x}} \cos \phi + \hat{\mathbf{y}} \sin \phi$ ), respectively.

### 2.4.1 AHE AND ITS THERMAL ANALOGUES

When the magnetization is out-of-plane, we can use the results from Sec. 2.3.3 and Sec. 2.3.4. We take the velocity Eq. (2.59) and the distribution functions Eqs. (2.48-2.49) into Eqs. (2.19-2.20) to calculate  $\mathbf{j}_c$  and  $\dot{\mathbf{Q}}_c$ , which are then decomposed to normal, side-jump, and skew scattering contributions.

$$\mathbf{j}_c \approx -e \sum_{\mathbf{k}} (\mathbf{v}_{\mathbf{k}c} + \boldsymbol{\omega}_{\mathbf{k}c}) \left( g_{k_c}^{(x)} \mathbf{k}_x + g_{k_c}^{(y)} \mathbf{k}_y \right) \approx \mathbf{j}_c^0 + \mathbf{j}_c^{\text{SJ}} + \mathbf{j}_c^{\text{SS}}, \quad (2.61)$$

$$\dot{\mathbf{Q}}_c \approx \sum_{\mathbf{k}} (\varepsilon - \varepsilon_F) (\mathbf{v}_{\mathbf{k}c} + \boldsymbol{\omega}_{\mathbf{k}c}) \left( g_{k_c}^{(x)} \mathbf{k}_x + g_{k_c}^{(y)} \mathbf{k}_y \right) \approx \dot{\mathbf{Q}}_c^0 + \dot{\mathbf{Q}}_c^{\text{SJ}} + \dot{\mathbf{Q}}_c^{\text{SS}}, \quad (2.62)$$

where

$$\mathbf{j}_c^0 \equiv -e \sum_{\mathbf{k}} \mathbf{v}_{\mathbf{k}c} g_{k_c}^{(x)} \mathbf{k}_x = \hat{\mathbf{x}} \frac{\tilde{\sigma}_c}{e} \partial_x (\bar{\mu}_c - e S_c T) \quad (2.63)$$

$$\dot{\mathbf{Q}}_c^0 \equiv \sum_{\mathbf{k}} (\varepsilon - \varepsilon_F) \mathbf{v}_{\mathbf{k}c} g_{k_c}^{(x)} \mathbf{k}_x = \hat{\mathbf{x}} \frac{\tilde{\sigma}_c}{e} T_0 \partial_x (\tilde{S}_c \mu_c - e \mathcal{L}_0 T), \quad (2.64)$$

are the ‘‘normal’’ electric and heat currents as introduced in Eq. (2.29) and only the electric conductivity  $\tilde{\sigma}_c = e^2 N_c v_c^2 \tilde{\tau}_c / 3$  and the Seebeck coefficient  $\tilde{S}_c = -e \mathcal{L}_0 T \partial_\varepsilon \ln \tilde{\sigma}_c |_{\mu_0}$  are slightly modified by the SOC.

$$\mathbf{j}_c^{\text{SJ}} \equiv -e \sum_{\mathbf{k}} \boldsymbol{\omega}_{\mathbf{k}c} g_{k_c}^{(x)} \mathbf{k}_x = \zeta \hat{\mathbf{y}} e^{-1} \sigma_{\text{H},c}^{\text{SJ}} \partial_x (\bar{\mu}_c - e S_{\text{H},c}^{\text{SJ}} T) \quad (2.65)$$

$$\dot{\mathbf{Q}}_c^{\text{SJ}} \equiv \sum_{\mathbf{k}} (\varepsilon - \varepsilon_F) \boldsymbol{\omega}_{\mathbf{k}c} g_{k_c}^{(x)} \mathbf{k}_x = \zeta \hat{\mathbf{y}} e^{-1} \sigma_{\text{H},c}^{\text{SJ}} T_0 \partial_x (S_{\text{H},c}^{\text{SJ}} \mu_c - e \mathcal{L}_0 T) \quad (2.66)$$

$$\mathbf{j}_c^{\text{SS}} \equiv -e \sum_{\mathbf{k}} \mathbf{v}_{\mathbf{k}c} g_{k_c}^{(y)} \mathbf{k}_y = \zeta \hat{\mathbf{y}} e^{-1} \sigma_{\text{H},c}^{\text{SS}} \partial_x (\bar{\mu}_c - e S_{\text{H},c}^{\text{SS}} T) \quad (2.67)$$

$$\dot{\mathbf{Q}}_c^{\text{SS}} \equiv \sum_{\mathbf{k}} (\varepsilon - \varepsilon_F) \mathbf{v}_{\mathbf{k}c} g_{k_c}^{(y)} \mathbf{k}_y = \zeta \hat{\mathbf{y}} e^{-1} \sigma_{\text{H},c}^{\text{SS}} T_0 \partial_x (S_{\text{H},c}^{\text{SS}} \mu_c - e \mathcal{L}_0 T). \quad (2.68)$$

are the ‘‘anomalous Hall’’ electric and heat currents induced by the side-jump (SJ) and skew scattering (SS), respectively. The required parameters are  $\sigma_{\text{H},c}^{\text{SJ(SS)}}(\varepsilon) \equiv \alpha_{\text{H},c}^{\text{SJ(SS)}}(\varepsilon) \tilde{\sigma}_c(\varepsilon)$ ,  $S_{\text{H},c}^{\text{SJ(SS)}} \equiv -e \mathcal{L}_0 T_0 \left( \partial_\varepsilon \log \sigma_{\text{H},c}^{\text{SJ(SS)}} |_{\varepsilon_F} \right)$ . The fundamental functions that

govern the anomalous Hall response are therefore the spectral functions  $\bar{\sigma}_\zeta(\varepsilon)$ ,  $\alpha_{\text{H},\zeta}^{\text{SJ}}(\varepsilon)$ , and  $\alpha_{\text{H},\zeta}^{\text{SS}}(\varepsilon)$ .

Combining the contributions of SJ and SS to the electric and heat Hall currents in spin channel  $\zeta$

$$\mathbf{j}_\zeta^{\text{H}} = \mathbf{j}_\zeta^{\text{SJ}} + \mathbf{j}_\zeta^{\text{SS}} = \zeta \hat{y} e^{-1} \sigma_{\text{H},\zeta} \partial_x (\bar{\mu}_\zeta - e S_{\text{H},\zeta} T) \quad (2.69)$$

$$\dot{\mathbf{Q}}_\zeta^{\text{H}} = \dot{\mathbf{Q}}_\zeta^{\text{SJ}} + \dot{\mathbf{Q}}_\zeta^{\text{SS}} = \zeta \hat{y} e^{-1} \sigma_{\text{H},\zeta} T_0 \partial_x (S_{\text{H},\zeta} \mu_\zeta - \mathcal{L}_0 T), \quad (2.70)$$

where the anomalous Hall conductivity and thermopower are defined as

$$\sigma_{\text{H},\zeta} = \sigma_{\text{H},\zeta}^{\text{SJ}} + \sigma_{\text{H},\zeta}^{\text{SS}}, \quad (2.71)$$

$$S_{\text{H},\zeta} = -e \mathcal{L}_0 T_0 (\partial_\varepsilon \log \sigma_{\text{H},\zeta} |_{\varepsilon_F}). \quad (2.72)$$

According to Eqs. (2.6-2.9), we have

$$\begin{pmatrix} \mathbf{J}_c \\ \mathbf{J}_s \\ \dot{\mathbf{Q}}_c \end{pmatrix} = (\hat{\mathbf{x}} \mathbf{G}_0 + \hat{\mathbf{y}} \mathbf{G}_1) \begin{pmatrix} \frac{1}{e} \partial_x \mu_c \\ \frac{1}{e} \partial_x \mu_s / 2 \\ -\frac{1}{T_0} \partial_x T_c \end{pmatrix}, \quad (2.73)$$

where the first term on the RHS is the normal response Eq. (2.30) with slight SOC modulation, while the second term is the anomalous Hall response, which reads

$$\mathbf{G}_1 \equiv \sigma_{\text{H}} \begin{pmatrix} P_{\text{H}} & 1 & P'_{\text{H}} S_{\text{H}} T_0 \\ 1 & P_{\text{H}} & S_{\text{H}} T_0 \\ P'_{\text{H}} S_{\text{H}} T_0 & S_{\text{H}} T_0 & P_{\text{H}} \mathcal{L}_0 T_0^2 \end{pmatrix}, \quad (2.74)$$

where the necessary parameters are defined as  $\sigma_{\text{H}} = \sigma_{\text{H},\uparrow} + \sigma_{\text{H},\downarrow}$  the electric conductivity,  $S_{\text{H}} = -e \mathcal{L}_0 T_0 (\partial_\varepsilon \log \sigma_{\text{H}} |_{\varepsilon_F})$  the thermopower,  $P_{\text{H}} \equiv (\sigma_{\text{H},\uparrow} - \sigma_{\text{H},\downarrow}) / (\sigma_{\text{H},\uparrow} + \sigma_{\text{H},\downarrow})$  the polarization of electric Hall conductivity, and  $P'_{\text{H}} \equiv (\sigma'_{\text{H},\uparrow} - \sigma'_{\text{H},\downarrow}) / (\sigma'_{\text{H},\uparrow} + \sigma'_{\text{H},\downarrow})$  the polarization of the derivative of the anomalous Hall conductivity as well as their energy dependences.

## 2.4.2 AMR, PHE, AND THEIR THERMAL ANALOGUES

For an in-plane magnetization, we take Eqs. (2.53-2.54) from Sec. 2.3.3 and follow the same procedure in Sec. 2.4.1. The response relation in this case reads

$$\begin{pmatrix} \mathbf{J}_c \\ \mathbf{J}_s \\ \dot{\mathbf{Q}}_c \end{pmatrix} = [\hat{\mathbf{x}} (\mathbf{G}_0 + \mathbf{G}_2 \cos^2 \phi) + \hat{\mathbf{y}} \mathbf{G}_2 \cos \phi \sin \phi] \begin{pmatrix} \frac{1}{e} \partial_x \mu_c \\ \frac{1}{e} \partial_x \mu_s / 2 \\ -\frac{1}{T_0} \partial_x T_c \end{pmatrix}, \quad (2.75)$$

where  $\mathbf{G}_0$  is the normal response as defined above and

$$\mathbf{G}_2 \equiv \sigma_A \begin{pmatrix} 1 & P_A & S_A T_0 \\ P_A & 1 & P'_A S_A T_0 \\ S_A T_0 & P'_A S_A T_0 & \mathcal{L}_0 T_0^2 \end{pmatrix}, \quad (2.76)$$

is the AMR response matrix with the parameters defined as  $\sigma_A = \sigma_{A,\uparrow} + \sigma_{A,\downarrow}$  the anisotropic conductivity  $S_A = -e\mathcal{L}_0 T_0 (\partial_\epsilon \log \sigma_A|_{\epsilon_F})$  the thermopower,  $P_A \equiv (\sigma_{A,\uparrow} - \sigma_{A,\downarrow}) / (\sigma_{A,\uparrow} + \sigma_{A,\downarrow})$  the polarization of anisotropic conductivity, and  $P'_A \equiv (\sigma'_{A,\uparrow} - \sigma'_{A,\downarrow}) / (\sigma'_{A,\uparrow} + \sigma'_{A,\downarrow})$  the polarization of the derivative of the anisotropic conductivity. The parameter  $\sigma_{A,\zeta}$  is defined as

$$\sigma_{A,\zeta} \equiv \frac{2\tau_\zeta^{(i)}}{5\tau_\zeta^{(a)}} \tilde{\sigma}_\zeta. \quad (2.77)$$

## 2.5 CONCLUSION

We developed a complete semiclassical theory for the thermoelectric transport properties of ferromagnetic metal films with the SOC, including the anisotropic magnetothermopower and anomalous/planer thermoelectric Hall effects. The linear response relation between the currents and driving forces has been derived for the cases of an out-of-plane and an in-plane magnetization, respectively. In the out-of-plane configuration, there are anomalous thermoelectric Hall effects linear to the SOC constant, while in the in-plane configuration, there are thermoelectric AMR and PHE in the second order SOC. In the present study we assumed thin films and disregarded transport normal to the boundaries. In Ref. [68], we relax that limitation and find that the AHE can also contribute to the transport properties for an in-plane magnetization. The response matrices are expressed by the microscopic parameters and therefore a more systematic study and classification of different transport studies. The distribution of the charge, spin, and heat requires discussion of the diffusion equations and boundary conditions in real systems of interests to quantitatively analyze experiments.

## 2.6 APPENDIX: COLLISION TERMS IN THE BOLTZMANN EQUATION

In this section, we work out the collision terms of the Boltzmann equation, which read

$$\left( \frac{\partial f_{\mathbf{k}\zeta}}{\partial t} \right)_{\text{scatt.}} = \sum_{\mathbf{k}'\zeta'} \left[ P_{\mathbf{k}\mathbf{k}'}^{\zeta\zeta'} f_{\mathbf{k}'\zeta'} - P_{\mathbf{k}'\mathbf{k}}^{\zeta'\zeta} f_{\mathbf{k}\zeta} \right], \quad (2.78)$$

where  $P_{\mathbf{k}'\mathbf{k}}^{\zeta'\zeta}$  is the scattering probability from a state  $\hat{\mathbf{k}}\zeta$  to  $\hat{\mathbf{k}}'\zeta'$ , which can be written as (Fermi's golden rule)

$$P_{\mathbf{k}'\mathbf{k}}^{\zeta'\zeta}(\varepsilon';\varepsilon) = \frac{2\pi}{\hbar} |\langle \mathbf{k}'\zeta' | T | \mathbf{k}\zeta \rangle|^2 \delta(\varepsilon - \varepsilon'), \quad (2.79)$$

where  $T$  is the so-called  $T$ -matrix operator that describes multiple impurity scattering process in principle exactly:

$$T = U + U \frac{1}{E - H_0 + i\delta} U + U \frac{1}{E - H_0 + i\delta} U \frac{1}{E - H_0 + i\delta} U + \dots \quad (2.80)$$

The first terms of the matrix elements in Eq. (2.79) then read

$$\langle \mathbf{k}'\zeta' | V_{\text{imp}} | \mathbf{k}\zeta \rangle = \frac{1}{\mathcal{V}} \sum_i (\mathbf{1} V_i + J \boldsymbol{\sigma} \cdot \mathbf{S}_i)_{\zeta'\zeta} e^{i(\mathbf{k}-\mathbf{k}') \cdot \bar{\mathbf{r}}_i} = \langle \mathbf{k}\zeta | V_{\text{imp}} | \mathbf{k}'\zeta' \rangle^\dagger, \quad (2.81)$$

$$\langle \mathbf{k}'\zeta' | V_{\text{so}} | \mathbf{k}\zeta \rangle = -i \left[ \frac{\eta_{\text{so}}}{\mathcal{V}} \boldsymbol{\sigma} \cdot (\mathbf{k} \times \mathbf{k}') \sum_i (\mathbf{1} V_i + J \boldsymbol{\sigma} \cdot \mathbf{S}_i) \right]_{\zeta'\zeta} e^{i(\mathbf{k}-\mathbf{k}') \cdot \bar{\mathbf{r}}_i} = \langle \mathbf{k}\zeta | V_{\text{so}} | \mathbf{k}'\zeta' \rangle^\dagger. \quad (2.82)$$

### 2.6.1 FIRST ORDER TERMS WITHOUT SOC

To lowest order in  $V$  and in the absence of SOC,  $T = V_{\text{imp}}$ , and the collision terms read

$$\begin{aligned} \left( \frac{\partial f_{\mathbf{k}\zeta}}{\partial t} \right)_{\text{scatt.}} &\approx \frac{2\pi}{\hbar} \sum_{\mathbf{k}'\zeta'} \left[ |\langle \mathbf{k}\zeta | V_{\text{imp}} | \mathbf{k}'\zeta' \rangle|^2 \delta(\varepsilon' - \varepsilon) f_{\mathbf{k}'\zeta'} - |\langle \mathbf{k}'\zeta' | V_{\text{imp}} | \mathbf{k}\zeta \rangle|^2 \delta(\varepsilon - \varepsilon') f_{\mathbf{k}\zeta} \right] \\ &= \frac{2\pi}{\hbar} \left[ \sum_{\mathbf{k}'\zeta'} |\langle \mathbf{k}\zeta | V_{\text{imp}} | \mathbf{k}'\zeta' \rangle|^2 \delta(\varepsilon' - \varepsilon) f_{\zeta'}^0 - f_{\mathbf{k}\zeta} \sum_{\mathbf{k}'\zeta'} |\langle \mathbf{k}'\zeta' | V_{\text{imp}} | \mathbf{k}\zeta \rangle|^2 \delta(\varepsilon - \varepsilon') \right] \\ &= \frac{2\pi}{\hbar} \left[ -g_{\mathbf{k}\zeta}^a \sum_{\mathbf{k}'\zeta'} |\langle \mathbf{k}'\zeta' | V_{\text{imp}} | \mathbf{k}\zeta \rangle|^2 \delta(\varepsilon - \varepsilon') - (f_{\zeta}^0 - f_{-\zeta}^0) \sum_{\mathbf{k}'} |\langle \mathbf{k}' - \zeta | V_{\text{imp}} | \mathbf{k}\zeta \rangle|^2 \delta(\varepsilon - \varepsilon') \right] \\ &\equiv -g_{\mathbf{k}\zeta}^a \left( \tau_{\text{sc}0,\zeta}^{-1}(\varepsilon) + \tau_{\text{sf}0,\zeta}^{-1}(\varepsilon) \right) - (f_{\zeta}^0 - f_{-\zeta}^0) \tau_{\text{sf}0,\zeta}^{-1}(\varepsilon), \quad (2.83) \end{aligned}$$

where spin-conserved and spin-flip relaxation times are defined as

$$\tau_{\text{sc}0,\zeta}^{-1}(\varepsilon) \equiv \frac{2\pi}{\hbar} \sum_{\mathbf{k}'} |\langle \mathbf{k}'\zeta | V_{\text{imp}} | \mathbf{k}\zeta \rangle|^2 \delta(\varepsilon - \varepsilon'), \quad (2.84)$$

$$\tau_{\text{sf}0,\zeta}^{-1}(\varepsilon) \equiv \frac{2\pi}{\hbar} \sum_{\mathbf{k}'} |\langle \mathbf{k}' - \zeta | V_{\text{imp}} | \mathbf{k}\zeta \rangle|^2 \delta(\varepsilon - \varepsilon'). \quad (2.85)$$

The configurational averages of the squared matrix elements are

$$\begin{aligned}
& \overline{|\langle \mathbf{k}'\zeta | V_{\text{imp}} | \mathbf{k}\zeta \rangle|^2} \\
&= \frac{1}{\mathcal{V}^2} \overline{\sum_{i,j} (V_i + J\boldsymbol{\sigma}_{\zeta\zeta} \cdot \mathbf{S}_i) e^{i(\mathbf{k}-\mathbf{k}') \cdot \mathbf{r}_i} (V_j + J\boldsymbol{\sigma}_{\zeta\zeta} \cdot \mathbf{S}_j) e^{-i(\mathbf{k}-\mathbf{k}') \cdot \mathbf{r}_j}} \\
&= \mathcal{V}^{-N_{\text{imp}}-2} \int d\mathbf{r}_1 \cdots d\mathbf{r}_{N_{\text{imp}}} \left( \sum_{i,j} (V_i + J\boldsymbol{\sigma}_{\zeta\zeta} \cdot \mathbf{S}_i) e^{i(\mathbf{k}-\mathbf{k}') \cdot \mathbf{r}_i} (V_j + J\boldsymbol{\sigma}_{\zeta\zeta} \cdot \mathbf{S}_j) e^{-i(\mathbf{k}-\mathbf{k}') \cdot \mathbf{r}_j} \right) \\
&= \mathcal{V}^{-N_{\text{imp}}-2} \int d\mathbf{r}_1 \cdots d\mathbf{r}_{N_{\text{imp}}} \sum_{i=1}^{N_{\text{imp}}} (V_i + J\boldsymbol{\sigma}_{\zeta\zeta} \cdot \mathbf{S}_i)^2 \\
&= \mathcal{V}^{-2} \sum_{i=1}^{N_{\text{imp}}} \overline{(V_i + J\boldsymbol{\sigma}_{\zeta\zeta} \cdot \mathbf{S}_i)^2} \\
&= \mathcal{V}^{-1} n_{\text{imp}} \overline{(V + J\boldsymbol{\sigma}_{\zeta\zeta} \cdot \mathbf{S})^2} \\
&= \mathcal{V}^{-1} n_{\text{imp}} \left( \overline{V^2} + J^2 \frac{\overline{S^2}}{3} + 2\zeta J \hat{\mathbf{M}} \cdot \overline{V\mathbf{S}} \right) \\
&= \mathcal{V}^{-1} n_{\text{imp}} \left( \overline{V^2} + J^2 \frac{\overline{S^2}}{3} \right), \tag{2.86}
\end{aligned}$$

$$\begin{aligned}
& \overline{|\langle \mathbf{k}' - \zeta | V_{\text{imp}} | \mathbf{k}\zeta \rangle|^2} \\
&= \frac{1}{\mathcal{V}^2} \overline{\sum_{i,j} (J\boldsymbol{\sigma}_{-\zeta\zeta} \cdot \mathbf{S}_i) e^{i(\mathbf{k}-\mathbf{k}') \cdot \mathbf{r}_i} (J\boldsymbol{\sigma}_{-\zeta\zeta} \cdot \mathbf{S}_j) e^{-i(\mathbf{k}-\mathbf{k}') \cdot \mathbf{r}_j}} \\
&= \mathcal{V}^{-1} n_{\text{imp}} J^2 \overline{(\boldsymbol{\sigma}_{-\zeta\zeta} \cdot \mathbf{S})^2} \\
&= \mathcal{V}^{-1} n_{\text{imp}} J^2 \frac{|\boldsymbol{\sigma}_{-\zeta\zeta}|^2 \overline{S^2}}{3} \\
&= \mathcal{V}^{-1} n_{\text{imp}} J^2 \frac{2\overline{S^2}}{3}, \tag{2.87}
\end{aligned}$$

where we have used

$$\boldsymbol{\sigma}_{\uparrow\uparrow} = (1, i, 0) = \boldsymbol{\sigma}_{\uparrow\downarrow}^* \Rightarrow |\boldsymbol{\sigma}_{\uparrow\uparrow}|^2 = |\boldsymbol{\sigma}_{\uparrow\downarrow}|^2 = 2. \tag{2.88}$$

Therefore,

$$\tau_{\text{sc}0,\zeta}^{-1}(\varepsilon) = \frac{2\pi}{\hbar} n_{\text{imp}} \overline{(V + J\boldsymbol{\sigma}_{\zeta\zeta} \cdot \mathbf{S})^2} \frac{1}{\mathcal{V}} \sum_{\mathbf{k}'} \delta(\varepsilon_{\mathbf{k}'\zeta} - \varepsilon) = \frac{2\pi}{\hbar} N_{\zeta}(\varepsilon) n_{\text{imp}} \left( \overline{V^2} + J^2 \frac{\overline{S^2}}{3} \right), \quad (2.89)$$

$$\tau_{\text{sf}0,\zeta}^{-1}(\varepsilon) \equiv \frac{2\pi}{\hbar} n_{\text{imp}} J^2 \frac{2\overline{S^2}}{3} \frac{1}{\mathcal{V}} \sum_{\mathbf{k}'} \delta(\varepsilon_{\mathbf{k}'-\zeta} - \varepsilon) = \frac{2\pi}{\hbar} n_{\text{imp}} N_{-\zeta}(\varepsilon) J^2 \frac{2\overline{S^2}}{3}, \quad (2.90)$$

where  $N_{\zeta}(\varepsilon) = \sum_{\mathbf{k}'} \delta(\varepsilon_{\mathbf{k}'\zeta} - \varepsilon) / \mathcal{V}$  is the density of states. For random impurity spin directions the spin dependence of the relaxation time originates from the density of states.

## 2.6.2 FIRST ORDER TERMS WITH SOC

With  $T = U = V_{\text{imp}} + V_{\text{so}}$  and repeating the similar calculation, the collision terms read

$$\begin{aligned} \left( \frac{\partial f_{\mathbf{k}\zeta}}{\partial t} \right)_{\text{scatt.}} &\approx \frac{2\pi}{\hbar} \sum_{\mathbf{k}'\zeta'} \left[ \overline{|\langle \mathbf{k}\zeta | V_{\text{imp}} + V_{\text{so}} | \mathbf{k}'\zeta' \rangle|^2} \delta(\varepsilon' - \varepsilon) f_{\mathbf{k}'\zeta'} - \overline{|\langle \mathbf{k}'\zeta' | V_{\text{imp}} + V_{\text{so}} | \mathbf{k}\zeta \rangle|^2} \delta(\varepsilon - \varepsilon') f_{\mathbf{k}\zeta} \right] \\ &= \frac{2\pi}{\hbar} \sum_{\mathbf{k}'\zeta'} \overline{|\langle \mathbf{k}\zeta | V_{\text{imp}} | \mathbf{k}'\zeta' \rangle|^2} \delta(\varepsilon' - \varepsilon) f_{\zeta'}^0 + \frac{2\pi}{\hbar} \sum_{\mathbf{k}'\zeta'} \overline{|\langle \mathbf{k}\zeta | V_{\text{so}} | \mathbf{k}'\zeta' \rangle|^2} \delta(\varepsilon' - \varepsilon) f_{\zeta'}^0 \\ &\quad - f_{\mathbf{k}\zeta} \frac{2\pi}{\hbar} \sum_{\mathbf{k}'\zeta'} \overline{|\langle \mathbf{k}'\zeta' | V_{\text{imp}} | \mathbf{k}\zeta \rangle|^2} \delta(\varepsilon - \varepsilon') - f_{\mathbf{k}\zeta} \frac{2\pi}{\hbar} \sum_{\mathbf{k}'\zeta'} \overline{|\langle \mathbf{k}'\zeta' | V_{\text{so}} | \mathbf{k}\zeta \rangle|^2} \delta(\varepsilon - \varepsilon') \\ &\equiv -g_{\mathbf{k}\zeta}^a \left( \tau_{\text{sc}0,\zeta}^{-1}(\varepsilon) + \tau_{\text{sf}0,\zeta}^{-1}(\varepsilon) + \tau_{\text{sc}1,\zeta}^{-1}(\varepsilon) + \tau_{\text{sf}1,\zeta}^{-1}(\varepsilon) \right) - (f_{\zeta}^0 - f_{-\zeta}^0) \left( \tau_{\text{sf}0,\zeta}^{-1}(\varepsilon) + \tau_{\text{sf}1,\zeta}^{-1}(\varepsilon) \right) \\ &\equiv -\frac{g_{\mathbf{k}\zeta}^a}{\tau_{\zeta}} - \frac{f_{\zeta}^0 - f_{-\zeta}^0}{\tau_{\text{sf},\zeta}}, \end{aligned} \quad (2.91)$$

where we introduce the relaxation times due to the SOC

$$\tau_{\text{sc}1,\zeta}^{-1}(\varepsilon) \equiv \frac{2\pi}{\hbar} \sum_{\mathbf{k}'} \overline{|\langle \mathbf{k}'\zeta | V_{\text{so}} | \mathbf{k}\zeta \rangle|^2} \delta(\varepsilon - \varepsilon'), \quad (2.92)$$

$$\tau_{\text{sf}1,\zeta}^{-1}(\varepsilon) \equiv \frac{2\pi}{\hbar} \sum_{\mathbf{k}'} \overline{|\langle \mathbf{k}' - \zeta | V_{\text{so}} | \mathbf{k}\zeta \rangle|^2} \delta(\varepsilon - \varepsilon'). \quad (2.93)$$

The configurational averages are

$$\begin{aligned} \overline{|\langle \mathbf{k}'_\zeta | V_{so} | \mathbf{k}_\zeta \rangle|^2} &= \mathcal{V}^{-2} \sum_i \left| -i\eta_{so} \boldsymbol{\sigma}_{\zeta\zeta} \cdot (\mathbf{k} \times \mathbf{k}') (V_i + \boldsymbol{\sigma}_{\zeta\zeta} \cdot \mathbf{S}_i) \right|^2 \\ &\approx \mathcal{V}^{-1} n_{\text{imp}} \eta_{so}^2 \left( \overline{V^2} + \frac{1}{3} J^2 \overline{S^2} \right) |\boldsymbol{\sigma}_{\zeta\zeta} \cdot (\mathbf{k} \times \mathbf{k}')|^2. \end{aligned} \quad (2.94)$$

$$\begin{aligned} \overline{|\langle \mathbf{k}'_{-\zeta} | V_{so} | \mathbf{k}_\zeta \rangle|^2} &= \mathcal{V}^{-2} \sum_i \left| -i\eta_{so} \boldsymbol{\sigma}_{-\zeta\zeta} \cdot (\mathbf{k} \times \mathbf{k}') (V_i + \boldsymbol{\sigma}_{-\zeta\zeta} \cdot \mathbf{S}_i) \right|^2 \\ &= \mathcal{V}^{-1} n_{\text{imp}} \eta_{so}^2 \left( \overline{V^2} + \frac{2}{3} J^2 \overline{S^2} \right) |\boldsymbol{\sigma}_{-\zeta\zeta} \cdot (\mathbf{k} \times \mathbf{k}')|^2. \end{aligned} \quad (2.95)$$

The summation over  $\mathbf{k}'$  are done by

$$\begin{aligned} \sum_{\mathbf{k}'} |\boldsymbol{\sigma}_{\zeta\zeta} \cdot (\mathbf{k} \times \mathbf{k}')|^2 \delta(\varepsilon_{k\zeta} - \varepsilon_{k'\zeta}) &= \sum_{\mathbf{k}'} |\mathbf{k}' \cdot (\boldsymbol{\sigma}_{\zeta\zeta} \times \mathbf{k})|^2 \delta(\varepsilon_{k\zeta} - \varepsilon_{k'\zeta}) \\ &= \frac{\mathcal{V}}{8\pi^3} \int |\mathbf{k}' \cdot (\boldsymbol{\sigma}_{\zeta\zeta} \times \mathbf{k})|^2 \delta(\varepsilon_{k\zeta} - \varepsilon_{k'\zeta}) d\mathbf{k}' \\ &= \frac{\mathcal{V}}{2\pi^2} \frac{|\boldsymbol{\sigma}_{\zeta\zeta} \times \mathbf{k}|^2}{3} \int (k')^4 \delta(\varepsilon_{k\zeta} - \varepsilon_{k'\zeta}) dk' \\ &= \mathcal{V} N_\zeta \frac{|\boldsymbol{\sigma}_{\zeta\zeta} \times \hat{\mathbf{k}}|^2}{3} \left[ \frac{2m_\zeta(\varepsilon - \zeta\Delta)}{\hbar^2} \right]^2, \end{aligned} \quad (2.96)$$

$$\begin{aligned} \sum_{\mathbf{k}'} |\boldsymbol{\sigma}_{-\zeta\zeta} \cdot (\mathbf{k} \times \mathbf{k}')|^2 \delta(\varepsilon_{k\zeta} - \varepsilon_{k'_{-\zeta}}) &= \sum_{\mathbf{k}'} |\mathbf{k}' \cdot (\boldsymbol{\sigma}_{-\zeta\zeta} \times \mathbf{k})|^2 \delta(\varepsilon_{k\zeta} - \varepsilon_{k'_{-\zeta}}) \\ &= \frac{\mathcal{V}}{8\pi^3} \int |\mathbf{k}' \cdot (\boldsymbol{\sigma}_{-\zeta\zeta} \times \mathbf{k})|^2 \delta(\varepsilon_{k\zeta} - \varepsilon_{k'_{-\zeta}}) d\mathbf{k}' \\ &= \frac{\mathcal{V}}{2\pi^2} \frac{|\boldsymbol{\sigma}_{-\zeta\zeta} \times \mathbf{k}|^2}{3} \int (k')^4 \delta(\varepsilon_{k\zeta} - \varepsilon_{k'_{-\zeta}}) dk' \\ &= \mathcal{V} N_{-\zeta} \frac{|\boldsymbol{\sigma}_{-\zeta\zeta} \times \hat{\mathbf{k}}|^2}{3} \left[ \frac{2m_\zeta(\varepsilon - \zeta\Delta)}{\hbar^2} \right] \left[ \frac{2m_{-\zeta}(\varepsilon + \zeta\Delta)}{\hbar^2} \right] \\ &= \mathcal{V} N_{-\zeta} \frac{2 - |\boldsymbol{\sigma}_{\zeta\zeta} \times \hat{\mathbf{k}}|^2}{3} \left[ \frac{2m_\zeta(\varepsilon - \zeta\Delta)}{\hbar^2} \right] \left[ \frac{2m_{-\zeta}(\varepsilon + \zeta\Delta)}{\hbar^2} \right], \end{aligned} \quad (2.97)$$

Then

$$\tau_{\text{sc}1,\zeta}^{-1}(\varepsilon) = \frac{2\pi}{\hbar} n_{\text{imp}} N_\zeta(\varepsilon) \left( \overline{V^2} + \frac{1}{3} J^2 \overline{S^2} \right) (\tilde{\eta}_{so,\zeta}(\varepsilon))^2 \frac{|\boldsymbol{\sigma}_{\zeta\zeta} \times \hat{\mathbf{k}}|^2}{3}, \quad (2.98)$$

$$\tau_{\text{sf}1,\zeta}^{-1}(\varepsilon) = \frac{2\pi}{\hbar} N_{-\zeta}(\varepsilon) n_{\text{imp}} \left( \tilde{\eta}_{so}^{sf}(\varepsilon) \right)^2 \left( \overline{V^2} + \frac{2}{3} J^2 \overline{S^2} \right) \frac{2 - |\boldsymbol{\sigma}_{\zeta\zeta} \times \hat{\mathbf{k}}|^2}{3}, \quad (2.99)$$

where

$$(\tilde{\eta}_{so,\zeta}(\varepsilon))^2 \equiv \left[ \eta_{so} \frac{2m_\zeta(\varepsilon - \zeta\Delta)}{\hbar^2} \right]^2, \quad (2.100)$$

$$(\tilde{\eta}_{so}^{sf}(\varepsilon))^2 \equiv \eta_{so}^2 \left[ \frac{2m_\zeta(\varepsilon - \zeta\Delta)}{\hbar^2} \right] \left[ \frac{2m_{-\zeta}(\varepsilon + \zeta\Delta)}{\hbar^2} \right]. \quad (2.101)$$

### 2.6.3 SECOND ORDER TERM WITH SOC

Taking Eq. (2.80) in the second order approximation

$$T = U + U \frac{1}{E - H_0 + i\delta} U, \quad (2.102)$$

the collision terms read

$$\begin{aligned} \left( \frac{\partial f_{\mathbf{k}\zeta}}{\partial t} \right)_{\text{scatt.}} &\approx -\frac{g_{\mathbf{k}\zeta}^a}{\tau_\zeta} - \frac{f_\zeta^0 - f_{-\zeta}^0}{\tau_{\text{sf},\zeta}} \\ &+ \frac{4\pi}{\hbar} \sum_{\mathbf{k}'\zeta'} f_{\mathbf{k}'\zeta'} \text{Re} \left[ \langle \vec{k}_\zeta | V_{\text{so}} | \vec{k}'\zeta' \rangle^* \sum_{\bar{q}} \frac{\langle \vec{k}_\zeta | V_{\text{imp}} | \bar{q}\zeta \rangle \langle \bar{q}\zeta | V_{\text{imp}} | \vec{k}'\zeta' \rangle}{\varepsilon_{\vec{k}_\zeta} - \varepsilon_{\bar{q}\zeta} + i\delta} \right] \delta(\varepsilon' - \varepsilon) \\ &- \frac{4\pi}{\hbar} \sum_{\mathbf{k}'\zeta'} f_{\mathbf{k}'\zeta'} \text{Re} \left[ \langle \vec{k}'\zeta' | V_{\text{so}} | \vec{k}_\zeta \rangle^* \sum_{\bar{q}} \frac{\langle \vec{k}'\zeta' | V_{\text{imp}} | \bar{q}\zeta \rangle \langle \bar{q}\zeta | V_{\text{imp}} | \vec{k}_\zeta \rangle}{\varepsilon_{\vec{k}'\zeta'} - \varepsilon_{\bar{q}\zeta} + i\delta} \right] \delta(\varepsilon - \varepsilon') \\ &\approx -\frac{g_{\mathbf{k}\zeta}^a}{\tau_\zeta} - \frac{f_\zeta^0 - f_{-\zeta}^0}{\tau_{\text{sf},\zeta}} \\ &+ \frac{4\pi}{\hbar} \sum_{\mathbf{k}'} g_{\mathbf{k}'\zeta}^a \text{Re} \left[ \langle \vec{k}_\zeta | V_{\text{so}} | \vec{k}'\zeta \rangle^* \sum_{\bar{q}} \frac{\langle \vec{k}_\zeta | V_{\text{imp}} | \bar{q}\zeta \rangle \langle \bar{q}\zeta | V_{\text{imp}} | \vec{k}'\zeta \rangle}{\varepsilon_{\vec{k}_\zeta} - \varepsilon_{\bar{q}\zeta} + i\delta} \right] \delta(\varepsilon' - \varepsilon) \\ &\equiv -\frac{g_{\mathbf{k}\zeta}^a}{\tau_\zeta} - \frac{f_\zeta^0 - f_{-\zeta}^0}{\tau_{\text{sf},\zeta}} + \sum_{\mathbf{k}'} g_{\mathbf{k}'\zeta}^a P_{\mathbf{k}\zeta}^{\zeta\zeta'(2)}, \end{aligned} \quad (2.103)$$

where the second order scattering rate is

$$P_{\mathbf{k}'\zeta}^{\zeta\zeta'(2)} = \frac{4\pi}{\hbar} \eta_{so} [(\mathbf{k}' \times \mathbf{k}) \cdot \boldsymbol{\sigma}_{\zeta\zeta}] n_{\text{imp}} N_\zeta(\varepsilon) \overline{V_\zeta^3} \delta_{\zeta\zeta'} \delta(\varepsilon_{k_\zeta} - \varepsilon_{k'\zeta'}). \quad (2.104)$$

## REFERENCES

- [1] S. D. Bader and S. S. P. Parkin, *Ann. Rev. Cond. Matt. Phys.* **1**, 71 (2010).
- [2] G. E. W. Bauer, E. Saitoh, and B. J. van Wees, *Nature Mat.* **11**, 391 (2012).

- [3] M. Johnson and R. H. Silsbee, *Phys. Rev. B* **35**, 4959 (1987).
- [4] L. Gravier, S. S.-Guisan, F. Reuse, and J.-Ph. Ansermet, *Phys. Rev. B* **73**, 024419 (2006); **73**, 052410 (2006).
- [5] M. Hatami, and G. E. W. Bauer, Q. Zhang, and P. J. Kelly, *Phys. Rev. B* **79**, 174426 (2009).
- [6] A. Slachter, F. L. Bakker, J. P. Adam, and B. J. van Wees, *Nature Phys.* **6**, 879 (2010).
- [7] J. Flipse, F. L. Bakker, A. Slachter, F. K. Dejene, and B. J. van Wees, *Nature Nanotech.* **7**, 166 (2012).
- [8] F. K. Dejene, J. Flipse, G. E. W. Bauer, and B. J. van Wees, *Nature Phys.* **9**, 636 (2013).
- [9] T. T. Heikkilä, M. Hatami, G. E. W. Bauer, *Solid State Commun.* **150**, 475 (2010).
- [10] K. Uchida, S. Takahashi, K. Harii, J. Ieda, W. Koshibae, K. Ando, S. Maekawa, and E. Saitoh, *Nature* **455**, 778 (2008).
- [11] J. Xiao, G. E. W. Bauer, K. Uchida, E. Saitoh, and S. Maekawa, *Phys. Rev. B* **81**, 214418 (2010).
- [12] E. H. Hall, *Am. J. Math.* **2**, 287 (1879).
- [13] H. B. Callen, *Phys. Rev.* **48**, 1349 (1948).
- [14] For a review see: N. Nagaosa, J. Sinova, S. Onoda, A. H. MacDonald, and N. P. Ong, *Rev. Mod. Phys.* **82**, 1539 (2010).
- [15] R. Karplus and J. M. Luttinger, *Phys. Rev.* **95**, 1154 (1954).
- [16] Y. Yao, L. Kleinman, A. H. MacDonald, J. Sinova, T. Jungwirth, D. S. Wang, E. Wang, and Q. Niu, *Phys. Rev. Lett.* **92**, 037204 (2004).
- [17] X. Wang, J. R. Yates, I. Souza, and D. Vanderbilt, *Phys. Rev. B* **74**, 195118 (2006).
- [18] X. Wang, D. Vanderbilt, J. R. Yates, and I. Souza, *Phys. Rev. B* **76**, 195109 (2007).
- [19] L. Berger *Phys. Rev. B* **2**, 4559 (1970).
- [20] A. A. Kovalev, J. Sinova, and Y. Tserkovnyak, *Phys. Rev. Lett.* **105**, 036601 (2010).
- [21] J. Weischenberg, F. Freimuth, J. Sinova, Stefan Blügel, and Yuriy Mokrousov, *Phys. Rev. Lett.* **107**, 106601 (2011).

- [22] J. Smit, *Physica* **21**, 877 (1955).
- [23] S. Onoda, N. Sugimoto, N. Nagaosa, *Phys. Rev. Lett.* **97**, 126602 (2006).
- [24] S. Onoda, N. Sugimoto, N. Nagaosa, *Phys. Rev. B* **77**, 165103 (2008), and references therein.
- [25] T. Miyasato, N. Abe, T. Fujii, A. Asamitsu, S. Onoda, Y. Onose, N. Nagaosa, and Y. Tokura, *Phys. Rev. Lett.* **99**, 086602 (2007).
- [26] M. Mizuguchi, S. Ohata, K. Hasegawa, K. Uchida, E. Saitoh, and K. Takanashi, *Applied Physics Express* **5**, 093002 (2012); Y. Sakuraba, K. Hasegawa, M. Mizuguchi, T. Kubota, S. Mizukami, T. Miyazaki, and K. Takanashi, *Applied Physics Express* **6**, 033003 (2013).
- [27] S. Lowitzer, D. Ködderitzsch, and H. Ebert, *Phys. Rev. Lett.* **105**, 266604 (2010).
- [28] D. A. Thompson, L. T. Romankiw, and A. E. Mayadas, *IEEE Trans. Magn.* **MAG-11**, 1039 (1975).
- [29] T. R. McGuire and R. I. Potter, *IEEE Trans. Magn.* **MAG-11**, 1018 (1975).
- [30] K. M. Seemann, F. Freimuth, H. Zhang, S. Blügel, Y. Mokrousov, D. E. Bürgler, and C. M. Schneider, *Phys. Rev. Lett.* **107**, 086603 (2011).
- [31] S. Kokado, M. Tsunoda, K. Harigaya, and A. Sakuma, *J. Phys. Soc. Jpn.* **81**, 024705 (2012).
- [32] H. X. Tang, R. K. Kawakami, D. D. Awschalom, and M. L. Roukes, *Phys. Rev. Lett.* **90**, 107201 (2003).
- [33] J. Smit, *Physica* **17**, 612 (1951).
- [34] V. D. Ky, *Phys. stat. sol.* **22**, 729 (1967).
- [35] R. I. Potter, *Phys. Rev. B* **10**, 4626 (1974).
- [36] Th. G. S. M. Rijks, R. Coehoorn, M. J. M. de Jong, and W. J. M. de Jonge, *Phys. Rev. B* **51**, 283 (1995).
- [37] T. Jungwirth, M. Abolfath, J. Sinova, J. Kušera, and A. H. MacDonald, *Appl. Phys. Lett.* **81**, 4029 (2002).
- [38] M. Trushin, K. Výborný, P. Moraczewski, A. A. Kovalev, J. Schliemann, and T. Jungwirth, *Phys. Rev. B* **80**, 134405 (2009).

- [39] T. Kato, T. Ishikawa, H. Itoh, and J. Inoue, Phys. Rev. B **77**, 233404 (2008).
- [40] Y. Pu, D. Chiba, F. Matsukura, H. Ohno, and J. Shi, Phys. Rev. Lett. **101**, 117208 (2008).
- [41] C. M. Jaworski and J. P. Heremans, Phys. Rev. B **85**, 033204 (2012).
- [42] W. L. Lee, S. Watauchi, V. L. Miller, R. J. Cava, and N. P. Ong, Phys. Rev. Lett. **93**, 226601 (2004).
- [43] S. Hu and T. Kimura, Phys. Rev. B **87**, 014424 (2013).
- [44] T. Seki, Y. Hasegawa, S. Mitani, S. Takahashi, H. Imamura, S. Maekawa, J. Nitta, K. Takanashi, Nature Mater. **7**, 125 (2008); T. Seki, I. Sugai, Y. Hasegawa, S. Mitani, and K. Takanashi, Solid State Commun. **150**, 496 (2010).
- [45] A. Slachter, F. L. Bakker, and B. J. van Wees, Phys. Rev. B **84**, 020412(R) (2011).
- [46] M. Weiler, M. Althammer, F. Czeschka, H. Huebl, M. S. Wagner, M. Opel, I. Imort, G. Reiss, A. Thomas, R. Gross, and S. T. B. Goennenwein, Phys. Rev. Lett. **108**, 106602 (2012).
- [47] Y. Pu, E. Johnston-Halperin, D. D. Awschalom, and J. Shi, Phys. Rev. Lett. **97**, 036601 (2006).
- [48] A. D. Avery, M. R. Pufall, and B. L. Zink, Phys. Rev. Lett. **109**, 196602 (2012).
- [49] J. Kimling, J. Gooth, and K. Nielsch, Phys. Rev. B **87**, 094409 (2013).
- [50] S. L. Yin, Q. Mao, Q. Y. Meng, D. Li, and H. W. Zhao, Phys. Rev. B **88**, 064410 (2013).
- [51] M. Schmid, S. Srichandan, D. Meier, T. Kuschel, J.-M. Schmalhorst, M. Vogel, G. Reiss, C. Strunk, and C. H. Back, Phys. Rev. Lett. **111**, 187201 (2013).
- [52] M. Mizuguchi, *et al.*, private discussion.
- [53] L. Smrčka and P. Středa, J. Phys. C **10**, 2153 (1977).
- [54] D. Xiao, Y. Yao, Z. Fang and Q. Niu, Phys. Rev. Lett. **97**, 026603 (2006).
- [55] J. Weischenberg, F. Freimuth, S. Blügel, and Y. Mokrousov, Phys. Rev. B **87**, 060406(R) (2013).
- [56] H. Katsura, N. Nagaosa, and P. A. Lee, Phys. Rev. Lett. **104**, 066403 (2011).

- [57] T. Qin, Q. Niu, and J. Shi, *Phys. Rev. Lett.* **107**, 236601 (2011).
- [58] R. Matsumoto and S. Murakami, *Phys. Rev. B* **84**, 184406 (2011).
- [59] J.-E. Wegrowe, H.-J. Drouhin, and D. Lacour, arXiv:1311.4868 (cond-mat.mes-hall) (2013).
- [60] S. Wimmer, D. Ködderitzsch, and H. Ebert, arXiv:1311.2498 (cond-mat.mes-hall) (2013).
- [61] S. Takahashi, H. Imamura, and S. Maekawa, in *Concepts in Spin Electronics*, edited by S. Maekawa (Oxford University Press, U.K., 2006), pp. 343-370.
- [62] H. Akera and H. Suzuura, *Phys. Rev. B* **87**, 075301 (2013).
- [63] M. Hatami, G. E. W. Bauer, S. Takahashi, and S. Maekawa, *Solid State Commun.* **150**, 480 (2010).
- [64] N. W. Ashcroft and N. D. Mermin, *Solid State Physics* (Saunders, Philadelphia, 1976).
- [65] L. Onsager, *Phys. Rev.* **37**, 405 (1931).
- [66] T. Heikkilä, M. Hatami, and G. E. W. Bauer, *Phys. Rev. B* **81**, 100408(R) (2010).
- [67] Y. Tian, L. Ye, and X. Jin, *Phys. Rev. Lett.* **103**, 087206 (2009).
- [68] Y.-T. Chen, S. Takahashi, and G. E. W. Bauer, in preparation.
- [69] N. Mott and H. Wills, *Proc. R. Soc.* **153**, 699 (1936).
- [70] S. K. Lyo and T. Holstein, *Phys. Rev. Lett.* **7**, 423 (1972).

# 3

## THEORY OF SPIN HALL MAGNETORESISTANCE

**Yan-Ting CHEN**

*We present a theory of the spin Hall magnetoresistance (SMR) in multilayers made from an insulating ferromagnet  $F$ , such as yttrium iron garnet (YIG), and a normal metal  $N$  with spin-orbit interactions, such as platinum (Pt). The SMR is induced by the simultaneous action of spin Hall and inverse spin Hall effects and therefore a non-equilibrium proximity phenomenon. We compute the SMR in  $F|N$  and  $F|N|F$  layered systems, treating  $N$  by spin-diffusion theory with quantum mechanical boundary conditions at the interfaces in terms of the spin-mixing conductance. Our results explain the experimentally observed spin Hall magnetoresistance in  $N|F$  bilayers. For  $F|N|F$  spin valves we predict an enhanced SMR amplitude when magnetizations are collinear. The SMR and the spin-transfer torques in these trilayers can be controlled by the magnetic configuration.*

---

Parts of this chapter have been collaborated with Saburo Takahashi, Hiroyasu Nakayama, Matthias Althammer, Sebastian T. B. Goennenwein, Eiji Saitoh, and Gerrit E. W. Bauer.

### 3.1 INTRODUCTION

Spin currents are a central theme in spintronics since they are intimately associated with the manipulation and transport of spins in small structures and devices [1, 2]. Spin currents can be generated by means of the spin Hall effect (SHE) and detected by the inverse spin Hall effect (ISHE) [3]. Of special interest are multilayers made of normal metals (N) and ferromagnets (F). When an electric current flows through N, an SHE spin current flows towards the interfaces, where it can be absorbed as a spin-transfer torque (STT) on the ferromagnet. This STT affects the magnetization damping [4] or even switches the magnetization [5, 6]. The ISHE can be used to detect spin currents pumped by the magnetization dynamics excited by microwaves [7–10] or temperature gradients (spin Seebeck effect) [11, 12].

Recently, magnetic insulators have attracted the attention of the spintronics community. Yttrium iron garnets (YIG), a class of ferrimagnetic insulators with a large band gap, are interesting because of their very low magnetization damping. Their magnetization can be activated thermally to generate the spin Seebeck effect in YIG|Pt bilayers [13, 14]. By means of the SHE, spin waves can be electrically excited in YIG via a Pt contact, and, via the ISHE, subsequently detected electrically in another Pt contact [15]. Spin transport at an N|F interface is governed by the complex spin-mixing conductance  $G_{\uparrow\downarrow}$  [16]. The prediction of a large real part of  $G_{\uparrow\downarrow}$  for interfaces of YIG with simple metals by first principles calculations [17] has been confirmed by experiments [18].

Magnetoresistance (MR) is the property of a material to change the value of its electrical resistance under an external magnetic field. In normal metals its origin is the Lorentz force [19]. The dependence of the resistance on the angle between current and magnetization in metallic ferromagnets is called anisotropic magnetoresistance (AMR). The transverse component of the AMR is also called the planar Hall effect (PHE), *i.e.* the transverse (Hall) voltage found in ferromagnets when the magnetization is rotated in the plane of the film [20, 21]. Both effects are symmetric with respect to magnetization reversal, which distinguishes them from the anomalous Hall effect (AHE) for magnetizations normal to the film, which changes sign under magnetization reversal [22]. The physical origin of AMR, PHE, and AHE is the spin-orbit interaction, in contrast to the giant magnetoresistance (GMR), which reflects the change in resistance that accompanies the magnetic field-induced magnetic configuration in magnetic multilayers [23].

Here we propose a theory for a recently discovered magnetoresistance effect in Pt|YIG bilayer systems [14, 24–26]. This MR is remarkable since YIG is a very good electric insulator such that a charge current can only flow in Pt. We explain this unusual magnetoresistance not in terms of an equilibrium static magnetic proximity polarization in Pt [24], but rather in terms of a non-equilibrium proximity effect

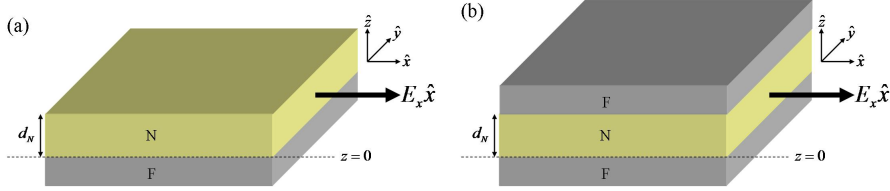


FIGURE 3.1: (a)N|F bilayer and (b) F|N|F trilayer systems considered here, where F is a ferromagnetic insulator and N a normal metal.

caused by the simultaneous action of the SHE and ISHE and therefore call it spin Hall magnetoresistance (SMR). This effect scales like the square of the spin Hall angle and is modulated by the magnetization direction in YIG via the spin-transfer at the N|F interface. Our explanation is similar to the Hanle effect-induced magnetoresistance in the two-dimensional electron gas proposed by Dyakonov [27]. Here we present the details of our theory, which is based on the spin-diffusion approximation in the N layer in the presence of spin-orbit interactions [28] and quantum mechanical boundary conditions at the interface in terms of the spin-mixing conductance [16, 17]. We also address F|N|F spin valves with electric currents applied parallel to the interface(s) with the additional degree of freedom of the relative angle between the two magnetizations directions.

This paper is organized as follows. We present the model, *i.e.* spin-diffusion with proper boundary conditions in Sec. 3.2. In Sec. 3.3, we consider an N|F bilayer as shown in Fig. 3.1 (a). We obtain spin accumulation, spin currents and finally the measured charge currents that are compared with the experimental SMR. We also find and discuss that the imaginary part of the spin-mixing conductance generates an AHE. F|N|F (Fig. 3.1 (b)) spin valves are investigated in Sec. 3.4, which show an enhanced SMR for spacers thinner than the spin-flip diffusion length. We summarize the results and give conclusions in Sec. 5.5.

## 3.2 TRANSPORT THEORY IN METALS IN CONTACT WITH A MAGNETIC INSULATOR

The spin current density in the non-relativistic limit

$$\vec{\mathbf{j}}_s = en \langle \vec{v} \otimes \vec{\sigma} + \vec{\sigma} \otimes \vec{v} \rangle / 2 = \left( \vec{j}_{sx}, \vec{j}_{sy}, \vec{j}_{sz} \right)^T = \left( \vec{j}_s^x, \vec{j}_s^y, \vec{j}_s^z \right) \quad (3.1)$$

is a second-order tensor (in units of the charge current density  $\vec{j}_c = en \langle \vec{v} \rangle$ ), where  $e = |e|$  is the electron charge,  $n$  is the density of the electrons,  $\vec{v}$  is the velocity

operator,  $\vec{\sigma}$  is the vector of Pauli spin matrices, and  $\langle \dots \rangle$  denotes an expectation value. The row vectors  $\vec{j}_{si} = en \langle \vec{v} \sigma_i + \sigma_i \vec{v} \rangle / 2$  in Eq. (5.6) are the spin current densities polarized in the  $\hat{i}$ -direction, while the column vectors  $\vec{j}_s^j = en \langle v_j \vec{\sigma} + \vec{\sigma} v_j \rangle / 2$  denote the spin current densities with polarization  $\vec{\sigma}$  flowing in the  $\hat{j}$ -direction. Ohm's law for metals with spin-orbit interactions can be summarized by the relation between thermodynamic driving forces and currents that reflects Onsager's reciprocity by the symmetry of the response matrix [28]:

$$\begin{pmatrix} \vec{j}_c \\ \vec{j}_{sx} \\ \vec{j}_{sy} \\ \vec{j}_{sz} \end{pmatrix} = \sigma \begin{pmatrix} 1 & \theta_{\text{SH}} \hat{x} \times & \theta_{\text{SH}} \hat{y} \times & \theta_{\text{SH}} \hat{z} \times \\ \theta_{\text{SH}} \hat{x} \times & 1 & 0 & 0 \\ \theta_{\text{SH}} \hat{y} \times & 0 & 1 & 0 \\ \theta_{\text{SH}} \hat{z} \times & 0 & 0 & 1 \end{pmatrix} \begin{pmatrix} -\vec{\nabla} \mu_0 / e \\ -\vec{\nabla} \mu_{sx} / (2e) \\ -\vec{\nabla} \mu_{sy} / (2e) \\ -\vec{\nabla} \mu_{sz} / (2e) \end{pmatrix}, \quad (3.2)$$

where  $\vec{\mu}_s = (\mu_{sx}, \mu_{sy}, \mu_{sz})^T - \mu_0 \hat{1}$  is the spin accumulation, *i.e.* the spin-dependent chemical potential relative to the charge chemical potential  $\mu_0$ ,  $\sigma$  is the electric conductivity,  $\theta_{\text{SH}}$  is the spin Hall angle, and “ $\times$ ” denotes the vector cross product operating on the gradients of the spin-dependent chemical potentials. The spin Hall effect is represented by the lower non-diagonal elements that generate the spin currents in the presence of an applied electric field, in the following chosen to be in the  $\hat{x}$ -direction  $\vec{E} = E_x \hat{x} = -\hat{x} \partial_x \mu_0 / e$ . The inverse spin Hall effect is governed by elements above the diagonal that connect the gradients of the spin accumulations to the charge current density.

The spin accumulation  $\vec{\mu}_s$  is obtained from the spin-diffusion equation in the normal metal

$$\nabla^2 \vec{\mu}_s = \frac{\vec{\mu}_s}{\lambda^2}, \quad (3.3)$$

where the spin-diffusion length  $\lambda = \sqrt{D\tau_{\text{sf}}}$  is expressed in terms of the charge diffusion constant  $D$  and spin-flip relaxation time  $\tau_{\text{sf}}$  [29]. For films with thickness  $d_N$  in the  $\hat{z}$ -direction

$$\vec{\mu}_s(z) = \vec{A} e^{-z/\lambda} + \vec{B} e^{z/\lambda}, \quad (3.4)$$

where the constant column vectors  $\vec{A}$  and  $\vec{B}$  are determined by the boundary conditions at the interfaces.

According to Eq. (4.8), the spin current in N consists of diffusion and spin Hall drift contributions. Since we are considering a system homogeneous in the  $x$ - $y$  plane, we focus on the spin current density flowing in the  $\hat{z}$ -direction

$$\vec{j}_s^z(z) = -\frac{\sigma}{2e} \partial_z \vec{\mu}_s - j_{s0}^{\text{SH}} \hat{y}, \quad (3.5)$$

where  $j_{s0}^{\text{SH}} = \theta_{\text{SH}} \sigma E_x$  is the bare spin Hall current, *i.e.*, the spin current generated directly by the SHE.

The boundary conditions require that  $\vec{j}_s^z(z)$  is continuous at the interfaces  $z = d_N$  and  $z = 0$ . The spin current at a vacuum (V) interface vanishes,  $\vec{j}_s^{(V)} = 0$ . The spin current density  $\vec{j}_s^{(F)}$  at a magnetic interface is governed by the spin accumulation and spin-mixing conductance [16]:

$$e\vec{j}_s^{(F)}(\hat{m}) = G_r \hat{m} \times (\hat{m} \times \vec{\mu}_s) + G_i (\hat{m} \times \vec{\mu}_s), \quad (3.6)$$

where  $\hat{m} = (m_x, m_y, m_z)^T$  is a unit vector along the magnetization and  $G_{\uparrow\downarrow} = G_r + iG_i$  the complex spin-mixing interface conductance per unit area. The imaginary part  $G_i$  can be interpreted as an effective exchange field acting on the spin accumulation. A positive current in Eq. (3.6) corresponds to up-spins flowing from F towards N. Since F is an insulator, this spin current density is proportional to the spin-transfer acting on the ferromagnet

$$\vec{\tau}_{\text{stt}} = -\frac{\hbar}{2e} \hat{m} \times (\hat{m} \times \vec{j}_s^{(F)}) = \frac{\hbar}{2e} \vec{j}_s^{(F)} \quad (3.7)$$

With these boundary conditions we determine the coefficients  $\vec{A}$  and  $\vec{B}$ , which leads to the spin accumulation

$$\vec{\mu}_s = \frac{2e\lambda}{\sigma} \left[ -\left( j_{s0}^{\text{SH}} \hat{y} + \vec{j}_s^z(d_N) \right) \cosh \frac{z}{\lambda} + \left( j_{s0}^{\text{SH}} \hat{y} + \vec{j}_s^{(F)}(\hat{m}) \right) \cosh \frac{z-d_N}{\lambda} \right] / \sinh \frac{d_N}{\lambda}, \quad (3.8)$$

where  $\vec{j}_s^z(d_N) = 0$  for F( $\hat{m}$ )|N|V bilayers and  $\vec{j}_s^z(d_N) = -\vec{j}_s^{(F)}(\hat{m}')$  for F( $\hat{m}$ )|N|F( $\hat{m}'$ ) spin valves.

### 3.3 N|F BILAYERS

In the bilayer the spin accumulation (3.8) is

$$\vec{\mu}_s(z) = -\hat{y}\mu_s^0 \frac{\sinh \frac{2z-d_N}{2\lambda}}{\sinh \frac{d_N}{2\lambda}} + \vec{j}_s^{(F)}(\hat{m}) \frac{2e\lambda}{\sigma} \frac{\cosh \frac{z-d_N}{\lambda}}{\sinh \frac{d_N}{\lambda}}, \quad (3.9)$$

where  $\mu_s^0 \equiv |\vec{\mu}_s(0)| = (2e\lambda/\sigma) j_{s0}^{\text{SH}} \tanh[d_N/(2\lambda)]$  is the spin accumulation at the interface in the absence of spin-transfer, *i.e.*, when  $G_{\uparrow\downarrow} = 0$ .

Using Eq. (3.6), the spin accumulation at  $z = 0$  becomes

$$\vec{\mu}_s(0) = \hat{y}\mu_s^0 + \frac{2\lambda}{\sigma} \{G_r [\hat{m}(\hat{m} \cdot \vec{\mu}_s(0)) - \vec{\mu}_s(0)] + G_i \hat{m} \times \vec{\mu}_s(0)\} \coth \frac{d_N}{\lambda}. \quad (3.10)$$

With

$$\hat{m} \cdot \vec{\mu}_s(0) = m_y \mu_s^0, \quad (3.11)$$

$$\hat{m} \times \vec{\mu}_s(0) = \mu_s^0 \frac{\sigma \hat{m} \times \hat{y} + \hat{m} m_y 2\lambda G_i \coth \frac{d_N}{\lambda}}{\sigma + 2\lambda G_r \coth \frac{d_N}{\lambda}} - \vec{\mu}_s(0) \frac{2\lambda G_i \coth \frac{d_N}{\lambda}}{\sigma + 2\lambda G_r \coth \frac{d_N}{\lambda}}, \quad (3.12)$$

$$\begin{aligned}
\vec{\mu}_s(0) = & \hat{y}\mu_s^0 \frac{1 + \frac{2\lambda}{\sigma} G_r \coth \frac{d_N}{\lambda}}{\left(1 + \frac{2\lambda}{\sigma} G_r \coth \frac{d_N}{\lambda}\right)^2 + \left(\frac{2\lambda}{\sigma} G_i \coth \frac{d_N}{\lambda}\right)^2} \\
& + \hat{m} m_y \mu_s^0 \frac{\frac{2\lambda}{\sigma} G_r \coth \frac{d_N}{\lambda} \left(1 + \frac{2\lambda}{\sigma} G_r \coth \frac{d_N}{\lambda}\right) + \left(\frac{2\lambda}{\sigma} G_i \coth \frac{d_N}{\lambda}\right)^2}{\left(1 + \frac{2\lambda}{\sigma} G_r \coth \frac{d_N}{\lambda}\right)^2 + \left(\frac{2\lambda}{\sigma} G_i \coth \frac{d_N}{\lambda}\right)^2} \\
& + (\hat{m} \times \hat{y}) \mu_s^0 \frac{\frac{2\lambda}{\sigma} G_i \coth \frac{d_N}{\lambda}}{\left(1 + \frac{2\lambda}{\sigma} G_r \coth \frac{d_N}{\lambda}\right)^2 + \left(\frac{2\lambda}{\sigma} G_i \coth \frac{d_N}{\lambda}\right)^2}, \quad (3.13)
\end{aligned}$$

the spin current through the F|N interface then reads

$$\vec{j}_s^{(F)} = \frac{\mu_s^0}{e} \hat{m} \times (\hat{m} \times \hat{y}) \sigma \operatorname{Re} \frac{G_{\uparrow\downarrow}}{\sigma + 2\lambda G_{\uparrow\downarrow} \coth \frac{d_N}{\lambda}} + \frac{\mu_s^0}{e} (\hat{m} \times \hat{y}) \sigma \operatorname{Im} \frac{G_{\uparrow\downarrow}}{\sigma + 2\lambda G_{\uparrow\downarrow} \coth \frac{d_N}{\lambda}}. \quad (3.14)$$

The spin accumulation

$$\frac{\vec{\mu}_s(z)}{\mu_s^0} = -\hat{y} \frac{\sinh \frac{2z-d_N}{2\lambda}}{\sinh \frac{d_N}{2\lambda}} + [\hat{m} \times (\hat{m} \times \hat{y}) \operatorname{Re} + (\hat{m} \times \hat{y}) \operatorname{Im}] \frac{2\lambda G_{\uparrow\downarrow}}{\sigma + 2\lambda G_{\uparrow\downarrow} \coth \frac{d_N}{\lambda}} \frac{\cosh \frac{z-d_N}{\lambda}}{\sinh \frac{d_N}{\lambda}}, \quad (3.15)$$

then leads to the distributed spin current in N

$$\frac{\vec{j}_s^z(z)}{j_{s0}^{\text{SH}}} = \hat{y} \frac{\cosh \frac{2z-d_N}{2\lambda} - \cosh \frac{d_N}{2\lambda}}{\cosh \frac{d_N}{2\lambda}} - [\hat{m} \times (\hat{m} \times \hat{y}) \operatorname{Re} + (\hat{m} \times \hat{y}) \operatorname{Im}] \frac{2\lambda G_{\uparrow\downarrow} \tanh \frac{d_N}{2\lambda}}{\sigma + 2\lambda G_{\uparrow\downarrow} \coth \frac{d_N}{\lambda}} \frac{\sinh \frac{z-d_N}{\lambda}}{\sinh \frac{d_N}{\lambda}}. \quad (3.16)$$

The ISHE drives a charge current in the  $x$ - $y$  plane by the diffusion spin current component flowing along the  $\hat{z}$ -direction. The total longitudinal (along  $\hat{x}$ ) and transverse or Hall (along  $\hat{y}$ ) charge currents become

$$\frac{j_{c,\text{long}}(z)}{j_c^0} = 1 + \theta_{\text{SH}}^2 \left[ \frac{\cosh \frac{2z-d_N}{2\lambda}}{\cosh \frac{d_N}{2\lambda}} + (1 - m_y^2) \operatorname{Re} \frac{2\lambda G_{\uparrow\downarrow} \tanh \frac{d_N}{2\lambda}}{\sigma + 2\lambda G_{\uparrow\downarrow} \coth \frac{d_N}{\lambda}} \frac{\sinh \frac{z-d_N}{\lambda}}{\sinh \frac{d_N}{\lambda}} \right], \quad (3.17)$$

$$\frac{j_{c,\text{trans}}(z)}{j_c^0} = \theta_{\text{SH}}^2 (m_x m_y \operatorname{Re} - m_z \operatorname{Im}) \frac{2\lambda G_{\uparrow\downarrow} \tanh \frac{d_N}{2\lambda}}{\sigma + 2\lambda G_{\uparrow\downarrow} \coth \frac{d_N}{\lambda}} \frac{\sinh \frac{z-d_N}{\lambda}}{\sinh \frac{d_N}{\lambda}}, \quad (3.18)$$

where  $j_c^0 = \sigma E_x$  is the charge current driven by the external electric field.

The charge current vector is the observable in the experiment that is usually expressed in terms of the longitudinal and transverse (Hall) resistivities. Averaging

the electric currents over the film thickness  $z$  and expanding the longitudinal resistivity governed by the current in the ( $x$ -)direction of the applied field to leading order in  $\theta_{\text{SH}}^2$ , we obtain

$$\rho_{\text{long}} = \sigma_{\text{long}}^{-1} = \left( \frac{\overline{j_{c,\text{long}}}}{E_x} \right)^{-1} \approx \rho + \Delta\rho_0 + \Delta\rho_1 (1 - m_y^2), \quad (3.19)$$

$$\rho_{\text{trans}} = -\frac{\sigma_{\text{trans}}}{\sigma_{\text{long}}^2} \approx -\frac{\overline{j_{c,\text{trans}}/E_x}}{\sigma^2} = \Delta\rho_1 m_x m_y + \Delta\rho_2 m_z, \quad (3.20)$$

where

$$\frac{\Delta\rho_0}{\rho} = -\theta_{\text{SH}}^2 \frac{2\lambda}{d_N} \tanh \frac{d_N}{2\lambda}, \quad (3.21)$$

$$\frac{\Delta\rho_1}{\rho} = \theta_{\text{SH}}^2 \frac{\lambda}{d_N} \text{Re} \frac{2\lambda G_{\uparrow\downarrow} \tanh^2 \frac{d_N}{2\lambda}}{\sigma + 2\lambda G_{\uparrow\downarrow} \coth \frac{d_N}{\lambda}}, \quad (3.22)$$

$$\frac{\Delta\rho_2}{\rho} = -\theta_{\text{SH}}^2 \frac{\lambda}{d_N} \text{Im} \frac{2\lambda G_{\uparrow\downarrow} \tanh^2 \frac{d_N}{2\lambda}}{\sigma + 2\lambda G_{\uparrow\downarrow} \coth \frac{d_N}{\lambda}}, \quad (3.23)$$

where  $\rho = \sigma^{-1}$  is the intrinsic electric resistivity of the bulk normal metal.  $\Delta\rho_0 < 0$  seems to imply that the resistivity is reduced by the spin-orbit interaction. However, this is an effect of the order of  $\theta_{\text{SH}}^2$  that becomes relevant only when  $d_N$  is sufficiently small. The spin-orbit interaction also generates spin-flip scattering that increases the resistance to leading order according to Matthiessen's rule. We see that  $\Delta\rho_1$  (caused mainly by  $G_r$ ) contributes to the SMR, while  $\Delta\rho_2$  (caused mainly by  $G_i$ ) contributes only when there is a magnetization component normal to the plane (AHE), as discussed below.

### 3.3.1 LIMIT OF $G_i = \text{Im} G_{\uparrow\downarrow} \ll \text{Re} G_{\uparrow\downarrow} = G_r$

According to first principles calculations [17],  $|G_i|$  is at least one order of magnitude smaller than  $G_r$  for YIG, so  $G_i = 0$  appears to be a good first approximation. In this limit, we plot normalized components of spin accumulation ( $\mu_{sx}$  and  $\mu_{sy}$ ) and spin current ( $j_{sx} = \vec{j}_s^z \cdot \hat{x}$  and  $j_{sy} = \vec{j}_s^z \cdot \hat{y}$ ) as functions of  $z$  for different magnetizations in Fig 3.2. When the magnetization of F is along  $\hat{y}$ , the spin current at the N|F interface ( $z = 0$ ) vanishes just as for the vacuum interface. By rotating the magnetization from  $\hat{y}$  to  $\hat{x}$ , the spin current at the N|F interface and the torque on the magnetization is activated, while the spin accumulation is dissipated correspondingly. We note that the  $x$ -components of both spin accumulation and spin

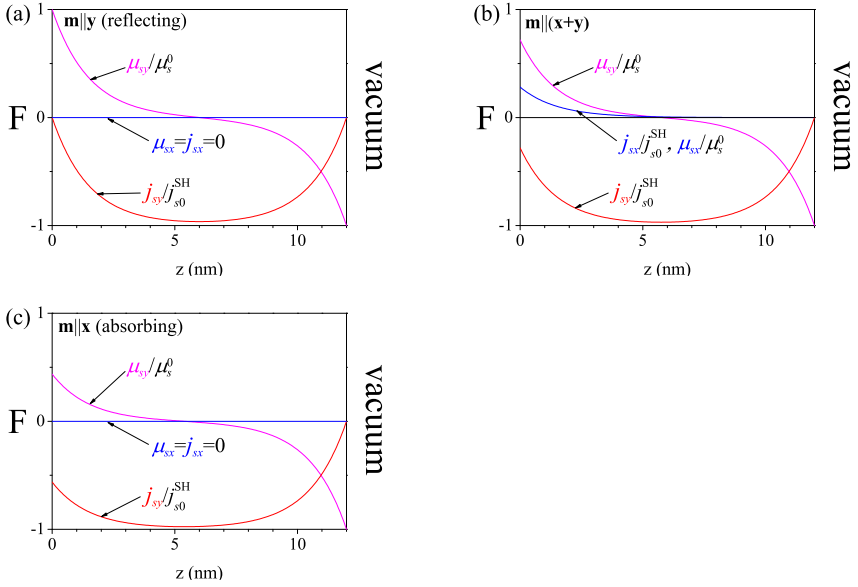


FIGURE 3.2: (Color online). Normalized  $\mu_{sx}$ ,  $\mu_{sy}$ ,  $j_{sx}$ , and  $j_{sy}$  as functions of  $z$  for magnetizations (a)  $\hat{m} = \hat{y}$ , (b)  $\hat{m} = (\hat{x} + \hat{y})/\sqrt{2}$ , and (c)  $\hat{m} = \hat{x}$  for a sample with  $d_N = 12$  nm. We adopt the transport parameters  $\rho = 8.6 \times 10^{-7} \Omega \text{m}$ ,  $\lambda = 1.5$  nm, and  $G_T = 5 \times 10^{14} \Omega^{-1} \text{m}^{-2}$ . For magnetizations  $\hat{m} = \hat{y}$  and  $\hat{m} = \hat{x}$ , both  $\mu_{sx}$  and  $j_{sx}$  are 0.

current vanish when the magnetization is along  $\hat{x}$  and  $\hat{y}$ , and reach a maximum value at  $(\hat{x} + \hat{y})/\sqrt{2}$ .

For  $G_i = 0$  the observable transport properties reduce to

$$\rho_{\text{long}} \approx \rho + \Delta\rho_0 + \Delta\rho_1 \left(1 - m_y^2\right), \quad (3.24)$$

$$\rho_{\text{trans}} \approx \Delta\rho_1 m_x m_y, \quad (3.25)$$

where

$$\frac{\Delta\rho_0}{\rho} = -\theta_{\text{SH}}^2 \frac{2\lambda}{d_N} \tanh \frac{d_N}{2\lambda}, \quad (3.26)$$

$$\frac{\Delta\rho_1}{\rho} = \theta_{\text{SH}}^2 \frac{\lambda}{d_N} \frac{2\lambda G_r \tanh^2 \frac{d_N}{2\lambda}}{\sigma + 2\lambda G_r \coth \frac{d_N}{\lambda}}. \quad (3.27)$$

Equations (3.24-3.25) fully explain the magnetization dependence of SMR in Ref. [25], while Eq. (3.27) shows that an SMR exists only when the spin-mixing conductance does not vanish. Since results do not depend on the  $z$ -component of magnetization, the AHE vanishes in our model when  $G_i = 0$ .

### 3.3.2 $G_r \gg \sigma / (2\lambda)$

Here we discuss the limit in which the spin current transverse to  $\hat{m}$  is completely absorbed as an STT without reflection. This ideal situation is actually not so far from reality for the recently found large  $G_r$  between YIG and noble metals [17, 18]. The spin current at the interface is then

$$\frac{\vec{j}_s^{(\text{F})}}{j_{s0}^{\text{SH}}} \stackrel{G_r \gg \sigma / (2\lambda)}{=} \hat{m} \times (\hat{m} \times \hat{y}) \tanh \frac{d_N}{\lambda} \tanh \frac{d_N}{2\lambda}, \quad (3.28)$$

and the maximum magnetoresistance for the bilayer is

$$\frac{\Delta\rho_1}{\rho} = \theta_{\text{SH}}^2 \frac{\lambda}{d_N} \tanh \frac{d_N}{\lambda} \tanh^2 \frac{d_N}{2\lambda}. \quad (3.29)$$

In Sec. 3.3.5 we test this limit with available parameters from experiments.

### 3.3.3 $\lambda / d_N \gg 1$

When the spin-diffusion length is much larger than the thickness of N

$$\frac{\vec{\mu}_s(z)}{\mu_s^0} \stackrel{\lambda / d_N \gg 1}{=} \hat{m} \times (\hat{m} \times \hat{y}) - \hat{y} \frac{2z - d_N}{d_N},$$

while spin current and magnetoresistance vanish. We can interpret this as multiple scattering of the spin current at the interfaces; the ISHE has both positive and negative charge current contributions that cancel each other.

### 3.3.4 SPIN HALL AHE

Recent measurements in YIG|Pt display a small AHE-like signal on top of the ordinary Hall effect, *i.e.* a transverse voltage when the magnetization is normal to the film [31]. As mentioned above, an imaginary part of the spin-mixing conductance  $G_i$  can cause a spin Hall AHE (SHAHE).

The component of the spin accumulation  $\mu_{sx}$

$$\frac{\mu_{sx}(z)}{\mu_s^0} = \frac{2\lambda}{\sigma} \frac{\cosh \frac{z-d_N}{\lambda}}{\sinh \frac{d_N}{\lambda}} [m_x m_y \operatorname{Re} - m_z \operatorname{Im}] \frac{\sigma G_{\uparrow\downarrow}}{\sigma + 2\lambda G_{\uparrow\downarrow} \coth \frac{d_N}{\lambda}} \quad (3.30)$$

contains a contribution that scales with  $m_z$  and contributes a charge current in the transverse ( $\hat{y}$ -) direction

$$\frac{j_{c,\text{trans}}^{(\text{SHAHE})}(z)}{j_c^0} = -2\lambda \theta_{\text{SH}}^2 m_z \frac{\sinh \frac{z-d_N}{\lambda}}{\sinh \frac{d_N}{\lambda}} \operatorname{Im} \frac{G_{\uparrow\downarrow} \tanh \frac{d_N}{2\lambda}}{\sigma + 2\lambda G_{\uparrow\downarrow} \coth \frac{d_N}{\lambda}}. \quad (3.31)$$

The transverse resistivity due to this current is

$$\rho_{\text{trans}}^{(\text{SHAHE})} \approx -\frac{\overline{j_{c,\text{trans}}^{(\text{SHAHE})}}/E_x}{\sigma^2} = -\Delta\rho_2 m_z, \quad (3.32)$$

where

$$\frac{\Delta\rho_2}{\rho} \approx \frac{2\lambda^2 \theta_{\text{SH}}^2}{d_N} \frac{\sigma G_i \tanh^2 \frac{d_N}{2\lambda}}{\left(\sigma + 2\lambda G_r \coth \frac{d_N}{\lambda}\right)^2 + \left(2\lambda G_i \coth \frac{d_N}{\lambda}\right)^2} \approx \frac{2\lambda^2 \theta_{\text{SH}}^2}{d_N} \frac{\sigma G_i \tanh^2 \frac{d_N}{2\lambda}}{\left(\sigma + 2\lambda G_r \coth \frac{d_N}{\lambda}\right)^2}.$$

### 3.3.5 COMPARISON WITH EXPERIMENTS

There are controversies about the values of the material parameters relevant for our theory, *i.e.* the spin-mixing conductance  $G_{\uparrow\downarrow}$  of the N|F interface, as well as spin-flip diffusion length  $\lambda$  and spin Hall angle  $\theta_{\text{SH}}$  in the normal metal.

Experimentally, Burrows *et al.* [18] found for an Au|YIG interface with  $G_0 = e^2/h$ .

$$\frac{G_r^{\text{exp}}}{G_0} = 5.2 \times 10^{18} \text{ m}^{-2}; \quad G_r^{\text{exp}} = 2 \times 10^{14} \Omega^{-1} \text{ m}^{-2}. \quad (3.33)$$

On the theory side, the spin-mixing conductance from scattering theory for an insulator reads [16]

$$\frac{G_{\uparrow\downarrow}}{G_0} = N_{\text{Sh}} - \sum_n r_{n\uparrow}^* r_{n\downarrow} = N_{\text{Sh}} - \sum_n e^{i(\delta_{n\downarrow} - \delta_{n\uparrow})}, \quad (3.34)$$

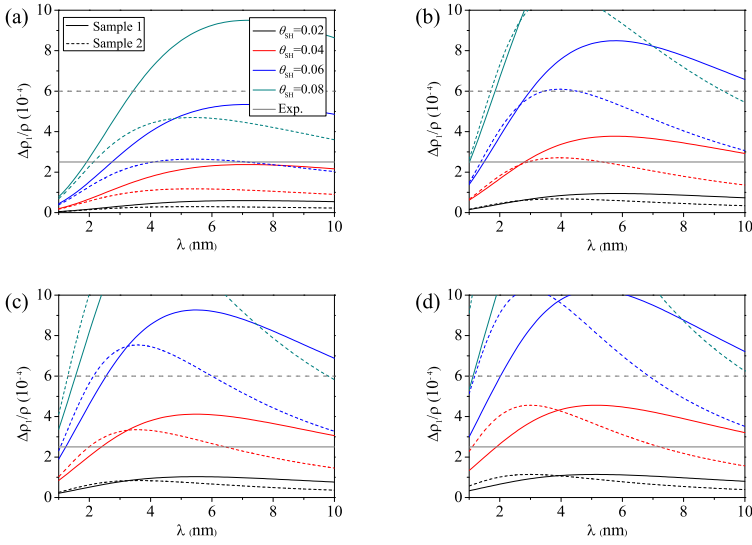


FIGURE 3.3: (Color online) Calculated  $\Delta\rho_1/\rho$  as a function of  $\lambda$  for different spin Hall angles  $\theta_{\text{SH}}$  with (a)  $G_r = 1 \times 10^{14} \Omega^{-1} \text{m}^{-2}$ , (b)  $G_r = 5 \times 10^{14} \Omega^{-1} \text{m}^{-2}$ , (c)  $G_r = 10 \times 10^{14} \Omega^{-1} \text{m}^{-2}$ , and (d) the ideal limit  $G_r \gg \sigma/(2\lambda)$ . The Pt layers are 12-nm-thick with resistivity  $8.6 \times 10^{-7} \Omega \text{m}$  (Sample 1, solid curve) and 7-nm-thick with resistivity  $4.1 \times 10^{-7} \Omega \text{m}$  (Sample 2, dashed curve). Experimental results are shown as horizontal lines for comparison [25].

where  $r_{n\uparrow(\downarrow)} = e^{i\delta_{n\uparrow(\downarrow)}}$  is the reflection coefficient of an electron in the quantum channel  $n$  on a unit area at the N|F interface with unit modulus and phase  $\delta_{n\uparrow(\downarrow)}$  for the majority (minority) spin, and  $N_{\text{Sh}}$  is the number of transport channels (per unit area) at the Fermi energy, *i.e.*  $N_{\text{Sh}}$  is the Sharvin conductance (for one spin). Therefore

$$\frac{G_r}{G_0} \leq 2N_{\text{Sh}}; \quad \frac{|G_i|}{G_0} \leq N_{\text{Sh}}, \quad (3.35)$$

Jia *et al.* [17] computed Eq. (3.34) for a Ag|YIG interface by first principles. The average of different crystal interfaces

$$G_r^{(0)} = 2.3 \times 10^{14} \Omega^{-1} \text{m}^{-2}, \quad (3.36)$$

is quite close to the Sharvin conductance of silver ( $N_{\text{Sh}}G_0 \approx 4.5 \times 10^{14} \Omega^{-1} \text{m}^{-2}$ ).

For comparison with experiment we have to include the Schep drift correction [32]:

$$\frac{1}{\tilde{G}_r/G_0} = \frac{1}{G_r^{(0)}/G_0} - \frac{1}{2N_{\text{Sh}}}, \quad (3.37)$$

which leads to

$$\tilde{G}_r \approx 3.1 \times 10^{14} \Omega^{-1} \text{m}^{-2}. \quad (3.38)$$

One should note that the mixing conductance of the Pt|YIG interface can then be estimated to be  $\tilde{G}_r \approx 10^{15} \Omega^{-1} \text{m}^{-2}$  since the Pt conduction electron density and Sharvin conductance are higher than those of noble metals.

Using parameters  $\rho = \sigma^{-1} = 8.6 \times 10^{-7} \Omega \text{m}$ ,  $d_N = 12 \text{ nm}$ , and  $\lambda = 1.5 \text{ nm}$  [30], we see that the absorbed transverse spin currents with  $G_r = \tilde{G}_r$  and  $G_r = G_r^{\text{max}}$  obtained from above for a Ag|YIG interface are 44% and 70% of the value for a perfect spin sink  $G_r \rightarrow \infty$ , respectively. For a Pt|YIG interface this value should be even larger.

In order to compare our results with the observed SMR, we have to fill in or fit the parameters. The values of the spin-diffusion length and the spin Hall angle differ widely [30]. In Fig. 3.3 we plot the SMR for three fixed values of  $G_r$ . We observe that the experiments can be explained by a sensible set of transport parameters ( $G_r$ ,  $\lambda$ ,  $\theta_{\text{SH}}$ ) that somewhat differ for the two representative samples reported in Ref. [25]. Generally, the SMR increases with a larger value of  $G_r$  but decreases when  $\lambda$  is getting longer. These features are in agreement with the discussion of the simple limits above. Sample 1 in Ref. [25] has a larger resistivity but a smaller SMR (ratio), implying a smaller spin Hall angle and/or smaller spin-diffusion length. When we fix the spin Hall angle  $\theta_{\text{SH}} = 0.06$  and the spin-mixing conductance  $G_r = 5 \times 10^{14} \Omega^{-1} \text{m}^{-2}$ , the corresponding estimated spin-diffusion lengths of Samples 1 and 2 are  $\lambda_1 \approx 1.5 \text{ nm}$  and  $\lambda_2 \approx 3.5 \text{ nm}$ , respectively.

Finally we discuss the AHE equivalent or SHAHE. From experiments  $\Delta\rho_2/\rho \approx 1.5 \times 10^{-5}$  for  $\rho = 4.1 \times 10^{-7} \Omega\text{m}$  and  $d_N = 7 \text{ nm}$  [31]. Choosing  $\theta_{\text{SH}} = 0.05$ ,  $\lambda = 1.5 \text{ nm}$ , and  $G_r = 5 \times 10^{14} \Omega^{-1} \text{ m}^{-2}$ , we would need a  $G_i = 6.2 \times 10^{13} \Omega^{-1} \text{ m}^{-2}$  to explain experiments, a number that is supported by first principles calculations [17].

### 3.4 SPIN VALVES

In this section we discuss F( $\hat{m}$ )|N|F( $\hat{m}'$ ) spin valves fabricated from magnetic insulators with magnetization directions  $\hat{m}$  and  $\hat{m}'$ . The general angle dependence for independent rotations of  $\hat{m}$  and  $\hat{m}'$  is straightforward but tedious. We discuss in the following two representative configurations in which the two magnetizations are parallel and perpendicular to each other. We disregard in the following the effective field due to  $G_i$  such that the parallel and antiparallel configurations  $\hat{m} = \pm \hat{m}'$  are equivalent. Moreover, we limit the discussion to the simple case of two identical F|N and N|F interfaces, *i.e.*, the spin-mixing conductances at both interfaces are the same.

#### 3.4.1 PARALLEL CONFIGURATION ( $\hat{m} \cdot \hat{m}' = \pm 1$ )

When the magnetizations are aligned in parallel or antiparallel configuration, the boundary condition  $\vec{j}_s^{(z)}(d_N) = -\vec{j}_s^{(\text{F})}$  applies. We proceed as in Sec. 3.3 to obtain the spin accumulation

$$\frac{\vec{\mu}_s}{\mu_s^0} = - \left[ \hat{y} + \hat{m} \times (\hat{m} \times \hat{y}) \frac{2\lambda G_r \tanh \frac{d_N}{2\lambda}}{\sigma + 2\lambda G_r \tanh \frac{d_N}{2\lambda}} \right] \frac{\sinh \frac{2z-d_N}{2\lambda}}{\sinh \frac{d_N}{2\lambda}}, \quad (3.39)$$

and the spin current

$$\frac{\vec{j}_s^z}{j_{s0}^{\text{SH}}} = \hat{y} \left( \frac{\cosh \frac{2z-d_N}{2\lambda}}{\cosh \frac{d_N}{2\lambda}} - 1 \right) + \hat{m} \times (\hat{m} \times \hat{y}) \frac{2\lambda G_r \tanh \frac{d_N}{2\lambda}}{\sigma + 2\lambda G_r \tanh \frac{d_N}{2\lambda}} \frac{\cosh \frac{2z-d_N}{2\lambda}}{\cosh \frac{d_N}{2\lambda}}.$$

The spin currents at the bottom and top of N are absorbed as STTs and read

$$\frac{\vec{j}_s^z(0)}{j_{s0}^{\text{SH}}} = \frac{\vec{j}_s^z(d_N)}{j_{s0}^{\text{SH}}} = \hat{m} \times (\hat{m} \times \hat{y}) \frac{2\lambda G_r \tanh \frac{d_N}{2\lambda}}{\sigma + 2\lambda G_r \tanh \frac{d_N}{2\lambda}}, \quad (3.40)$$

leading to opposite STTs at the bottom ( $\vec{\tau}_{\text{stt}}^{(\text{B})}$ ) and top ( $\vec{\tau}_{\text{stt}}^{(\text{T})}$ ) ferromagnets

$$\vec{\tau}_{\text{stt}}^{(\text{B})} = \frac{\hbar}{2e} \vec{j}_s^z(0) = -\vec{\tau}_{\text{stt}}^{(\text{T})} \quad (3.41)$$

since  $\vec{j}_s^{(\text{F})}(\hat{m}) = \vec{j}_s^z(0) = \vec{j}_s^z(d_N) = -\vec{j}_s^{(\text{F})}(\hat{m}')$ .

The longitudinal and transverse (Hall) charge currents are

$$\frac{j_{c,\text{long}}}{j_c^0} = 1 + \theta_{\text{SH}}^2 \left[ 1 - (1 - m_y^2) \frac{2\lambda G_r \tanh \frac{d_N}{2\lambda}}{\sigma + 2\lambda G_r \tanh \frac{d_N}{2\lambda}} \right] \frac{\cosh \frac{2z - d_N}{2\lambda}}{\cosh \frac{d_N}{2\lambda}}, \quad (3.42)$$

$$\frac{j_{c,\text{trans}}}{j_c^0} = -\theta_{\text{SH}}^2 m_x m_y \frac{2\lambda G_r \tanh \frac{d_N}{2\lambda}}{\sigma + 2\lambda G_r \tanh \frac{d_N}{2\lambda}} \frac{\cosh \frac{2z - d_N}{2\lambda}}{\cosh \frac{d_N}{2\lambda}}. \quad (3.43)$$

and the longitudinal and transverse resistivities read

$$\rho_{\text{long}} = \rho + \Delta\rho_0 + \Delta\rho_1 (1 - m_y^2), \quad (3.44)$$

$$\rho_{\text{trans}} = \Delta\rho_1 m_x m_y, \quad (3.45)$$

where

$$\frac{\Delta\rho_0}{\rho} = -\theta_{\text{SH}}^2 \frac{2\lambda}{d_N} \tanh \frac{d_N}{2\lambda}, \quad (3.46)$$

$$\frac{\Delta\rho_1}{\rho} = \frac{\theta_{\text{SH}}^2}{d_N} \frac{4\lambda^2 G_r \tanh^2 \frac{d_N}{2\lambda}}{\sigma + 2\lambda G_r \tanh \frac{d_N}{2\lambda}}. \quad (3.47)$$

Figure 3.4 shows  $\Delta\rho_1 / (\rho\theta_{\text{SH}}^2)$  with respect to the spin-diffusion length in an F|N|F spin valve with parallel magnetization configuration. Compared to N|F bilayers, the SMR in spin valves is larger and does not vanish in the limit of long spin-diffusion lengths.

### 3.4.2 LIMIT $\lambda/d_N \gg 1$

The spin accumulation for weak spin-flip reads

$$\frac{\vec{\mu}_s}{\mu_s^0} \stackrel{\lambda/d_N \gg 1}{\approx} - \left[ \hat{y} + \frac{d_N G_r}{\sigma + d_N G_r} \hat{m} \times (\hat{m} \times \hat{y}) \right] \frac{2z - d_N}{d_N}, \quad (3.48)$$

leading to the spin current

$$\frac{\vec{j}_s^z}{j_{s0}^{\text{SH}}} \stackrel{\lambda/d_N \gg 1}{\approx} \frac{d_N G_r}{\sigma + d_N G_r} \hat{m} \times (\hat{m} \times \hat{y}). \quad (3.49)$$

In contrast to the bilayer, we find a finite SMR in this limit for spin valves:

$$\frac{j_{c,\text{long}}}{j_c^0} \stackrel{\lambda/d_N \gg 1}{\approx} 1 + \theta_{\text{SH}}^2 \left[ 1 - \frac{d_N G_r}{\sigma + d_N G_r} (1 - m_y^2) \right] \stackrel{G_r \gg \sigma/d_N}{\approx} 1 + \theta_{\text{SH}}^2 m_y^2, \quad (3.50)$$

$$\frac{j_{c,\text{trans}}}{j_c^0} \stackrel{\lambda/d_N \gg 1}{\approx} -\theta_{\text{SH}}^2 \frac{d_N G_r}{\sigma + d_N G_r} m_x m_y \stackrel{G_r \gg \sigma/d_N}{\approx} -\theta_{\text{SH}}^2 m_x m_y \quad (3.51)$$

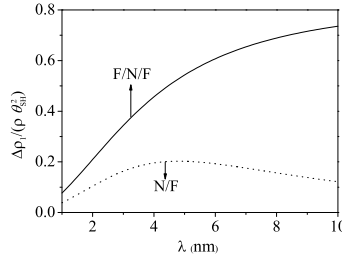


FIGURE 3.4: (Color online) Calculated  $\Delta\rho_1 / (\rho\theta_{\text{SH}}^2)$  in an F|N|F spin valve as a function of spin-diffusion length  $\lambda$  with  $d_N = 12$  nm,  $G_r = 5 \times 10^{14} \Omega^{-1} \text{m}^{-2}$ , and  $\rho = 8.6 \times 10^{-7} \Omega \text{m}$  chosen from Sample 1 in Ref. [25].  $\Delta\rho_1 / (\rho\theta_{\text{SH}}^2)$  in an N|F bilayer is plotted as a dotted line for comparison.

or

$$\frac{\Delta\rho_0}{\rho} = -\theta_{\text{SH}}^2, \quad (3.52)$$

$$\frac{\Delta\rho_1}{\rho} = \theta_{\text{SH}}^2 \frac{d_N G_r}{\sigma + d_N G_r} \stackrel{G_r \gg \sigma/d_N}{\approx} \theta_{\text{SH}}^2. \quad (3.53)$$

Here we find the maximum achievable SMR effects in metals with spin Hall angle  $\theta_{\text{SH}}$  by taking the limit of perfect spin current absorption. Clearly this requires spin valves with sufficiently thin spacer layers. We interpret these results in terms of spin angular momentum conservation: The finite SMR is achieved by using the ferromagnet as a spin sink that suppresses the back flow of spins and the ISHE. This process requires a source of angular momentum, which in bilayers can only be the lattice of the normal metal. Consequently, the SMR is suppressed in the F|N system when spin-flip is not allowed. In spin valves, however, the second ferromagnet layer can act as a spin current source, thereby allowing a finite SMR even in the absence of spin-flip scattering.

### 3.4.3 PERPENDICULAR CONFIGURATION ( $\hat{m} \cdot \hat{m}' = 0$ )

We may consider two in-plane magnetizations  $\hat{m} = (\cos \alpha, \sin \alpha, 0)$  and  $\hat{m}' = (-\sin \alpha, \cos \alpha, 0)$ , which are perpendicular to each other. When  $\alpha = 0$ , the first layer maximally absorbs the SHE spin current, while  $\hat{m}'$  is completely reflecting, just as the vacuum

interface in the bilayer. For general  $\alpha$ :

$$\frac{\mu_{sx}(z)}{\mu_s^0} = \frac{2\lambda G_r}{\sigma + 2\lambda G_r \coth \frac{d_N}{\lambda}} \left( \frac{\cosh \frac{z-d_N}{\lambda}}{\sinh \frac{d_N}{\lambda}} + \frac{\cosh \frac{z}{\lambda}}{\sinh \frac{d_N}{\lambda}} \right) \cos \alpha \sin \alpha, \quad (3.54)$$

$$\frac{\mu_{sy}(z)}{\mu_s^0} = -\frac{\sinh \frac{2z-d_N}{2\lambda}}{\sinh \frac{d_N}{2\lambda}} - \frac{2\lambda G_r}{\sigma + 2\lambda G_r \coth \frac{d_N}{\lambda}} \left( \frac{\cosh \frac{z-d_N}{\lambda}}{\sinh \frac{d_N}{\lambda}} \cos^2 \alpha - \frac{\cosh \frac{z}{\lambda}}{\sinh \frac{d_N}{\lambda}} \sin^2 \alpha \right), \quad (3.55)$$

$$\mu_{sz}(z) = 0, \quad (3.56)$$

which leads to the components of spin current normal to the interfaces

$$\frac{j_{sx}(z)}{j_{s0}^{\text{SH}}} = -\frac{2\lambda G_r \tanh \frac{d_N}{2\lambda}}{\sigma + 2\lambda G_r \coth \frac{d_N}{\lambda}} \left( \frac{\sinh \frac{z-d_N}{\lambda}}{\sinh \frac{d_N}{\lambda}} + \frac{\sinh \frac{z}{\lambda}}{\sinh \frac{d_N}{\lambda}} \right) \cos \alpha \sin \alpha, \quad (3.57)$$

$$\frac{j_{sy}(z)}{j_{s0}^{\text{SH}}} = \frac{\cosh \frac{2z-d_N}{2\lambda} - \cosh \frac{d_N}{2\lambda}}{\cosh \frac{d_N}{2\lambda}} + \frac{2\lambda G_r \tanh \frac{d_N}{2\lambda}}{\sigma + 2\lambda G_r \coth \frac{d_N}{\lambda}} \left( \frac{\sinh \frac{z-d_N}{\lambda}}{\sinh \frac{d_N}{\lambda}} \cos^2 \alpha - \frac{\sinh \frac{z}{\lambda}}{\sinh \frac{d_N}{\lambda}} \sin^2 \alpha \right). \quad (3.58)$$

The total current is the sum of those from the two ferromagnets at the top and bottom; in contrast to the parallel  $\hat{m} = \pm \hat{m}'$  configuration, they do not feel each other. We can extend the discussion from the previous subsection: the second F can be a spin current source, and we can switch this source on by rotating the magnetization from perpendicular to (anti)parallel configuration.

The longitudinal and transverse electric currents read

$$\frac{j_{c,\text{long}}(z)}{j_c^0} = 1 + \theta_{\text{SH}}^2 \frac{\cosh \frac{2z-d_N}{2\lambda}}{\cosh \frac{d_N}{2\lambda}} + \theta_{\text{SH}}^2 \frac{2\lambda G_r \tanh \frac{d_N}{2\lambda}}{\sigma + 2\lambda G_r \coth \frac{d_N}{\lambda}} \left( \frac{\sinh \frac{z-d_N}{\lambda}}{\sinh \frac{d_N}{\lambda}} \cos^2 \alpha - \frac{\sinh \frac{z}{\lambda}}{\sinh \frac{d_N}{\lambda}} \sin^2 \alpha \right), \quad (3.59)$$

$$\frac{j_{c,\text{trans}}(z)}{j_c^0} = \theta_{\text{SH}}^2 \frac{2\lambda G_r \tanh \frac{d_N}{2\lambda}}{\sigma + 2\lambda G_r \coth \frac{d_N}{\lambda}} \left( \frac{\sinh \frac{z-d_N}{\lambda}}{\sinh \frac{d_N}{\lambda}} + \frac{\sinh \frac{z}{\lambda}}{\sinh \frac{d_N}{\lambda}} \right) \cos \alpha \sin \alpha. \quad (3.60)$$

Since the angle-dependent contributions vanish upon integration over  $z$ , there is no magnetoresistance in the perpendicular configuration.

### 3.4.4 CONTROLLING THE SPIN-TRANSFER TORQUE

Like the SMR, the STT at the N|F interface depends on the relative orientation between  $\hat{m}$  and  $\hat{m}'$ , too. We may pin  $\hat{m} = \hat{x}$  and observe how the STT at the bottom

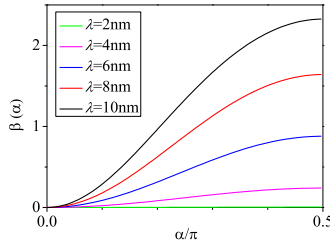


FIGURE 3.5: (Color online) The ratio  $\beta(\alpha)$  which characterizes how  $\bar{\tau}_{\text{stt}}^{(\text{B})}$  changes with respect to the relative orientation between  $\hat{m}$  and  $\hat{m}'$ . We adopt the transport parameters  $d_N = 12$  nm,  $\rho = 8.6 \times 10^{-7} \Omega\text{m}$ , and  $G_r = 5 \times 10^{14} \Omega^{-1}\text{m}^{-2}$ .

magnet,  $\bar{\tau}_{\text{stt}}^{(\text{B})}(\hat{m}, \hat{m}')$ , changes with rotating  $\hat{m}' = \hat{x} \cos \alpha + \hat{y} \sin \alpha$ . Figure 3.5 displays the ratio  $\beta$  defined as

$$\beta(\alpha) \equiv \frac{\left| \bar{\tau}_{\text{stt}}^{(\text{B})}(\hat{x}, \hat{x}) - \bar{\tau}_{\text{stt}}^{(\text{B})}(\hat{x}, \hat{x} \cos \alpha + \hat{y} \sin \alpha) \right|}{\left| \bar{\tau}_{\text{stt}}^{(\text{B})}(\hat{x}, \hat{x}) \right|}, \quad (3.61)$$

as a function of  $\alpha$  for some spin-diffusion lengths. Only when  $\lambda \ll d_N$ ,  $\beta$  remains constant under rotation of  $\hat{m}'$ . A larger spin-mixing conductance and smaller  $d_N$  enhances the SMR as well as angle dependence of  $\beta$ . This modification of the STT should lead to complex dynamics of the spin valve in the presence of an applied current and will be the subject of a subsequent study.

### 3.5 SUMMARY

We developed a theory for the SMR in N|F and F|N|F systems that takes into account the spin-orbit coupling in N as well as the spin-transfer at the N|F interface(s). In a N|F bilayer system, the SMR requires spin-flip in N and spin-transfer at the N|F interface. Our results explain the SMR measured in Ref. [25] both qualitatively and quantitatively with transport parameters that are consistent with other experiments. The degrees of spin accumulation in N that can be controlled by the magnetization direction is found to be very significant. In the presence of an imaginary part of the spin-mixing conductance  $G_i$  we predicted a AHE-like signal (SHAHE). Such a signal was observed in Ref. [31] and can be explained with values of  $G_i$  that agree with first principles calculations.[17] We furthermore analyzed F|N|F spin valves for parallel and perpendicular magnetization configurations. A

maximal SMR  $\sim \theta_{\text{SH}}^2$  is found for a collinear magnetization configuration in the limit that the spin-diffusion length is much larger than the thickness of the normal spacer. The SMR vanishes when rotating the two magnetizations into a fixed perpendicular constellation. The SMR torques under applied currents in N are expected to lead to magnetization dynamics of N|F and F|N|F structures.

## REFERENCES

- [1] S. D. Bader and S. S. P. Parkin, *Ann. Rev. Cond. Matt. Phys.* **1**, 71 (2010).
- [2] J. Sinova and I Žutić, *Nature Mater.* **11**, 368 (2012).
- [3] For a review see: T. Jungwirth, J. Wunderlich, and K. Olejník, *Nature Mater.* **11**, 382 (2012).
- [4] K. Ando, S. Takahashi, K. Harii, K. Sasage, J. Ieda, S. Maekawa, and E. Saitoh, *Phys. Rev. Lett.* **101**, 036601 (2008).
- [5] I. M. Miron, K. Garello, G. Gaudin, P.-J. Zermatten, M. V. Costache, S. Auffret, S. Bandiera, B. Rodmacq, A. Schuhl, and P. Gambardella, *Nature* **476**, 189 (2011).
- [6] L. Liu, C. F. Pai, Y. Li, H. W. Tseng, D. C. Ralph, and R. A. Buhrman, *Science* **336**, 555 (2012).
- [7] E. Saitoh, M. Ueda, H. Miyajima, and G. Tatara, *Appl. Phys. Lett.* **88**, 182509 (2006).
- [8] O. Mosendz, J. E. Pearson, F. Y. Fradin, G. E. W. Bauer, S. D. Bader, and A. Hoffmann, *Phys. Rev. Lett.* **104**, 046601 (2010).
- [9] O. Mosendz, V. Vlainck, J. E. Pearson, F. Y. Fradin, G. E. W. Bauer, S. D. Bader, and A. Hoffmann, *Phys. Rev. B* **82**, 214403 (2010).
- [10] F. D. Czeschka, L. Dreher, M. S. Brandt, M. Weiler, M. Althammer, I.-M. Imort, G. Reiss, A. Thomas, W. Schoch, W. Limmer, H. Huebl, R. Gross, and S. T. B. Goennenwein, *Phys. Lett. Rev.* **107**, 046601 (2011).
- [11] K. Uchida, S. Takahashi, K. Harii, J. Ieda, W. Koshibae, K. Ando, S. Maekawa, and E. Saitoh, *Nature* **455**, 778 (2008).
- [12] C. M. Jaworski, J. Yang, S. Mack, D. D. Awschalom, J. P. Heremans, and R. C. Myers, *Nature Mater.* **9**, 898 (2010).

- [13] K. Uchida, J. Xiao, H. Adachi, J. Ohe, S. Takahashi, J. Ieda, T. Ota, Y. Kajiwara, H. Umezawa, H. Kawai, G. E.W. Bauer, S. Maekawa, and E. Saitoh, *Nature Mater.* **9**, 894 (2010).
- [14] M. Weiler, M. Althammer, F. D. Czeschka, H. Huebl, M. S. Wagner, M. Opel, I.-M. Imort, G. Reiss, A. Thomas, R. Gross, and S. T. B. Goennenwein, *Phys. Rev. Lett.* **108**, 106602 (2012).
- [15] Y. Kajiwara, K. Harii, S. Takahashi, J. Ohe, K. Uchida, M. Mizuguchi, H. Umezawa, H. Kawai, K. Ando, K. Takanashi, S. Maekawa, and E. Saitoh, *Nature* **464**, 262 (2010).
- [16] A. Brataas, Yu. V. Nazarov, and G. E. W. Bauer, *Phys. Rev. Lett.* **84**, 2481 (2000); *Eur. Phys. J. B* **22**, 99 (2001).
- [17] X. Jia, K. Liu, K. Xia, and G. E. W. Bauer, *Eurphys. Lett.* **96**, 17005 (2011).
- [18] C. Burrowes, B. Heinrich, B. Kardasz, E. A. Montoya, E. Girt, Y. Sun, Y. Y. Song, and M. Wu, *Appl. Phys. Lett.* **100**, 092403 (2012).
- [19] N. W. Ashcroft and N. D. Mermin, *Solid State Physics* (Saunders, Philadelphia, 1976).
- [20] T. R. McGuire and R. I. Potter, *IEEE Trans. Magn.* **MAG-11**, 1018 (1975).
- [21] D. A. Thompson, L. T. Romankiw, and A. F. Mayadas, *IEEE Trans. Magn.* **MAG-11**, 1039 (1975).
- [22] N. Nagaosa, J. Sinova, S. Onoda, A. H. MacDonald, and N. P. Ong, *Rev. Mod. Phys.* **82**, 1539 (2010).
- [23] A. Fert, *Rev. Mod. Phys.* **80**, 1517 (2008).
- [24] S. Y. Huang, X. Fan, D. Qu, Y. P. Chen, W. G. Wang, J. Wu, T. Y. Chen, J. Q. Xiao, and C. L. Chien, *Phys. Rev. Lett.* **109**, 107204 (2012).
- [25] H. Nakayama, M. Althammer, Y.-T. Chen, K. Uchida, Y. Kajiwara, D. Kikuchi, T. Ohtani, S. Geprägs, M. Opel, S. Takahashi, R. Gross, G. E. W. Bauer, S. T. B. Goennenwein, and E. Saitoh, *Phys. Rev. Lett.* **110**, 206601 (2013).
- [26] N. Vlietstra, J. Shan, V. Castel, J. Ben Youssef, and B. J. van Wees, *Phys. Rev. B* **87**, 184421 (2013).
- [27] M. I. Dyakonov, *Phys. Rev. Lett.* **99**, 126601 (2007).

- 
- [28] S. Takahashi, H. Imamura, and S. Maekawa, in *Concepts in Spin Electronics*, edited by S. Maekawa (Oxford University Press, U.K., 2006), pp. 343-370.
- [29] T. Valet and A. Fert, *Phys. Rev. B* **48**, 7099 (1993).
- [30] L. Liu, R. A. Buhrman, and D. C. Ralph, arXiv:1111.3702 (cond-mat.mes-hall).
- [31] M. Althammer, S. Meyer, H. Nakayama, M. Schreier, S. Altmannshofer, M. Weiler, H. Huebl, S. Geprägs, M. Opel, R. Gross, D. Meier, C. Klewe, T. Kuschel, J.-M. Schmalhorst, G. Reiss, L. Shen, A. Gupta, Y.-T. Chen, G. E. W. Bauer, E. Saitoh, and S. T. B. Goennenwein, *Phys. Rev. B* **87**, 224401 (2013).
- [32] K. M. Schep, J. B. A. N. van Hoof, P. J. Kelly, G. E. W. Bauer, and J. E. Inglesfield, *Phys. Rev. B* **56**, 10805 (1997).

# 4

## SIZE EFFECT IN THE ANISOTROPIC MAGNETORESISTANCE OF FERROMAGNETIC THIN-FILMS

**Yan-Ting CHEN**

*We predict a new contribution of anisotropic magnetoresistance in metallic ferromagnets as simultaneous action of the anomalous Hall effect and its inverse. By diffusion theory, we compare this contribution with the conventional AMR, demonstrating that they can be distinguished experimentally by studying its dependence on the film thickness.*

---

Parts of this chapter have been collaborated with Saburo Takahashi and Gerrit E. W. Bauer

## 4.1 INTRODUCTION

The phenomenon that the electric resistance in metallic ferromagnets depends on the relative orientation between the electric current and the magnetization is called anisotropic magnetoresistance (AMR). It has been discovered a long time ago [1] and is of considerable interest as a convenient tool to measure the magnetization direction electrically thereby serving as magnetic field sensor [2]. The AMR in bulk ferromagnets is generally believed to have an extrinsic origin, caused by the spin-orbit coupling (SOC) in the  $s$ - $d$  scattering in ferromagnets, *i.e.*, the conduction electrons are scattered into localized electrons by impurities [3–7]. The AMR in the magnetic Rashba two-dimensional electron gas is strongly enhanced by magnetic impurities [8]. An intrinsic mechanism was reported to contribute to the transverse component of magnetoresistance (the planar Hall effect) [9]. Theoretical and experimental works on both the AMR and the AHE (anomalous Hall effect, see below) exist [8, 10], but these two effects are regarded as different physics and treated separately. For AMR studies, permalloy has been the material of choice because the effect is relatively large and its small magnetic anisotropy makes it easy to vary the magnetization angles with respect to the current direction [11]. Semiclassical calculations that take irregular boundaries into account showed that surface roughness [12] can explain the difference between the MR for magnetizations in- and out-of-plane in Py thin-films [13]. Surface roughness has been also invoked to explain a vanishing AMR in the thin-film limit [14]. Here we address the AMR in thin Py films in the absence of surface roughness. We predict that size effects should become observable in sufficiently smooth thin films.

The present study has been motivated by the recently discovered so-called spin Hall magnetoresistance (SMR) in bilayer systems of platinum (Pt) and yttrium iron garnet (YIG) [15–20]. This effect has been explained in terms of the combined action of spin Hall effect and inverse spin Hall effect which is modulated by the magnetization direction in YIG by the interface exchange interaction [17, 21]. An equilibrium proximity effect in which Pt becomes magnetic close to the interface was invoked to explain the observations as a thin-layer version of the AMR [16]. The nature and magnitude of such an MR is still an open question, though. The AMR and the SMR may coexist in multilayers of non-magnetic and ferromagnetic metals [22, 23]. The MR of bilayers made of Py|YIG [24, 25] is a puzzle, since the SMR theory cannot be directly applied to metallic ferromagnets and the nature of a magnetic proximity effect between two strong ferromagnets is not apparent. In this report, we generalize the SMR theory to the case of ferromagnetic films with inert substrate and capping, such as vacuum, which appear to be valid also when on top of a strongly exchange-coupled ferromagnetic insulator.

Another magnetotransport effect in ferromagnets caused by the SOC is the

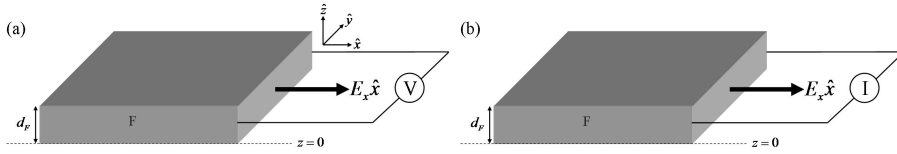


FIGURE 4.1: A thin-film made of metallic ferromagnet subject to an electric field in the  $\hat{x}$  direction with (a) open Hall and (b) short circuit contacts.

transverse Hall charge current in conducting ferromagnets referred to as anomalous Hall effect (AHE) [26]. The AHE exists in the limit of zero applied magnetic fields provided that the magnetization is pointing normal to both driving and Hall currents. We may interpret the AHE in terms of the spin current generated by the SHE that is converted into a charge current by the magnetic order parameter [27]. This argument allows us to generalize the SMR to ferromagnetic metal films. Consider a layer of a single-domain ferromagnetic metal magnetized along  $\hat{m}$  with a finite thickness  $d_F$  in the  $\hat{z}$  direction that is subject to an external electric field  $\vec{E} = E_x \hat{x}$  as shown in Fig. 4.1. The AHE charge current direction is governed by the cross product  $\vec{j}_c^H \propto \hat{m} \times \vec{E}$ . According to the two-current model, a charge current in a conducting ferromagnet is associated with a spin current with polarization along  $\hat{m}$ . Keeping the Hall contacts floating, these currents generate charge and spin accumulations at the Hall edges [28] that drive charge (spin) currents back into the sample. The AHE (ISHE) then generates charge currents in the same direction as the originally applied current that depends on the magnetization direction, thereby contributing to the MR that we find to depend on the film thickness and coexist with the conventional AMR. Below we introduce the theoretical model and formulate this mechanism in Sec. 5.2. The results for two extreme cases of Hall contacts are presented in Sec. 4.3. Conclusions are provided in Sec. 5.5.

## 4.2 THEORETICAL MODEL

The conventional AMR in a bulk ferromagnet  $\Delta\rho_b/\rho_F$  is defined as

$$\frac{\Delta\rho_b}{\rho_0} \equiv \frac{\rho_{\parallel} - \rho_{\perp}}{\rho_0}, \quad (4.1)$$

where  $\rho_{\parallel}$  ( $\rho_{\perp}$ ) is the resistivity for a magnetization parallel (transverse) to the applied current.  $\rho_0$  is an averaged value over directions. The latter has been defined differently in the literature, for example, as an average over the three principle directions as  $\rho_0 \equiv (\rho_{\parallel} + 2\rho_{\perp})/3$  in Ref. [2]. Defining  $\rho_{\parallel} = \rho_0 + \Delta\rho_b$  and  $\rho_{\perp} = \rho_0 - \Delta\rho_b$ , the dependence of the AMR on the magnetization direction with unit vector  $\hat{m}$  in an

isotropic (or cubic) material and charge current bias along the  $\hat{x}$  direction reads:

$$\rho_{\text{long}} = \rho_0 + \Delta\rho_b m_x^2, \quad (4.2)$$

$$\rho_{\text{trans}} = \Delta\rho_b m_x m_y, \quad (4.3)$$

where  $\rho_{\text{long}}$  is the longitudinal component of electric resistivity (along  $\hat{x}$ ),  $\rho_{\text{trans}}$  is the transverse component along  $\hat{y}$ , and  $m_i$  is the  $i$ -component of the magnetization direction unit vector.  $\Delta\rho_b$  can be derived microscopically from the  $s$ - $d$  model with a free  $s$ -electron conduction band and localized  $d$ -electrons with a strong exchange interaction and weaker SOC. Transport is carried by the conduction electrons with a contribution to the resistivity from scattering into the localized  $d$ -states by impurities that depends on the magnetization direction because of the SOC. The AMR ratio for strong ferromagnet then leads to [5]

$$\frac{\Delta\rho_b}{\rho_0} = \gamma \left( \frac{\rho_{s \rightarrow d\downarrow} - \rho_{s\uparrow}}{\rho_{s\downarrow}} \right) \quad (4.4)$$

where  $\gamma = (3/4)(\lambda/H_{\text{ex}})$  with  $\lambda = \hbar^2/(4m_0^2c^2)$  is the SOC constant and  $H_{\text{ex}}$  the exchange field of the  $d$ -states.  $\rho_{s\uparrow}$  is the resistivity of  $s$ -state electrons with majority spin ( $\uparrow$ ) and  $\rho_{s \rightarrow d\downarrow}$  a resistivity due to the  $s$ - $d$  scattering into minority-spin  $d$  states ( $\downarrow$ ). Eq. (4.4) has been refined by taking into account more scattering processes [6] but assuming  $\rho_{s\uparrow} = \rho_{s\downarrow}$  leading to a positive definite value

$$\frac{\Delta\rho_b}{\rho_0} = \frac{\gamma(\rho_{s \rightarrow d\downarrow} - \rho_{s \rightarrow d\uparrow})^2}{(\rho_s + \rho_{s \rightarrow d\downarrow})(\rho_s + \rho_{s \rightarrow d\uparrow})}. \quad (4.5)$$

Experimentally,  $\Delta\rho_b$  is indeed larger than zero for most ferromagnets, but exceptions have been observed [29, 30] and computed by a model that includes spin-dependent effective masses and number density of electrons in the conduction band [7]. In thin films  $\Delta\rho_b$  was found to be affected by surface roughness [12]. In the following we assume specular surfaces, keeping in mind that this is an oversimplification for ultrathin films.

#### 4.2.1 SPIN CURRENTS IN FERROMAGNETS

The spin current density in a homogeneous metal in the non-relativistic limit

$$\vec{\mathbf{j}}_s = en \langle \vec{v} \otimes \boldsymbol{\sigma} + \boldsymbol{\sigma} \otimes \vec{v} \rangle / 2 = \left( \vec{j}_{sx}, \vec{j}_{sy}, \vec{j}_{sz} \right)^T = \left( \vec{j}_s^x, \vec{j}_s^y, \vec{j}_s^z \right) \quad (4.6)$$

is a second-rank tensor (in the same units as the charge current density  $\vec{j}_c = en \langle \vec{v} \rangle$ ), where  $e = |e|$  is the electron charge,  $n$  is the density of the electrons,  $\vec{v}$  is the velocity operator,  $\boldsymbol{\sigma}$  is the vector of Pauli spin matrices, and  $\langle \dots \rangle$  denotes an expectation

value. The row vectors  $\vec{j}_{si} = en \langle \vec{v} \sigma_i + \sigma_i \vec{v} \rangle / 2$  in Eq. (5.6) are the spin current density directions polarized along  $\hat{i}$ , while the column vectors  $\vec{j}_s^j = en \langle v_j \sigma + \sigma v_j \rangle / 2$  denote the spin current density polarizations when flowing into the  $\hat{j}$  direction.

We consider a strong ferromagnet in which the exchange field amounts to  $\sim 10^4$  Tesla, implying that spin currents and accumulations with polarization not collinear with the magnetization direction  $\hat{m}$  are absorbed immediately as a spin transfer torque by the magnetic texture. We consider here only sufficiently weak currents such that current-induced magnetization dynamics can be disregarded. The particle spin current polarization is then locked to  $\hat{m}$ , so Eq. (5.6) can be rewritten as

$$\vec{j}_s = (\hat{m} \otimes \vec{j}_s + \vec{j}_s \otimes \hat{m}) / 2, \quad (4.7)$$

where  $\vec{j}_s$  is the spin current density *direction*.

### 4.2.2 LINEAR RESPONSE

In ferromagnets, the direct response to an applied electric field  $\vec{E}$  is a charge current density  $\vec{j}_c = \sigma_F \vec{E}$  with  $\sigma_F = \sigma_\uparrow + \sigma_\downarrow$  the electric (charge) conductivity, which is the sum of the conductivities ( $\sigma_{\uparrow(\downarrow)}$ ) of the two spin species in the two-current model. The conductivities of electrons in opposite spin channels are asymmetric such that any charge current  $\vec{j}_c$  is associated with a spin current  $P \vec{j}_c$  flowing in the same direction and  $P = (\sigma_\uparrow - \sigma_\downarrow) / \sigma_F$  is the current spin polarization. In a system with SOC, an applied charge current  $\vec{j}_c$  drives a transverse charge current  $\theta_{\text{AH}} (\hat{m} \times \vec{j}_c)$  and correspondingly a transverse spin current  $\theta_{\text{SH}} (\hat{m} \times \vec{j}_c)$  via the AHE and SHE, which defines  $\theta_{\text{AH}}$  ( $\theta_{\text{SH}}$ ), the anomalous (spin) Hall angle. There are also currents from higher order SOC effects. For example, an electric field generates a SHE current, which again generates an ISHE current due to the SOC. Following the derivation in Appendix 4.6, the linear response relation between currents and forces in a ferromagnetic metal reads

$$\begin{pmatrix} \vec{j}_c \\ \vec{j}_s \end{pmatrix} = \sigma_F \begin{pmatrix} 1 + \mathcal{C}_{\text{AHE}} + \mathcal{C}_{\text{ISH}}^{(2)} & P + \mathcal{C}_{\text{SHE}}^{(1)} \\ P + \mathcal{C}_{\text{SHE}}^{(1)} & 1 + \mathcal{C}_{\text{AHE}} + \mathcal{C}_{\text{ISH}}^{(2)} \end{pmatrix} \begin{pmatrix} -\vec{\nabla} \mu_c / e + E_x \hat{x} \\ -\vec{\nabla} \mu_s / (2e) \end{pmatrix}, \quad (4.8)$$

where the AHE, SHE, and ISHE are included by the operators

$$\mathcal{C}_{\text{AHE}} \approx \theta_{\text{AH}} [\hat{m} \times + \theta_{\text{AH}} \hat{m} \times (\hat{m} \times)], \quad (4.9)$$

$$\mathcal{C}_{\text{SHE}}^{(1)} \approx \theta_{\text{SH}} \hat{m} \times, \quad (4.10)$$

$$\mathcal{C}_{\text{SHE}}^{(2)} \approx \theta_{\text{SH}}^2 \hat{m} \times (\hat{m} \times), \quad (4.11)$$

with “ $\times$ ” denotes the vector cross product operating on the gradients of the charge ( $-\vec{\nabla} \mu_c + e E_x \hat{x}$ ) and spin ( $-\vec{\nabla} \mu_s / 2$ ) chemical potentials. In the following, we disre-

gard terms proportional to  $\theta_{\text{AH(SH)}}^2$  when solving for the charge (spin) accumulation, but take them into account when calculating the currents since they are of the same order as the diffuse currents driven by the charge (spin) accumulation gradients (which is linear to the Hall angle).

In the two-current model including impurity SOC [28, 31] the Hall current in each spin channel ( $\zeta = \uparrow / \downarrow \equiv \pm 1$ ) reads

$$\vec{j}_{\zeta}^{\text{H}} = \alpha_{\text{H},\zeta} (\zeta \hat{m} \times \sigma_{\zeta} \vec{E}), \quad (4.12)$$

where  $\alpha_{\text{H},\zeta} > 0$  is the spin-dependent Hall angle. The anomalous Hall current  $\vec{j}_{c0}^{\text{AH}}$  and spin Hall current  $\vec{j}_{s0}^{\text{SH}}$  then read

$$\vec{j}_{c0}^{\text{AH}} = (\alpha_{\text{H},\uparrow} \sigma_{\uparrow} - \alpha_{\text{H},\downarrow} \sigma_{\downarrow}) (\hat{m} \times \vec{E}) = \theta_{\text{AH}} (\hat{m} \times \sigma_F \vec{E}), \quad (4.13)$$

$$\vec{j}_{s0}^{\text{SH}} = (\alpha_{\text{H},\uparrow} \sigma_{\uparrow} + \alpha_{\text{H},\downarrow} \sigma_{\downarrow}) (\hat{m} \times \vec{E}) = \theta_{\text{SH}} (\hat{m} \times \sigma_F \vec{E}), \quad (4.14)$$

Therefore

$$\theta_{\text{AH}} = P_{\text{H}} \theta_{\text{SH}}, \quad (4.15)$$

where

$$P_{\text{H}} = \frac{\alpha_{\text{H},\uparrow} \sigma_{\uparrow} - \alpha_{\text{H},\downarrow} \sigma_{\downarrow}}{\alpha_{\text{H},\uparrow} \sigma_{\uparrow} + \alpha_{\text{H},\downarrow} \sigma_{\downarrow}} \quad (4.16)$$

is the Hall current spin polarization with  $0 \leq |P_{\text{H}}| \leq 1$ .  $P_{\text{H}} = P$  when  $\alpha_{\text{H},\uparrow} = \alpha_{\text{H},\downarrow}$  or  $|P| = 1, 0$ .

### 4.2.3 DIFFUSION EQUATIONS

$\mu_c$  and  $\mu_s$  in Eq. (4.8) are solutions of the spin and charge diffusion equations [32, 33]

$$\nabla^2 \mu_s = \frac{\mu_s}{\lambda_F^2}, \quad (4.17)$$

$$\nabla^2 \left( \mu_c + \frac{P}{2} \mu_s \right) = 0. \quad (4.18)$$

The coefficients  $A, B$  in the general solutions to Eqs. (4.17-4.18)

$$\mu_s = A_s e^{-z/\lambda_F} + B_s e^{z/\lambda_F}, \quad (4.19)$$

$$\mu_c = -\frac{P}{2} \mu_s + A_{cy} y + A_{cz} z \quad (4.20)$$

depend on the boundary conditions. We assume that the spin current vanishes at the top and bottom of the ferromagnet, implying the absence of spin-flips induced

by e.g. disordered surfaces with strong spin-orbit interaction and static magnetizations. When the surfaces are good spin sinks, e.g., if the ferromagnet is attached to a normal metal, there is a finite spin current flows through the interface governed by the parameter spin mixing conductance [44]. We consider the two limiting cases in which the Hall contacts are open (floating) or short-circuited. In the following, we treat these two cases separately. Quite different results are found, which is caused by the charge build up at the Hall edges for the open configuration that are absent when the Hall currents are allowed to flow.

## 4.3 RESULTS

### 4.3.1 FLOATING HALL EDGES (OPEN-CIRCUIT CONFIGURATION)

When the Hall edges are electrically floating as shown in Fig. 4.1(a), a transverse charge accumulation is induced along  $\hat{y}$ , which is measurable by a high-impedance voltmeter. The vanishing Hall charge current fixes the coefficient  $A_{cy}$  in Eq. (4.20) to

$$A_{cy} = \theta_{\text{AH}} e E_x m_z, \quad (4.21)$$

while the vanishing charge current condition normal to the film plane

$$\vec{j}_c \cdot \hat{z} = \frac{\sigma_F}{e} (-\partial_z \mu_c - \theta_{\text{AH}} e E_x m_y - P \partial_z \mu_s / 2) = 0, \quad (4.22)$$

is satisfied when

$$A_{cz} = -\theta_{\text{AH}} e E_x m_y. \quad (4.23)$$

With

$$\vec{j}_s(z) \cdot \hat{z} = \frac{\sigma_F}{e} (-P \partial_z \mu_c(z) - \theta_{\text{SH}} e E_x m_y - \partial_z \mu_s(z) / 2) \quad (4.24)$$

$\vec{j}_s(0) \cdot \hat{z} = \vec{j}_s(d_N) \cdot \hat{z} = 0$  leads to a spin accumulation

$$\mu_s = 2 \frac{1 - P P_H}{1 - P^2} \theta_{\text{SH}} e E_x m_y \lambda_F \sinh\left(\frac{d_F - 2z}{2\lambda_F}\right) / \cosh\left(\frac{d_F}{2\lambda_F}\right). \quad (4.25)$$

When  $P = P_H$  the result is identical to that of the spin Hall effect of a normal metal, i.e. when  $P = P_H \rightarrow 0$ . The spin Hall current is then compensated by the spin diffusion and there is no charge accumulation.

From Eq. (4.8) includes the lowest order contribution, the longitudinal and

transverse components of charge current (along  $\hat{x}$ ) then read

$$\frac{j_{c,\text{long}}}{\sigma_F E_x} = 1 + (m_x^2 - 1)\theta_{\text{SH}}^2 + \frac{(\theta_{\text{SH}} - \theta_{\text{AH}}P)^2}{1 - P^2} \frac{\cosh \frac{d_F - 2z}{2\lambda_F}}{\cosh \frac{d_F}{2\lambda_F}} m_y^2, \quad (4.26)$$

$$\frac{j_{c,\text{trans}}}{\sigma_F E_x} = \theta_{\text{AH}} m_z + m_x m_y \theta_{\text{SH}}^2 - \frac{(\theta_{\text{SH}} - \theta_{\text{AH}}P)^2}{1 - P^2} \frac{\cosh \frac{d_F - 2z}{2\lambda_F}}{\cosh \frac{d_F}{2\lambda_F}} m_x m_y. \quad (4.27)$$

The total current is obtained by integrating over the film thickness (*i.e.* the  $z$ -direction)

$$\frac{\overline{j_{c,\text{long}}}}{\sigma_F E_x} = \frac{\sigma_{\text{long}}}{\sigma_F} = 1 + (m_x^2 - 1)\theta_{\text{SH}}^2 + m_y^2 \frac{(\theta_{\text{SH}} - \theta_{\text{AH}}P)^2}{1 - P^2} \frac{2\lambda_F}{d_F} \tanh \frac{d_F}{2\lambda_F}, \quad (4.28)$$

$$\frac{\overline{j_{c,\text{trans}}}}{\sigma_F E_x} = \frac{\sigma_{\text{trans}}}{\sigma_F} = \theta_{\text{AH}} m_z + m_x m_y \theta_{\text{SH}}^2 - m_x m_y \frac{(\theta_{\text{SH}} - \theta_{\text{AH}}P)^2}{1 - P^2} \frac{2\lambda_F}{d_F} \tanh \frac{d_F}{2\lambda_F}. \quad (4.29)$$

Using

$$\rho_{\text{long}} = \frac{\sigma_{\text{long}}}{\sigma_{\text{long}}^2 - \sigma_{\text{trans}}^2}, \quad (4.30)$$

$$\rho_{\text{trans}} = -\frac{\sigma_{\text{trans}}}{\sigma_{\text{long}}^2 - \sigma_{\text{trans}}^2}, \quad (4.31)$$

for small spin Hall angles, we can expand the longitudinal (AMR) and transverse components (planar Hall effect and AHE) of the electric resistivity (to the order of  $\theta_{\text{AH/SH}}^2$ ), we have

$$\rho_{\text{long}} \approx 1 + \Delta\rho_1 m_z^2 + \Delta\rho_2 m_y^2 + \Delta\rho_3 (m_x^2 - 1), \quad (4.32)$$

$$\rho_{\text{trans}} \approx -\theta_{\text{AH}} \rho_F m_z - \Delta\rho_2 m_x m_y + \Delta\rho_3 m_x m_y, \quad (4.33)$$

where the magnetoresistance ratios are

$$\frac{\Delta\rho_1}{\rho_F} = -\theta_{\text{AH}}^2, \quad (4.34)$$

$$\frac{\Delta\rho_2}{\rho_F} = -\frac{(\theta_{\text{SH}} - \theta_{\text{AH}}P)^2}{1 - P^2} \frac{2\lambda_F}{d_F} \tanh \frac{d_F}{2\lambda_F}, \quad (4.35)$$

$$\frac{\Delta\rho_3}{\rho_F} = -\theta_{\text{SH}}^2. \quad (4.36)$$

Eqs. (4.34-4.36) predict three contributions to the AMR that to the best of our knowledge have not been reported earlier. Both  $\Delta\rho_1$  and  $\Delta\rho_2$  are negative and have different magnetization dependences from that of the conventional AMR. These characteristics enable separating  $\Delta\rho_1$  and  $\Delta\rho_2$  from  $\Delta\rho_b$ , because the latter is usually positive and has an  $m_x^2$  magnetization dependence. On the other hand,  $\Delta\rho_3$  is negative but has the same magnetization dependence as that of  $\Delta\rho_b$ , which seems just renormalize the conventional AMR.

$\Delta\rho_1$  does not depend on thickness and therefore should exist also in bulk samples. This term simply comes from the off-diagonal elements of the conductivity tensor. Note that this term is always there when we convert the conductivity tensor to the resistivity tensor including the AHE.  $\Delta\rho_3$  does not depend on thickness neither. This term can be understood as the combined action of the SHE and ISHE: the electric field generates a SHE current, which again generates in ISHE current contributing on both longitudinal and transverse directions. Such a non-local term has apparently been missed in previous treatises of the AMR, implying that old experiments might have to be reinterpreted.

The physical mechanism behind the second contribution to the AMR ( $\Delta\rho_2$ ) is similar to that of the SMR in normal metals in contact with a ferromagnet, being caused by the SHE and ISHE and therefore has an identical magnetization dependence to the SMR [17, 21]. This contribution is strongly thickness-dependent and vanishes when  $d_F \gg \lambda_F$ . In the thin-film limit ( $d_F \ll \lambda_F$ ),  $\Delta\rho_2$  becomes

$$\frac{\Delta\rho_2}{\rho_F} \xrightarrow{d_F \ll \lambda_F} -\frac{(\theta_{\text{SH}} - \theta_{\text{AHP}})^2}{1 - P^2} \left(1 - \frac{d_F^2}{12\lambda_F^2}\right). \quad (4.37)$$

### 4.3.2 SHORT-CIRCUIT CONFIGURATION

Short-circuiting the Hall edges as shown in Fig. 4.1(b) is equivalent to a system with translational invariance in the film ( $x$ - $y$ ) plane and  $A_{cy} = 0$ , while  $A_{cz}$  and  $\mu_s$  are not modified. The longitudinal and transverse components of the electric current density in the short-circuit configuration are

$$\frac{j_{c,\text{long}}}{\sigma_F E_x} = 1 + (m_x^2 - 1)\theta_{\text{SH}}^2 - m_z^2\theta_{\text{AH}}^2 + m_y^2 \frac{(\theta_{\text{SH}} - \theta_{\text{AHP}})^2}{1 - P^2} \cosh\left(\frac{d_F - 2z}{2\lambda_F}\right) / \left(\cosh\left(\frac{d_F}{2\lambda_F}\right)\right), \quad (4.38)$$

$$\frac{j_{c,\text{trans}}}{\sigma_F E_x} = \theta_{\text{AH}}m_z + m_x m_y \theta_{\text{SH}}^2 - m_x m_y \frac{(\theta_{\text{SH}} - \theta_{\text{AHP}})^2}{1 - P^2} \cosh\left(\frac{d_F - 2z}{2\lambda_F}\right) / \cosh\left(\frac{d_F}{2\lambda_F}\right). \quad (4.39)$$

The total currents are obtained by integrating over the film thickness (*i.e.* the  $z$ -direction)

$$\frac{\overline{j_{c,\text{long}}}}{\sigma_F E_x} = \frac{\sigma_{\text{long}}}{\sigma_F} = 1 + (m_x^2 - 1)\theta_{\text{SH}}^2 - m_z^2\theta_{\text{AH}}^2 + m_y^2 \frac{(\theta_{\text{SH}} - \theta_{\text{AH}}P)^2}{1 - P^2} \frac{2\lambda_F}{d_F} \tanh \frac{d_F}{2\lambda_F}, \quad (4.40)$$

$$\frac{\overline{j_{c,\text{trans}}}}{\sigma_F E_x} = \frac{\sigma_{\text{trans}}}{\sigma_F} = \theta_{\text{AH}}m_z + m_x m_y \theta_{\text{SH}}^2 - m_x m_y \frac{(\theta_{\text{SH}} - \theta_{\text{AH}}P)^2}{1 - P^2} \frac{2\lambda_F}{d_F} \tanh \frac{d_F}{2\lambda_F}. \quad (4.41)$$

For small spin Hall angles, we expand the longitudinal and transverse components of the electric resistivity in the Hall angles to leading order as

$$\rho_{\text{long}} \approx \rho_F + \Delta\rho_2 m_y^2 + \Delta\rho_3 (m_x^2 - 1) \quad (4.42)$$

$$\rho_{\text{trans}} \approx -\theta_{\text{AH}}\rho_F m_z - \Delta\rho_2 m_x m_y + \Delta\rho_3 m_x m_y. \quad (4.43)$$

We observe that the transverse charge accumulation strongly modifies the magnetoresistance because of the transverse current-backflow that arises from the zero Hall current condition.

#### 4.4 EXPERIMENTAL TESTS

According to Matthiessen's Rule, the conventional AMR and the contribution of size effect are additive. The longitudinal components of resistivity with open (oc) and short-circuited (sc) Hall edges then read

$$\rho_{\text{long}}^{(\text{oc})} = \rho_0 + \Delta\rho_b m_x^2 + \Delta\rho_1 m_z^2 + \Delta\rho_2 m_y^2 + \Delta\rho_3 (m_x^2 - 1), \quad (4.44)$$

$$\rho_{\text{long}}^{(\text{sc})} = \rho_0 + \Delta\rho_b m_x^2 + \Delta\rho_2 m_y^2 + \Delta\rho_3 (m_x^2 - 1). \quad (4.45)$$

By in-plane and out-of-plane measurements and comparing the open and short-circuited Hall edge configurations, we can in principle distinguish  $\Delta\rho_b$  from  $\Delta\rho_1$  and  $\Delta\rho_2$  since the magnetization-dependences are different.  $\Delta\rho_2$  can be extracted by thickness-dependence studies.  $\Delta\rho_3$  just renormalizes  $\Delta\rho_b$ , so is hard to be distinguished from the conventional AMR.

We then check the amplitudes of  $\Delta\rho_1$  and  $\Delta\rho_2$ . Judging by the parameters from Table 4.1  $\Delta\rho_1/\Delta\rho_b$  is rather small. However, this contribution may be observable in materials with large anomalous Hall angle and relatively small bulk AMR. For example, gadolinium (Gd) has a large  $\theta_{\text{AH}} \approx 0.1$  at 200 K, while the AMR at the same temperature is  $\Delta\rho_b/\rho_F = 0.2\%$ . [2, 39] Thus in Gd  $\Delta\rho_1/\Delta\rho_F$  should not be overwhelmed by  $\Delta\rho_b/\rho_F$ .

Mater.	$\rho_F$ (n $\Omega$ m)	$\lambda_F$ (nm)	$P$ (%)	$\Delta\rho_b/\rho_F$ (%)	$\theta_{AH}$ (%)
Fe (300K)	40 (ref. [36])	8.5 (ref. [36])	40 (ref. [37])	0.3 (ref. [29])	0.4 (ref. [39])
Co (300K)	60 (ref. [36])	40 (ref. [36])	35 (ref. [37])	2 (ref. [29])	3.6 (ref. [39])
Ni (300K)	33 (ref. [36])	21 (ref. [36])	23 (ref. [37])	2.2 (ref. [29])	0.2 (ref. [39])
Gd (200K)	131 (ref. [36])	< 0.5 (ref. [36])	14 (ref. [35])	2 (ref. [38])	0.1 (ref. [40])
Py (300K)	120 (ref. [36])	5.5 (ref. [36])	70 (ref. [35])	4 (ref. [38])	0.25 (ref. [40])

TABLE 4.1: Parameters governing  $\Delta\rho_1$  and  $\Delta\rho_2$  in metallic ferromagnets as well as the conventional bulk AMR ratios.

As for  $\Delta\rho_2$ ,  $d_F$  can be experimentally controlled, while the remaining parameters are  $\rho_F$ ,  $\lambda_F$ ,  $P$ ,  $\theta_{AH}$  and  $\theta_{SH}$ . The first four can be independently measured and are known for many ferromagnetic metals: Table 4.1 lists these parameters for Fe, Co, Ni, and Py. On the other hand, the SHE in ferromagnets is basically unexplored, which means also  $\Delta\rho_3$  is hardly known yet. Miao *et al.* [24] observed the spin Seebeck effect in YIG|Py bilayers, *i.e.* a Hall voltage in Py induced by a temperature gradient. They extracted  $\theta_{SH}(\text{Py}) \approx 0.4 \times \theta_{SH}(\text{Pt})$  assuming a rather small  $\lambda_F(\text{Py}) \approx 2.5$  nm. However, the accuracy of this parameter fit is difficult to judge, since the nature of the spin Seebeck effect at purely ferromagnetic interfaces is unknown and the effect of ferromagnetism on the Hall voltage was not taken into account. The spin Hall angle ( $\theta_{SH}$ ) of Py has recently been measured via the ISHE [24, 41]. Tsukahara *et al.* [41] detected the transverse electric voltage in YIG|Py under ferromagnetic resonance conditions, extracting a spin Hall angle of  $\theta_{SH} = 0.5\% - 1\%$ . Nevertheless, the spin pumping physics in purely ferromagnetic bilayers is likely to be different from that in bilayers with normal metals, so this estimate should be taken with a grain of salt as well, as experimentally verified recently [42]. Another study of voltage generation in YIG|Py under FMR conditions was not analyzed in terms of a spin Hall angle [43]. In Figure 4.2, we plot  $|\Delta\rho_2|/\rho_F$  of Py as a function of  $d_F$  for several values of  $\theta_{SH}$  and other required parameters from Table 4.1. We see that for  $\theta_{SH} = 0.08$ ,  $|\Delta\rho_2|/\rho_F > 1\%$  when  $d_F < 10$  nm, which is comparable with the conventional AMR  $\Delta\rho_b/\rho_F = 4\%$  and therefore experimentally observable in epitaxial films. On the other hand  $|\Delta\rho_1|/\rho_F = 6 \times 10^{-6}$  is negligibly small for Py.

## 4.5 SUMMARY

We predict a size effect in the magnetoresistance of magnetic thin films that originates from the spin Hall and anomalous Hall effects. The mechanism of the present MR is reminiscent of the SMR [17, 21] in bilayers of normal metal and magnetic insulator (FI), in which the spin Hall current is modulated and partially absorbed

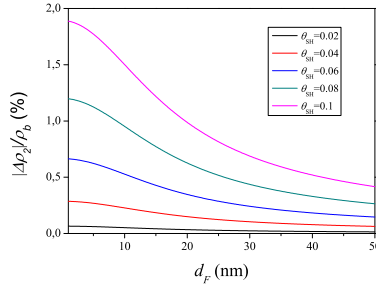


FIGURE 4.2:  $|\Delta\rho_2|/\rho_F$  of Py as a function of  $d_F$  and several values of  $\theta_{SH}$  using parameters from Table 4.1.

## 4

as a spin transfer torque at the N|YIG interface. A transverse spin current cannot be completely absorbed by an FI interface with a finite spin mixing conductance. On the other hand, if generated in a metallic ferromagnet, the transverse spin current is absorbed completely by the ferromagnetic order parameter on a length scale that is atomic in elemental ferromagnets with large exchange splittings, which does explain the similarity of the SMR and thin-film AMR reported here.

The extra contribution to the MR has a magnetization dependence different from that of the conventional AMR and is always negative. While the conventional AMR is usually positive, the new contribution is always negative. We also find a contribution to the AMR generated by the AMR that survives in the thin film limit. This term appears to have been overlooked previously and should be observable in ferromagnets with a large anomalous Hall angle and small AMR, such as Gd.

Miao *et al.* [24] suggest that the similarity of the MR found in bilayers made of Py|YIG and Pt|YIG would be proof for a proximity effect in Pt, claiming that SMR theory fails to explain the former. We show here that while the physics of transport in these two systems is quite different, an SMR type of mechanism can be at work as well in Py|YIG. When the magnetizations are homogeneous over the interface, it should make no difference whether the Py borders to vacuum or YIG and the size effects predicted here should be expected, although possibly concealed by surface roughness. scattering [13].

## 4.6 APPENDIX: LINEAR RESPONSE MATRIX

Here we construct the full linear response in Eq. (4.8) including all the higher order SOC effects. Without the SOC, the linear response relation between currents and

driving forces in a ferromagnetic metal reads

$$\begin{pmatrix} \vec{j}_c \\ \vec{j}_s \end{pmatrix} = \sigma_F \begin{pmatrix} 1 & P \\ P & 1 \end{pmatrix} \begin{pmatrix} -\vec{\nabla}\mu_c/e + E_x \hat{x} \\ -\vec{\nabla}\mu_s/(2e) \end{pmatrix}. \quad (4.46)$$

Now we want to include the contributions of the AHE, the SHE, the ISHE, and their higher order effects. First we focus on the element in the matrix which corresponds to the electric current driven by the electric field (more generally, the gradient of electrochemical potential). This element is contributed by the AHE and its higher order currents, and the ISHE currents from all orders of SHE currents. The total current from all the AHE-related terms  $\mathcal{C}_{\text{AH}} \vec{j}_c^{\vec{0}}$  is summed up

$$\begin{aligned} \mathcal{C}_{\text{AH}} \vec{j}_c^{\vec{0}} &= \theta_{\text{AH}} \hat{m} \times \vec{j}_c^{\vec{0}} + \theta_{\text{AH}}^2 \hat{m} \times (\hat{m} \times \vec{j}_c^{\vec{0}}) + \theta_{\text{AH}}^3 \hat{m} \times [\hat{m} \times (\hat{m} \times \vec{j}_c^{\vec{0}})] + \dots \\ &= \theta_{\text{AH}} \hat{m} \times \vec{j}_c^{\vec{0}} + \theta_{\text{AH}}^2 \hat{m} \times (\hat{m} \times \vec{j}_c^{\vec{0}}) - \theta_{\text{AH}}^3 \hat{m} \times \vec{j}_c^{\vec{0}} + \dots \\ &= \frac{\theta_{\text{AH}}}{1 + \theta_{\text{AH}}^2} \hat{m} \times \vec{j}_c^{\vec{0}} + \frac{\theta_{\text{AH}}^2}{1 + \theta_{\text{AH}}^2} \hat{m} \times (\hat{m} \times \vec{j}_c^{\vec{0}}) \\ &= \frac{\theta_{\text{AH}}}{1 + \theta_{\text{AH}}^2} [\hat{m} \times + \theta_{\text{AH}} \hat{m} \times (\hat{m} \times)] \vec{j}_c^{\vec{0}}, \end{aligned} \quad (4.47)$$

where  $\vec{j}_c^{\vec{0}} = \sigma_F \vec{E}$  is the applied current. Therefore

$$\mathcal{C}_{\text{AH}} = \frac{\theta_{\text{AH}}}{1 + \theta_{\text{AH}}^2} [\hat{m} \times + \theta_{\text{AH}} \hat{m} \times (\hat{m} \times)]. \quad (4.48)$$

The total ISHE current from all orders of spin current  $\mathcal{C}_{\text{ISHE}} \vec{j}_c^{\vec{0}}$  is

$$\begin{aligned} \mathcal{C}_{\text{SHE}}^{(2)} \vec{j}_c^{\vec{0}} &= \theta_{\text{SH}}^2 \hat{m} \times (\hat{m} \times \vec{j}_c^{\vec{0}}) - \theta_{\text{SH}}^4 \hat{m} \times (\hat{m} \times \vec{j}_c^{\vec{0}}) + \dots \\ &= \frac{\theta_{\text{SH}}^2}{1 + \theta_{\text{SH}}^2} \hat{m} \times (\hat{m} \times \vec{j}_c^{\vec{0}}). \end{aligned} \quad (4.49)$$

Thus

$$\mathcal{C}_{\text{SHE}}^{(2)} = \frac{\theta_{\text{SH}}^2}{1 + \theta_{\text{SH}}^2} \hat{m} \times (\hat{m} \times). \quad (4.50)$$

The spin current generated by an electric field has to take into account all orders of SHE currents  $\mathcal{C}_{\text{SHE}}^{(1)} \vec{j}_c^{\vec{0}}$

$$\begin{aligned} \mathcal{C}_{\text{SHE}}^{(1)} \vec{j}_c^{\vec{0}} &= \theta_{\text{SH}} \hat{m} \times \vec{j}_c^{\vec{0}} + \theta_{\text{SH}}^3 \hat{m} \times [\hat{m} \times (\hat{m} \times \vec{j}_c^{\vec{0}})] + \dots \\ &= \frac{\theta_{\text{SH}}}{1 + \theta_{\text{SH}}^2} \hat{m} \times \vec{j}_c^{\vec{0}}. \end{aligned} \quad (4.51)$$

Then

$$\mathcal{C}_{\text{SHE}}^{(1)} = \frac{\theta_{\text{SH}}}{1 + \theta_{\text{SH}}^2} \hat{m} \times \quad (4.52)$$

The rest two matrix elements can be worked out similarly.

We may define the effective Hall angles

$$\theta_{\text{AH(SH)}}^{\text{eff}} \equiv \frac{\theta_{\text{AH(SH)}}}{1 + \theta_{\text{AH(SH)}}^2}, \quad (4.53)$$

because  $\theta_{\text{AH(SH)}}^{\text{eff}}$  is actually the Hall angle measured experimentally if we fix  $\hat{m} = \hat{z}$ . The effective Hall angle can be expanded as

$$\theta_{\text{AH(SH)}}^{\text{eff}} = \frac{\theta_{\text{AH(SH)}}}{1 + \theta_{\text{AH(SH)}}^2} = \theta_{\text{AH(SH)}} (1 - \theta_{\text{AH(SH)}}^2 + \dots) \approx \theta_{\text{AH(SH)}} - \theta_{\text{AH(SH)}}^3. \quad (4.54)$$

Since we mostly consider the currents proportional to the Hall angle square, we may disregard the cubic term here. This simplifies the elements in the response matrix

$$\mathcal{C}_{\text{AHE}} \approx \theta_{\text{AH}} [\hat{m} \times + \theta_{\text{AH}} \hat{m} \times (\hat{m} \times)], \quad (4.55)$$

$$\mathcal{C}_{\text{SHE}}^{(1)} \approx \theta_{\text{SH}} \hat{m} \times, \quad (4.56)$$

$$\mathcal{C}_{\text{SHE}}^{(2)} \approx \theta_{\text{SH}}^2 \hat{m} \times (\hat{m} \times). \quad (4.57)$$

As the result, the general response relation which includes all the AHE and SHE effects reads

$$\begin{pmatrix} \vec{j}_c \\ \vec{j}_s \end{pmatrix} = \sigma_F \begin{pmatrix} 1 + \mathcal{C}_{\text{AHE}} + \mathcal{C}_{\text{SHE}}^{(2)} & P + \mathcal{C}_{\text{SHE}}^{(1)} \\ P + \mathcal{C}_{\text{SHE}}^{(1)} & 1 + \mathcal{C}_{\text{AHE}} + \mathcal{C}_{\text{SHE}}^{(2)} \end{pmatrix} \begin{pmatrix} -\vec{\nabla} \mu_c / e + E_x \hat{x} \\ -\vec{\nabla} \mu_s / (2e) \end{pmatrix}. \quad (4.58)$$

In the main text, we calculate the charge and spin accumulations to the order linear to the Hall angles such that they contribute to the currents to the order of Hall angle square. This means we disregarded the terms proportional to  $\theta_{\text{AH(SH)}}$  when solving the charge and spin accumulations.

## REFERENCES

- [1] W. Thomson, Proc. R. Soc. London **8**, 546 (1857)
- [2] T. R. McGuire and R. I. Potter, IEEE Trans. Magn. **11**, 1018 (1975).
- [3] J. Smit, Physica **16**, 612 (1951).

- [4] L. Berger, *Physica* **30**, 1141 (1964).
- [5] I. A. Campbell, A. Fert, and O. Jaoul, *J. Phys. C* **3**, S95 (1975).
- [6] A. P. Malozemoff, *Phys. Rev. B* **32**, 6080 (1985); *Phys. Rev. B* **34**, 1853 (1986).
- [7] S. Kokado, M. Tsunoda, K. Harigaya, and A. Sakuma, *J. Phys. Soc. Jpn.* **81**, 024705 (2012).
- [8] A. A. Kovalev, Y. Tserkovnyak, K. Výborný, and J. Sinova, *Phys. Rev. B* **79**, 195129 (2009).
- [9] K.-J. Friedland, M. Bowen, J. Herfort, H. P. Schönherr, and K. H. Ploog, *J. Phys. Condens. Matter* **18**, 2641 (2006).
- [10] M. Bibes, V. Laukhin, S. Valencia, B. Martínez, J. Fontcuberta, O. Yu. Gorbenko, A. R. Kaul, and J. L. Martínez, *J. Phys. C* **17**, 2733 (2005).
- [11] H. D. Arnold and G. W. Elmen, *J. Frank. Inst.* **195**, 621 (1923).
- [12] Th. G. S. M. Rijks, R. Coehoorn, M. J. M. de Jong, and W. J. M. de Jonge, *Phys. Rev. B* **51**, 283 (1995).
- [13] Th. G. S. M. Rijks, S. K. J. Lenczowski, R. Coehoorn, and W. J. M. de Jonge, *Phys. Rev. B* **56**, 362 (1997).
- [14] A. T. Hindmarch *et al*, unpublished.
- [15] M. Weiler, M. Althammer, F. D. Czeschka, H. Huebl, M. S. Wagner, M. Opel, I.-M. Imort, G. Reiss, A. Thomas, R. Gross, and S. T. B. Goennenwein, *Phys. Rev. Lett.* **108**, 106602 (2012).
- [16] S. Y. Huang, X. Fan, D. Qu, Y. P. Chen, W. G. Wang, J. Wu, T. Y. Chen, J. Q. Xiao, and C. L. Chien, *Phys. Rev. Lett.* **109**, 107204 (2012).
- [17] H. Nakayama, M. Althammer, Y.-T. Chen, K. Uchida, Y. Kajiwara, D. Kikuchi, T. Ohtani, S. Geprägs, M. Opel, S. Takahashi, R. Gross, G. E. W. Bauer, S. T. B. Goennenwein, and E. Saitoh, *Phys. Rev. Lett.* **110**, 206601 (2013).
- [18] C. Hahn, G. de Loubens, O. Klein, M. Viret, V. V. Naletov, and J. Ben Youssef, *Phys. Rev. B* **87**, 174417 (2013).
- [19] N. Vlietstra, J. Shan, V. Castel, J. Ben Youssef, and B. J. van Wees, *Phys. Rev. B* **87**, 184421 (2013).

- [20] M. Althammer, S. Meyer, H. Nakayama, M. Schreier, S. Altmannshofer, M. Weiler, H. Huebl, S. Geprägs, M. Opel, R. Gross, D. Meier, C. Klewe, T. Kuschel, J.-M. Schmalhorst, G. Reiss, L. Shen, A. Gupta, Y.-T. Chen, G. E. W. Bauer, E. Saitoh, and S. T. B. Goennenwein, *Phys. Rev. B* **87**, 224401 (2013).
- [21] Y.-T. Chen, S. Takahashi, H. Nakayama, M. Althammer, S. T. B. Goennenwein, E. Saitoh, G. E. W. Bauer, *Phys. Rev. B* **87**, 144411 (2013).
- [22] A. Kobs, S. Heße, W. Kreuzpaintner, G. Winkler, D. Lott, P. Weinberger, A. Schreyer, and H. P. Oepen, *Phys. Rev. Lett.* **106**, 217207 (2011).
- [23] Y. M. Lu, J. W. Cai, S. Y. Huang, D. Qu, B. F. Miao, and C. L. Chien, *Phys. Rev. B* **87**, 220409(R) (2013).
- [24] B. F. Miao, S. Y. Huang, D. Qu, and C. L. Chien, *Phys. Rev. Lett.* **111**, 066602 (2013).
- [25] E. Saitoh *c.s.*, private communication.
- [26] For a review, see, N. Nagaosa, J. Sinova, S. Onoda, A. H. MacDonald, and N. P. Ong, *Rev. Mod. Phys.* **82**, 1539 (2010).
- [27] Í. Adagideli, G. E. W. Bauer, and B. I. Halperin, *Phys. Rev. Lett.* **97**, 256601 (2006).
- [28] S. Zhang, *Phys. Rev. Lett.* **85**, 393 (2000).
- [29] T. R. McGuire, J. A. Aboaf, and E. Klokholm, *IEEE Trans. Magn.* **20**, 972 (1984).
- [30] M. Tsunoda, Y. Komasaki, S. Kokado, S. Isogami, C.-C. Chen, and M. Takahashi, *Appl. Phys. Express* **2**, 083001 (2009).
- [31] S. Takahashi, H. Imamura, and S. Maekawa, in *Concepts in Spin Electronics*, edited by S. Maekawa (Oxford University Press, U.K., 2006), pp. 343-370.
- [32] P. C. van Son, H. van Kempen, and P. Wyder, *Phys. Rev. Lett.* **58**, 2271 (1987).
- [33] S. Hershfield and H. L. Zhao, *Phys. Rev. B* **56**, 3296 (1997).
- [34] M. Haidar and M. Bailleul, *Phys. Rev. B* **88**, 054417 (2013).
- [35] A. A. Starikov, P. J. Kelly, A. Brataas, Y. Tserkovnyak, and G. E. W. Bauer, *Phys. Rev. Lett.* **105**, 236601 (2010).
- [36] J. Bass and W. P. Pratt, *J. Phys. Condens. Matter* **19**, 183201 (2007).

- [37] R. Merservey and P. M. Tedrow, *Phys. Rep.* **238**, 173 (1994).
- [38] R. M. Bozorth, *Phys. Rev.* **70**, 923 (1946).
- [39] T. Miyasato, N. Abe, T. Fujii, A. Asamitsu, S. Onoda, Y. Onose, N. Nagaosa, and Y. Tokura, *Phys. Rev. Lett.* **99**, 086602 (2007); S. Onoda, N. Sugimoto, and N. Nagaosa, *Phys. Rev. B* **77**, 165103 (2008).
- [40] J. Banhart and H. Ebert, *Europhys. Lett.* **32**, 517 (1995).
- [41] A. Tsukahara, Y. Kitamura, E. Shikoh, Y. Ando, T. Shinjo, and M. Shiraishi, arXiv:1301.3580.
- [42] A. Azevedo, O. Alves Santos, G. A. Fonseca Guerra, R. O. Cunha, R. Rodríguez-Suàrez, and S. M. Rezende, accepted by *Appl. Phys. Lett.*
- [43] P. Hyde, L. Bai, D.M.J. Kumar, B.W. Southern, S.Y. Huang, B.F. Miao, C.L. Chien, C.-M. Hu, arXiv:1310.4840.
- [44] A. Brataas, Yu. V. Nazarov, and G. E. W. Bauer, *Phys. Rev. Lett.* **84**, 2481 (2000); A. Brataas, Y.V. Nazarov, and G.E.W. Bauer, *Eur. Phys. J. B* **22**, 99 (2001).
- [45] H. X. Tang, R. K. Kawakami, D. D. Awschalom, and M. L. Roukes, *Phys. Rev. Lett.* **90**, 107201 (2003).



# 5

## FUCHS-SONDHEIMER THEORY OF THE SPIN HALL EFFECT

**Yan-Ting CHEN**

*We present a Boltzmann analysis of the surface/interface scattering effects on the spin Hall physics in bilayers of a metal (N) with a magnetic insulator (FI). The spin Hall angle is modulated by the surface scattering and becomes thickness-dependent in the thin-film limit. We propose that due to spin-dependent scattering at the N\FI interface, a spin polarized current is generated when applying an electric field parallel to the interface. When the magnetization is out-of-plane, this spin-polarized current contributes a transverse charge current via the inverse spin Hall effect.*

---

Parts of this chapter have been collaborated with Eiji Saitoh, Saburo Takahashi, and Gerrit E. W. Bauer

## 5.1 INTRODUCTION

Since the discovery of the giant magnetoresistance (GMR) [1] a large part of the magnetism/spintronics community has been interested in magnetic multilayers [2, 3]. Recently, bilayers made from a heavy normal metal (N) such as platinum and a ferromagnet (F) have attracted attention since a strong spin-orbit coupling (SOC) in N may lead to a transfer of spin angular momentum through the N|F interface in the form of spin transfer torques (STTs). The injected angular momentum may modulate or even switch the magnetization, thereby providing a promising mechanism for new types of magnetic storage devices [4–6]. The STTs in this type of systems is often ascribed to the spin Hall effect (SHE), i.e., the transverse spin current/accumulation generated by a charge current/voltage bias [7]. Another possible source of STTs is the Rashba/Edelstein effect in conductors with broken inversion symmetry [8]. The bilayer systems studied in this context all contain ferromagnetic metals. However, it is known that large spin transfer torques exist also at the interface to magnetic insulators (FI) such as yttrium iron garnet (YIG) [9, 10], a material of considerable technological interest because of its very low magnetization damping [11]. Moreover, in FI|N the electric current only flows in N, which importantly simplifies the interpretation of experiments.

The essential parameters of the FI|N bilayer are the spin Hall angle and spin diffusion length in N as well as the interface spin-mixing conductance. They can be determined by fitting a model based on diffusion theory to a set of experimental data. For the most commonly used N=Pt different experiments have converged to some degree [12, 13], although most groups arrive a spin-flip lengths of Pt that are suspiciously short, i.e. of the order of a nm. Furthermore, the Pt electrical conductivity turn out to be strongly thickness dependent, indicating the increasing importance of interface roughness (or deterioration of the sample quality) with reduced film thickness. Transport in thin-films with rough surfaces can characterize by a specularity parameter that interpolates between the limits of completely specular and completely diffusive scatterings [14, 15]. This approach has been adopted to analyze the current-in-plane (CIP) GMR [16] and the anisotropic magnetoresistance (AMR) in ultra-thin films [17, 18].

A recently discovered effect in FI|N bilayers is the so-called spin magnetoresistance (SMR), i.e. the dependence of the charge transport in N on the magnetization direction in F, in spite of the fact that electrons cannot penetrate the FI. This effect can be quantitatively explained in terms of the simultaneous action of the SHE and the inverse spin Hall effect (ISHE) [20–22], although an alternative, qualitative interpretation as an equilibrium magnetic proximity effect has been put forward as well [23]. The theory predicts an anomalous Hall like contribution from the SMR, i.e. a finite Hall resistance when the magnetization is normal to the films, which

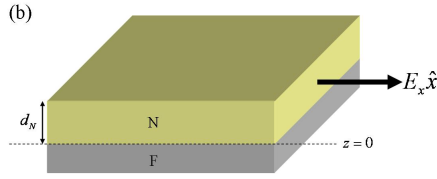


FIGURE 5.1: N|FI bilayer, where FI is a magnetic insulator.

is proportional to the imaginary part of the spin-mixing conductance  $g_i$  [22]. This effect was indeed observed [24] and found to be consistent with diffusion theory and band structure calculations for  $g_i$ . However, there is an alternative explanation that does not involve  $g_i$ : The scattering at an FI|N interface is spin-dependent in the presence of roughness, which can spin-polarize an applied charge current. The ISHE then may generate a Hall voltage with identical phenomenology as the AHE.

A numerical study in metallic bilayers in the presence of both SHE and Rashba (Edelstein) effects focussed on spin transfer torques [25]. Here we analyze the simpler problem of semiclassical transport FI|N bilayers as shown in Fig. 5.1, which allows an analytical treatment. We generalize the Fuchs-Sondheimer approach [14, 15], taking into account the contributions from the spin-orbit interaction in N in the collision terms [26]. Surface roughness is found to affect the effective spin Hall angle, as well as inducing an AHE-like effect similar to that of the imaginary spin mixing conductance [22]. This article is organized as following: In Sec. 5.2, we present the Boltzmann theory in the relaxation time approximation. We apply the theory to study the AHE induced by spin-dependent roughness in Sec. 5.3, and provide a procedure to analyze the correction of roughness on the conventional in Sec. 5.4, respectively. We summarize conclusions in Sec. 5.5.

## 5.2 RELAXATION TIME APPROXIMATION

### 5.2.1 BASICS

We are interested in the transport properties of thin metallic films in the presence of disorder and spin-orbit interactions (SOI) at ambient temperatures. The semiclassical Boltzmann equation is well suited to describe the spatiotemporal distribution of electrons in the presence of applied electric fields. We assume that the SOI is mediated by impurity scattering only. This is probably not the case in heavy metal such as Pt in which the electronic structure is strongly affected by SOI. However, the intrinsic terms only modify the parameter values and e.g. their tempera-

tures dependence, but do not change the phenomenology. We consider thin films, either suspended in vacuum or deposited on top of an FI substrate (see Fig. 1). The system is translationally invariant in the  $x$ - $y$  film plane,  $\hat{x}$  being the transport direction, and finite in the  $\hat{z}$  direction.

The distribution function in a normal metal in the weakly relativistic limit can be expressed as a  $2 \times 2$  matrix in (Pauli) spin space

$$\hat{f}_{\vec{k}} = \begin{pmatrix} f_{\uparrow\uparrow} & f_{\uparrow\downarrow} \\ f_{\downarrow\uparrow} & f_{\downarrow\downarrow} \end{pmatrix} = f_{\vec{k}0} \hat{1} + \vec{\sigma} \cdot \vec{f}_{\vec{k}s}, \quad (5.1)$$

where  $f_{\vec{k}0}$  is the particle (charge) distribution,  $\hat{1}$  is a  $2 \times 2$  identity matrix,  $\vec{\sigma}$  is the vector of the Pauli matrices, and  $\vec{f}_{\vec{k}s} = (f_{\vec{k}x}, f_{\vec{k}y}, f_{\vec{k}z})^T$  is the net spin polarization. In order to simplify the problem we assume that the spin polarization is along a Cartesian axis. This is the case when the FI magnetization is as well oriented along Cartesian axes and when precession of the spin accumulation in external magnetic fields or the imaginary part of spin mixing conductance at the interface is disregarded.

The elements of the matrix in Eq. (5.1) are expressed by particle and spin distributions

$$f_{\uparrow\uparrow} = f_{\vec{k}0} + f_{\vec{k}z}, \quad (5.2)$$

$$f_{\downarrow\downarrow} = f_{\vec{k}0} - f_{\vec{k}z}, \quad (5.3)$$

$$f_{\downarrow\uparrow} = f_{\vec{k}x} - i f_{\vec{k}y}, \quad (5.4)$$

$$f_{\uparrow\downarrow} = f_{\vec{k}x} + i f_{\vec{k}y}. \quad (5.5)$$

The spin current density in the non-relativistic limit

$$\vec{j}_s = en \langle \vec{v} \otimes \vec{\sigma} + \vec{\sigma} \otimes \vec{v} \rangle / 2 = (\vec{j}_{sx}, \vec{j}_{sy}, \vec{j}_{sz})^T \quad (5.6)$$

is a second-rank tensor (here in units of the charge current density  $\vec{j}_c = en \langle \vec{v} \rangle$ ), where  $e = |e|$  is the electron charge,  $n$  is the density of the electrons,  $\vec{v}$  is the velocity operator,  $\vec{\sigma}$  is the vector of Pauli spin matrices, and  $\langle \dots \rangle$  denotes an expectation value. The row vectors  $\vec{j}_{si} = en \langle \vec{v} \sigma_i + \sigma_i \vec{v} \rangle / 2$  in Eq. (5.6) are the spin current densities polarized in the  $\hat{i}$ -direction. In the present formulation with particle and spin distributions, the charge and each component of the spin current densities then read [26]

$$\vec{j}_c = e \sum_{\vec{k}} \left( \vec{v}_{\vec{k}}^{(0)} f_{\vec{k}0} + \sum_i \vec{\omega}_{\vec{k}i} f_{\vec{k}i} \right), \quad (5.7)$$

$$\vec{j}_{si} = e \sum_{\vec{k}} \left( \vec{v}_{\vec{k}}^{(0)} f_{\vec{k}i} + \vec{\omega}_{\vec{k}i} f_{\vec{k}0} \right), \quad (5.8)$$

where  $\vec{v}_{\vec{k}}^{(0)} = \hbar \vec{k} / m$  is the normal velocity,  $\hat{k} = \vec{k} / |\vec{k}|$ , and

$$\vec{\omega}_{\vec{k}l} = \alpha_{\text{H}}^{\text{SJ}} \left( \hat{l} \times \frac{\hbar \vec{k}}{m} \right) \quad (5.9)$$

is the anomalous velocity for electrons polarized along  $\hat{l}$  from side-jump scattering characterized by the parameter

$$\alpha_{\text{H}}^{\text{SJ}} = \frac{m \eta_{so}}{\hbar \tau}, \quad (5.10)$$

where  $\eta_{so} = \hbar^2 / (4m_0^2 c^2)$  is the SOC constant and  $\tau$  the relaxation time [26, 27]. We can associate the first term in Eq. (5.8) to skew scattering and second one to the side-jump mechanism.

## 5.2.2 BOLTZMANN EQUATIONS

The steady-state distribution function  $\hat{f}_{\vec{k}}(\epsilon, \vec{r})$  solves the Boltzmann equation matrix

$$\vec{v}_{\vec{k}}^{(0)} \cdot \vec{\nabla} \hat{f}_{\vec{k}} - \frac{e \vec{E}}{\hbar} \cdot \vec{\nabla}_{\vec{k}} \hat{f}_{\vec{k}} = \left( \frac{\partial \hat{f}_{\vec{k}}}{\partial t} \right)_{\text{scatt}}, \quad (5.11)$$

where  $\vec{E} = E \hat{x}$  is the applied electric field. The collision terms on the RHS of the equation govern the scattering by non-magnetic impurities in the bulk metal. The spin-(in)dependent scattering at the interface/surface will be taken into account by the boundary conditions.

With the linearization ( $\chi = 0, x, y, z$ )

$$f_{\vec{k}\chi} \rightarrow f^0 \delta_{\chi,0} - \frac{\partial f^0}{\partial \epsilon} \mu_{\chi} + g_{\vec{k}\chi}^a, \quad (5.12)$$

where  $f^0$  is the Fermi-Dirac distribution,  $\hat{f}_{\vec{k}}$  can be expanded as

$$\hat{f}_{\vec{k}} \rightarrow f^0 \hat{1} - \frac{\partial f^0}{\partial \epsilon} \hat{\mu} + \hat{g}_{\vec{k}}^a. \quad (5.13)$$

Collecting the leading terms

$$\begin{aligned}
& \vec{v}_{\hat{k}}^{(0)} \cdot \vec{\nabla} \hat{f}_{\hat{k}} - \frac{e\vec{E}}{\hbar} \cdot \vec{\nabla}_{\hat{k}} \hat{f}_{\hat{k}} \\
& \approx \vec{v}_{\hat{k}}^{(0)} \cdot \left( \vec{\nabla} \hat{f}_{\hat{k}} - e\vec{E} \frac{\partial f^0}{\partial \varepsilon} \hat{1} \right) \\
& = \vec{v}_{\hat{k}}^{(0)} \cdot \left( -\frac{\partial f^0}{\partial \varepsilon} \vec{\nabla} \hat{\mu} + \vec{\nabla} \hat{g}_{\hat{k}}^a - \frac{\partial f^0}{\partial \varepsilon} e\vec{E} \hat{1} \right) \\
& = v_k^{(z)} \left( -\frac{\partial f^0}{\partial \varepsilon} \partial_z \hat{\mu} + \partial_z \hat{g}_{\hat{k}}^a \right) - v_k^{(x)} eE \frac{\partial f^0}{\partial \varepsilon} \hat{1}. \tag{5.14}
\end{aligned}$$

The Boltzmann equation Eq. (5.11) can be decomposed into four equations for particle and spin distributions taking into account the SO terms (in the relaxation time approximation) [25, 26, 28]

$$v_k^{(z)} \partial_z \left( g_{\hat{k}0}^a - \frac{\partial f^0}{\partial \varepsilon} \mu_0 \right) - v_k^{(x)} eE \frac{\partial f^0}{\partial \varepsilon} = -\frac{g_{\hat{k}0}^a}{\tau} - \frac{\alpha_{\text{H}}^{\text{SS}}}{\tau} \sum_{\chi=x,y,z} \sum_{\hat{k}'} (\hat{k} \times \hat{k}')_{\chi} g_{\hat{k}'\chi}^a, \tag{5.15}$$

$$v_k^{(z)} \partial_z \left( g_{\hat{k}x}^a - \frac{\partial f^0}{\partial \varepsilon} \mu_x \right) = -\frac{g_{\hat{k}x}^a}{\tau} - \frac{\mu_x}{\tau_{\text{sf}}} + \frac{\alpha_{\text{H}}^{\text{SS}}}{\tau} \sum_{\hat{k}'} (\hat{k} \times \hat{k}')_x g_{\hat{k}'0}^a, \tag{5.16}$$

$$v_k^{(z)} \partial_z \left( g_{\hat{k}y}^a - \frac{\partial f^0}{\partial \varepsilon} \mu_y \right) = -\frac{g_{\hat{k}y}^a}{\tau} - \frac{\mu_y}{\tau_{\text{sf}}} + \frac{\alpha_{\text{H}}^{\text{SS}}}{\tau} \sum_{\hat{k}'} (\hat{k} \times \hat{k}')_y g_{\hat{k}'0}^a, \tag{5.17}$$

$$v_k^{(z)} \partial_z \left( g_{\hat{k}z}^a - \frac{\partial f^0}{\partial \varepsilon} \mu_z \right) = -\frac{g_{\hat{k}z}^a}{\tau} - \frac{\mu_z}{\tau_{\text{sf}}} + \frac{\alpha_{\text{H}}^{\text{SS}}}{\tau} \sum_{\hat{k}'} (\hat{k} \times \hat{k}')_z g_{\hat{k}'0}^a, \tag{5.18}$$

where the spin dissipation is characterized by the spin-flip relaxation time  $\tau_{\text{sf}}$ , and the skew scattering by the parameter  $\alpha_{\text{H}}^{\text{SS}}$ .

### 5.3 AHE

We are interested in the leading corrections due to spin orbit interaction and spin-dependent interface roughness to the anomalous Hall effect-like signal. We set the magnetization in FI  $\hat{m} = \hat{z}$  and discard the  $x$  and  $y$  polarization components that not interfere with the AHE to leading order. Those can be analyzed independently below in another section (or paper). Then we just have the Boltzmann equation for particle and  $\hat{z}$ -polarized spin distributions. Neither the SOC nor the roughness can drive a  $z$ -polarized spin current flow into the  $z$ -direction, so the ansatz should

be  $g_{\hat{k}z}^a = g_z^x \kappa_x + g_z^y \kappa_y$ , where  $\hat{k} = (\kappa_x, \kappa_y, \kappa_z)$ . Integrating the Boltzmann equation

$$v_k^{(z)} \partial_z \left( g_z^x \kappa_x + g_z^y \kappa_y - \frac{\partial f^0}{\partial \varepsilon} \mu_z \right) = -\frac{g_z^x \kappa_x + g_z^y \kappa_y}{\tau} - \frac{\mu_z}{\tau_{\text{sf}}} + \frac{\alpha_{\text{H}}^{\text{SS}}}{\tau} \sum_{\hat{k}'} (\hat{k} \times \hat{k}')_z g_{\hat{k}'0}^a \quad (5.19)$$

over momentum space directly leads to  $\mu_z = 0$ , i.e. the spin accumulation vanishes since every term is odd in  $\kappa_i$  except for  $\mu_z/\tau_{\text{sf}}$ . Also,  $\partial_z \mu_0 = 0$  since no charge current flows in the  $\hat{z}$  direction. The Boltzmann equations then read

$$v_k^{(z)} \partial_z g_{\hat{k}0}^a - v_k^{(x)} eE \frac{\partial f^0}{\partial \varepsilon} = -\frac{g_{\hat{k}0}^a}{\tau} - \frac{\alpha_{\text{H}}^{\text{SS}}}{\tau} \sum_{\hat{k}'} (\hat{k} \times \hat{k}')_z g_{\hat{k}'z}^a, \quad (5.20)$$

$$v_k^{(z)} \partial_z g_{\hat{k}z}^a = -\frac{g_{\hat{k}z}^a}{\tau} + \frac{\alpha_{\text{H}}^{\text{SS}}}{\tau} \sum_{\hat{k}'} (\hat{k} \times \hat{k}')_z g_{\hat{k}'0}^a, \quad (5.21)$$

Two mechanisms give rise to an AHE-like transport phenomenon. The first one is the combination of the spin current  $g_{\hat{k}z}^a$  (due to spin-dependent roughness) and the anomalous velocity (due to side jump). The second one is the skew-scattering correction to  $g_{\hat{k}0}^a$  by  $g_{\hat{k}z}^a$  in Eq. (5.20).

To leading order in the perturbations (interface roughness and spin-orbit interaction)  $g_{\hat{k}z}^a$  can be obtained from Eq. (5.21) by disregarding the SOC term since the spin current is generated by the roughness. Substituting  $g_{\hat{k}z}^a$  into Eq. (5.20), we obtain the skew scattering correction on  $g_{\hat{k}0}^a$ . In the absence of SOC, we can adopt the two-channel model. According to Eqs. (5.2-5.3), the anisotropic distribution of electron along  $\hat{z}$  ( $-\hat{z}$ ) can be written as  $g_{\hat{k}\uparrow}^a$  ( $g_{\hat{k}\downarrow}^a$ ). The charge and spin distribution are related by

$$g_{\hat{k}0}^a = \frac{g_{\hat{k}\uparrow}^a + g_{\hat{k}\downarrow}^a}{2}, \quad (5.22)$$

$$g_{\hat{k}z}^a = g_{\hat{k}\uparrow}^a - g_{\hat{k}\downarrow}^a. \quad (5.23)$$

The specularity at the top of N is spin-independent ( $p_0$ ) while the specularity at the bottom is spin-dependent. We use  $p_p$  ( $p_{\text{ap}}$ ) to denote the specularity in the case polarization of electrons is (anti-) parallel to the magnetization. The boundary

conditions are

$$g_{k\uparrow}^-(z = d_N) = p_0 g_{k\uparrow}^+(z = d_N), \quad (5.24)$$

$$g_{k\downarrow}^-(z = d_N) = p_0 g_{k\downarrow}^+(z = d_N), \quad (5.25)$$

$$g_{k\uparrow}^+(z = 0) = p_p g_{k\uparrow}^-(z = 0), \quad (5.26)$$

$$g_{k\downarrow}^+(z = 0) = p_{ap} g_{k\downarrow}^-(z = 0), \quad (5.27)$$

leading to the solutions

$$g_{k\uparrow}^{(x)+}(|v_k^{(z)}|, z) = \tau v_k^{(x)} eE \frac{\partial f^0}{\partial \varepsilon} \left[ 1 - \frac{e^{\frac{d_N}{\tau|v_k^{(z)}|}} (1 - p_p) + p_p (1 - p_0) e^{-\frac{z}{\tau|v_k^{(z)}|}}}{e^{\frac{d_N}{\tau|v_k^{(z)}|}} - p_0 p_p e^{-\frac{d_N}{\tau|v_k^{(z)}|}}} \right], \quad (5.28)$$

$$g_{k\downarrow}^{(x)+}(|v_k^{(z)}|, z) = \tau v_k^{(x)} eE \frac{\partial f^0}{\partial \varepsilon} \left[ 1 - \frac{e^{\frac{d_N}{\tau|v_k^{(z)}|}} (1 - p_{ap}) + p_{ap} (1 - p_0) e^{-\frac{z}{\tau|v_k^{(z)}|}}}{e^{\frac{d_N}{\tau|v_k^{(z)}|}} - p_0 p_{ap} e^{-\frac{d_N}{\tau|v_k^{(z)}|}}} \right], \quad (5.29)$$

$$g_{k\uparrow}^{(x)-}(|v_k^{(z)}|, z) = \tau v_k^{(x)} eE \frac{\partial f^0}{\partial \varepsilon} \left[ 1 - \frac{e^{\frac{d_N}{\tau|v_k^{(z)}|}} (1 - p_0) + p_0 (1 - p_p) e^{\frac{z-d_N}{\tau|v_k^{(z)}|}}}{e^{\frac{d_N}{\tau|v_k^{(z)}|}} - p_0 p_p e^{-\frac{d_N}{\tau|v_k^{(z)}|}}} \right], \quad (5.30)$$

$$g_{k\downarrow}^{(x)-}(|v_k^{(z)}|, z) = \tau v_k^{(x)} eE \frac{\partial f^0}{\partial \varepsilon} \left[ 1 - \frac{e^{\frac{d_N}{\tau|v_k^{(z)}|}} (1 - p_0) + p_0 (1 - p_{ap}) e^{\frac{z-d_N}{\tau|v_k^{(z)}|}}}{e^{\frac{d_N}{\tau|v_k^{(z)}|}} - p_0 p_{ap} e^{-\frac{d_N}{\tau|v_k^{(z)}|}}} \right]. \quad (5.31)$$

When the spin-dependence of the interface scattering is weak

$$p_p = p_0 + \delta p, \quad (5.32)$$

$$p_{ap} = p_0 - \delta p, \quad (5.33)$$

in terms of the small parameter  $\delta p$ . When  $\delta p \ll p_0$ , the particle distribution is

simplified to

$$g_{k0}^{x+} = \tau v_k^{(x)} eE \frac{\partial f^0}{\partial \varepsilon} \left[ 1 - \frac{1 - p_0}{1 - p_0 \exp\left(-\frac{d_N}{\tau |v_k^{(z)}|}\right)} \exp\left(-\frac{z}{\tau |v_k^{(z)}|}\right) \right], \quad (5.34)$$

$$g_{k0}^{x-} = \tau v_k^{(x)} eE \frac{\partial f^0}{\partial \varepsilon} \left[ 1 - \frac{1 - p_0}{1 - p_0 \exp\left(-\frac{d_N}{\tau |v_k^{(z)}|}\right)} \exp\left(\frac{z - d_N}{\tau |v_k^{(z)}|}\right) \right], \quad (5.35)$$

while the spin distribution reads

$$\begin{aligned} g_{kz}^{x+} &= 2\delta p \tau v_k^{(x)} eE \frac{\partial f^0}{\partial \varepsilon} \frac{\exp\left(\frac{2d_N}{\tau |v_k^{(z)}|}\right) \left[ \exp\left(\frac{d_N}{\tau |v_k^{(z)}|}\right) - 1 \right]}{\left[ \exp\left(\frac{d_N}{\tau |v_k^{(z)}|}\right) - p_0 \right]^2 \left[ \exp\left(\frac{d_N}{\tau |v_k^{(z)}|}\right) + p_0 \right]} \exp\left(-\frac{z}{\tau |v_k^{(z)}|}\right) \\ &\equiv h^+ \exp\left(-\frac{z}{\tau |v_k^{(z)}|}\right), \end{aligned} \quad (5.36)$$

$$\begin{aligned} g_{kz}^{x-} &= 2\delta p p_0 \tau v_k^{(x)} eE \frac{\partial f^0}{\partial \varepsilon} \frac{\exp\left(\frac{d_N}{\tau |v_k^{(z)}|}\right) \left[ \exp\left(\frac{d_N}{\tau |v_k^{(z)}|}\right) - 1 \right]}{\left[ \exp\left(\frac{d_N}{\tau |v_k^{(z)}|}\right) - p_0 \right]^2 \left[ \exp\left(\frac{d_N}{\tau |v_k^{(z)}|}\right) + p_0 \right]} \exp\left(\frac{z - d_N}{\tau |v_k^{(z)}|}\right) \\ &\equiv h^- \exp\left(\frac{z - d_N}{\tau |v_k^{(z)}|}\right), \end{aligned} \quad (5.37)$$

where terms proportional to  $(\delta p)^2$  are disregarded.

### 5.3.1 ROUGHNESS EFFECT ON ELECTRIC CONDUCTIVITY

One can see that the particle distribution is the result for a thin-film with the same specularity at top and bottom, which was analyzed by Fuchs and Sondheimer [14,

15]. The charge current can be calculated by

$$\begin{aligned} \vec{j}_c &= e \sum_{\vec{k}, k_z > 0} \vec{v}_{\vec{k}}^{(0)} \int_0^{d_N} g_{k0}^+ dz / d_N + e \sum_{\vec{k}, k_z < 0} \vec{v}_{\vec{k}} \int_0^{d_N} g_{k0}^- dz / d_N \quad (5.38) \\ &= e^2 E \sum_{\vec{k}} \vec{v}_{\vec{k}}^{(0)} v_k^{(x)} \tau \frac{\partial f^0}{\partial \varepsilon} - e^2 E l / d_N (1 - p_0) \sum_{\vec{k}} \vec{v}_{\vec{k}}^{(0)} v_k^{(x)} \tau \frac{\partial f^0}{\partial \varepsilon} |\cos \theta| \frac{1 - e^{-\frac{d_N}{l|\cos \theta|}}}{1 - p_0 e^{-\frac{d_N}{l|\cos \theta|}}}, \quad (5.39) \end{aligned}$$

where we have defined the mean free path  $l \equiv \tau v_k$  and  $v_k^{(z)} = v_k \kappa_z = v_k \cos \theta$  with  $\theta$  the angle between  $\hat{k}$  and  $\hat{z}$ .

It is convenient to introduce the effective electric conductivity

$$\sigma = e^2 \sum_{\vec{k}} v_k^2 \kappa_x^2 \tau \frac{\partial f^0}{\partial \varepsilon} - e^2 l / d_N (1 - p_0) \sum_{\vec{k}} v_k^2 \kappa_x^2 \tau \frac{\partial f^0}{\partial \varepsilon} |\cos \theta| \frac{1 - e^{-\frac{d_N}{l|\cos \theta|}}}{1 - p_0 e^{-\frac{d_N}{l|\cos \theta|}}}. \quad (5.40)$$

Defining the electric conductivity for bulk (without roughness correction)

$$\sigma_0 \equiv e^2 \sum_{\vec{k}} v_k^2 \kappa_x^2 \tau \frac{\partial f^0}{\partial \varepsilon}, \quad (5.41)$$

we can see that

$$\frac{\sigma_0}{\sigma} = \frac{\sum_{\vec{k}} \kappa_x^2}{\sum_{\vec{k}} \kappa_x^2 - l / d_N (1 - p_0) \sum_{\vec{k}} \kappa_x^2 |\cos \theta| \frac{1 - e^{-\frac{d_N}{l|\cos \theta|}}}{1 - p_0 e^{-\frac{d_N}{l|\cos \theta|}}}}. \quad (5.42)$$

This is a complicated integral. It is shown in Ref. [15] that for thick-films  $d_N \gg l$ ,

$$\frac{\sigma_0}{\sigma} \approx 1 + \frac{3l}{8d_N} (1 - p_0), \quad (5.43)$$

while for thin-films  $d_N \ll l$ ,

$$\frac{\sigma_0}{\sigma} \approx \frac{4(1 - p_0)}{3(1 + p_0)} \frac{1}{d_N / l \log(l / d_N)}. \quad (5.44)$$

If the roughness at the top or bottom is different from  $p_0$ , e.g., characterized by  $p_1 \neq p_0$ , the correction can be calculated but involves tedious integrals which do not appear to be solvable analytically.

### 5.3.2 SPIN CURRENT DRIVEN BY SPIN-DEPENDENT ROUGHNESS AND AHE DUE TO SIDE-JUMP

We mainly interested in the spin distribution, Eqs. (5.36-5.37).  $g_{kz}^{x+}(z=0) \geq g_{kz}^{x-}(z=d_N)$  since  $p_0 \leq 1$  implies that spin-dependent scattering at  $z=0$  induces a spin current

$$\vec{j}_{sz} \equiv e \sum_{\vec{k}} \vec{v}_{\vec{k}}^{(0)} g_z^x \kappa_x \quad (5.45)$$

proportional to  $\delta p$  for small  $\delta p$ . When the anomalous velocity (due to the side-jump scattering) is taken into account, the spin current generates a charge current in the  $\hat{y}$ -direction (the AHE current)

$$\vec{j}_c^{\text{SJ}} \equiv e \sum_{\vec{k}} \tilde{\omega}_{\vec{k}} g_z^x \kappa_x = \alpha_{\text{H}}^{\text{SJ}} e \sum_{\vec{k}} (\hat{z} \times \vec{v}_{\vec{k}}) g_z^x \kappa_x = \alpha_{\text{H}}^{\text{SJ}} (\hat{z} \times \vec{j}_{sz}). \quad (5.46)$$

In the limit  $p_0 \approx 1 \gg \delta p$  (specular limit), the spin distribution is simplified to

$$g_z^{x+} = \delta p \tau v_k e E \frac{\partial f^0}{\partial \varepsilon} \left[ 1 + \coth \left( \frac{d_N}{l |\cos \theta|} \right) \right] \exp \left( - \frac{z}{l |\cos \theta|} \right), \quad (5.47)$$

$$g_z^{x-} = \delta p \tau v_k e E \frac{\partial f^0}{\partial \varepsilon} \text{csch} \left( \frac{d_N}{l |\cos \theta|} \right) \exp \left( \frac{z - d_N}{l |\cos \theta|} \right), \quad (5.48)$$

and the averaged (over  $z$ ) spin current reads

$$\begin{aligned} \vec{J}_{sz} &= \frac{1}{d_N} \int_0^{d_N} \vec{j}_{sz} dz = \frac{1}{d_N} \int_0^{d_N} e \sum_{\vec{k}} \vec{v}_{\vec{k}}^{(0)} g_z^x \kappa_x dz \\ &= \hat{x} \delta p \frac{l}{d_N} e^2 E \sum_{\vec{k}, k_z > 0} \tau v_k^2 \frac{\partial f^0}{\partial \varepsilon} |\cos \theta| \left[ 1 + \coth \left( \frac{d_N}{l |\cos \theta|} \right) \right] \left[ 1 - \exp \left( - \frac{d_N}{l |\cos \theta|} \right) \right] \kappa_x^2 \\ &\quad + \hat{x} \delta p \frac{l}{d_N} e^2 E \sum_{\vec{k}, k_z < 0} \tau v_k^2 \frac{\partial f^0}{\partial \varepsilon} |\cos \theta| \text{csch} \left( \frac{d_N}{l |\cos \theta|} \right) \left[ 1 - \exp \left( - \frac{d_N}{l |\cos \theta|} \right) \right] \kappa_x^2. \end{aligned} \quad (5.49)$$

The corresponding averaged AHE current due to side-jump can be estimated to scale like

$$\vec{J}_c^{\text{SJ}} = \alpha_{\text{H}}^{\text{SJ}} (\hat{z} \times \vec{J}_{sz}) \propto \eta_{so} \cdot \delta p \cdot l / d_N. \quad (5.50)$$

### 5.3.3 AHE DUE TO SKEW SCATTERING

In order to find the leading term caused by skew scattering, we substitute the spin distribution  $g_{\hat{k}z}^a$  Eqs. (5.36-5.37) from the two-current model into Eq. (5.20):

$$\begin{aligned} v_k^{(z)} \partial_z \left( g_{\hat{k}0}^a - \frac{\partial f^0}{\partial \varepsilon} \mu_0 \right) - v_k^{(x)} eE \frac{\partial f^0}{\partial \varepsilon} &= -\frac{g_{\hat{k}0}^a}{\tau} - \frac{\alpha_{\text{H}}^{\text{SS}}}{\tau} \sum_{\hat{k}'} (\hat{k} \times \hat{k}')_z g_{\hat{k}'z}^a \\ &= -\frac{g_{\hat{k}0}^a}{\tau} + \frac{4\pi\alpha_{\text{H}}^{\text{SS}}}{3\tau} g_z^x \kappa_y. \end{aligned} \quad (5.51)$$

With the ansatz  $g_{\hat{k}0}^a = g_0^x \kappa_x + g_0^y \kappa_y$ , we obtain the equation for the transverse ( $\hat{y}$ ) component

$$v_k^{(z)} \partial_z g_0^y = -\frac{g_0^y}{\tau} + \frac{4\pi\alpha_{\text{H}}^{\text{SS}}}{3\tau} g_z^x. \quad (5.52)$$

We can solve  $g_0^y$  by an integral since  $g_z^x$  is already known. We distinguish  $g_0^{y+}$  from  $g_0^{y-}$

$$\partial_z g_0^{y+} = -\frac{g_0^{y+}}{l \cos \theta} + \frac{4\pi\alpha_{\text{H}}^{\text{SS}}}{3l \cos \theta} h^+ \exp\left(-\frac{z}{l \cos \theta}\right), \quad (5.53)$$

$$\partial_z g_0^{y-} = -\frac{g_0^{y-}}{l \cos \theta} + \frac{4\pi\alpha_{\text{H}}^{\text{SS}}}{3l \cos \theta} h^- \exp\left(-\frac{z-d_N}{l \cos \theta}\right), \quad (5.54)$$

and write down the solution

$$g_0^{y+} = \left( B^+ + \frac{z}{l |\cos \theta|} \frac{4\pi\alpha_{\text{H}}^{\text{SS}} h^+}{3} \right) \exp\left(-\frac{z}{l |\cos \theta|}\right), \quad (5.55)$$

$$g_0^{y-} = \left( B^- - \frac{z}{l |\cos \theta|} \frac{4\pi\alpha_{\text{H}}^{\text{SS}} h^-}{3} \right) \exp\left(\frac{z-d_N}{l |\cos \theta|}\right), \quad (5.56)$$

where the coefficient  $B^\pm$  is governed by the roughness of the top and bottom interfaces. Assuming that they are the same:

$$g_0^{y+}(z=0) = p_0 g_0^{y-}(z=0), \quad (5.57)$$

$$g_0^{y-}(z=d_N) = p_0 g_0^{y+}(z=d_N), \quad (5.58)$$

$$B^+ = \frac{4\pi\alpha_{\text{H}}^{\text{SS}}}{3} \frac{d_N}{l |\cos \theta|} \frac{h^- + h^+ p_0 \exp\left(-\frac{d_N}{l |\cos \theta|}\right)}{1 - p_0^2 \exp\left(-\frac{2d_N}{l |\cos \theta|}\right)} p_0 \exp\left(-\frac{d_N}{l |\cos \theta|}\right), \quad (5.59)$$

$$B^- = \frac{4\pi\alpha_{\text{H}}^{\text{SS}}}{3} \frac{d_N}{l |\cos \theta|} \frac{h^- + h^+ p_0 \exp\left(-\frac{d_N}{l |\cos \theta|}\right)}{1 - p_0^2 \exp\left(-\frac{2d_N}{l |\cos \theta|}\right)}. \quad (5.60)$$

We arrive at

$$g_0^{y+} = \frac{4\pi\alpha_{\text{H}}^{\text{SS}}}{3} \frac{d_N}{l|\cos\theta|} \left( \frac{h^- + h^+ p_0 \exp\left(-\frac{d_N}{l|\cos\theta|}\right)}{1 - p_0^2 \exp\left(-\frac{2d_N}{l|\cos\theta|}\right)} p_0 \exp\left(-\frac{d_N}{l|\cos\theta|}\right) + \frac{z}{d_N} h^+ \right) \exp\left(-\frac{z}{l|\cos\theta|}\right), \quad (5.61)$$

$$g_0^{y-} = \frac{4\pi\alpha_{\text{H}}^{\text{SS}}}{3} \frac{d_N}{l|\cos\theta|} \left( \frac{h^- + h^+ p_0 \exp\left(-\frac{d_N}{l|\cos\theta|}\right)}{1 - p_0^2 \exp\left(-\frac{2d_N}{l|\cos\theta|}\right)} - \frac{z}{d_N} h^- \right) \exp\left(\frac{z - d_N}{l|\cos\theta|}\right). \quad (5.62)$$

The averaged AHE-like current from skew scattering can now be estimated

$$\bar{J}_c^{\text{SS}} = \frac{e}{d_N} \int_0^{d_N} \left[ \sum_{\hat{k}} \bar{v}_{\hat{k}}^{(0)} g_0^y \kappa_y \right] dz \propto \eta_{so} \cdot \delta p, \quad (5.63)$$

since the  $h^{\pm} \propto \delta p$ . This can be compared with the AHE current  $\delta p$  from side-jump scattering that is proportional to  $\eta_{so} \cdot \delta p \cdot l/d_N$ .

It is not clear yet whether the size-dependences of side-jump and skew scattering are so different because one has to perform the integrals.

## 5.4 CORRECTION DUE TO ROUGHNESS ON THE SMR

We want to know the role of roughness in the conventional SMR theory. For this we redefine the quantization axis along  $\hat{y}$  and follow the same procedure in Sec 5.3, focusing on the  $y$ -component of spin distribution since it is related to the SMR. In this case, we have the particle and spin Boltzmann equations

$$v_k^{(z)} \partial_z g_{\hat{k}0}^a - v_k^{(x)} eE \frac{\partial f^0}{\partial \varepsilon} = -\frac{g_{\hat{k}0}^a}{\tau} - \frac{\alpha_{\text{H}}^{\text{SS}}}{\tau} \sum_{\hat{k}'} (\hat{k} \times \hat{k}')_y g_{\hat{k}'y}^a, \quad (5.64)$$

$$v_k^{(z)} \partial_z \left( g_{\hat{k}y}^a - \frac{\partial f^0}{\partial \varepsilon} \mu_y \right) = -\frac{g_{\hat{k}y}^a}{\tau} - \frac{\mu_y}{\tau_{\text{sf}}} + \frac{\alpha_{\text{H}}^{\text{SS}}}{\tau} \sum_{\hat{k}'} (\hat{k} \times \hat{k}')_y g_{\hat{k}'0}^a. \quad (5.65)$$

The spin-dependent roughness can induce a  $\hat{y}$ -polarized current flows along  $\hat{x}$  when the magnetization  $\hat{m} = \hat{y}$ , similarly to Sec. 5.3. However, we discard from this contribution since it does not generate any further effect, and consider the ansatz  $g_{\hat{k}y}^a = g_y^z \kappa_z$  driven by the SOC. We integrate Eq. (5.65) over all directions and energy,

$$\frac{1}{3} v_k \partial_z g_y^z = -\frac{\mu_y}{\tau_{\text{sf}}}. \quad (5.66)$$

Multiplying Eq. (5.65) by  $\kappa_z$ , and integrating it over all directions and energy,

$$g_y^z = -\tau v_k \partial_z \mu_y + 3\alpha_H^{SS} \int d\Omega_{\hat{k}} \left[ \kappa_z \sum_{\hat{k}'} (\hat{k} \times \hat{k}')_y g_{\hat{k}'0}^a \right]. \quad (5.67)$$

Substituting Eq. (5.67) into Eq. (5.66), we obtain a modulated spin diffusion equation

$$\partial_z^2 \mu_y = \frac{\mu_y}{\lambda^2} - \frac{3\alpha_H^{SS}}{l} \partial_z \int d\Omega_{\hat{k}} \left[ \kappa_z \sum_{\hat{k}'} (\hat{k} \times \hat{k}')_y g_{\hat{k}'0}^a \right], \quad (5.68)$$

where  $\lambda$  is the spin diffusion length.

$\mu_y$  can be solved if we take the approximated solution  $g_{\hat{k}0}^a$  in Eqs. (5.34-5.35). The boundary conditions for  $\mu_y$  involve the spin current at the interface, which depends on both the magnetization in YIG and spin-mixing conductance. With  $\mu_y$  one can get  $g_y^z$  according to Eq. (5.67).

Finally one can derive the ISHE current which corresponds to the SMR. The side-jump contribution comes from  $g_{ky}^a = g_y^z \kappa_z$  and the anomalous velocity

$$\vec{j}_c^{SJ} \equiv e \sum_{\vec{k}} \tilde{\omega}_{\vec{k}} g_y^z \kappa_z = \alpha_H^{SJ} e \sum_{\vec{k}} \left( \hat{y} \times \vec{v}_{\vec{k}}^{(0)} \right) g_y^z \kappa_z = \alpha_H^{SJ} \left( \hat{y} \times \vec{j}_{sy} \right), \quad (5.69)$$

where the spin current flows in  $\hat{y}$  is

$$\vec{j}_{sy} \equiv e \sum_{\vec{k}} \vec{v}_{\vec{k}}^{(0)} g_y^z \kappa_z. \quad (5.70)$$

The ISHE current from skew scattering has to be found by solving  $g_{\hat{k}0}^a$  from Eq. (5.64), taking into account the correction due to  $g_{ky}^a = g_y^z \kappa_z$ .

## 5.5 SUMMARY

We carried out a semiclassical analysis based on the Fuchs-Sondheimer theory to quantify the spin Hall effect in the presence of surface/interface roughness. In a bilayer system made of N and FI, we predict an AHE-like transverse voltage induced by the spin-dependent scattering at the FI|N interface, which is competing with the spin precession of reflected spin as parameterized by the imaginary part of the mixing conductance. Furthermore, we conclude that the spin diffusion equation used to describe the conventional SMR has to be corrected by the surface/interface roughness in the limit of thin-films. Our model can be used to analyze the role of roughness in recent measurements on ultrathin layered systems.

**REFERENCES**

- [1] A. Fert, *Rev. Mod. Phys.* **80**, 1517 (2008).
- [2] S. D. Bader and S. S. P. Parkin, *Ann. Rev. Cond. Matt. Phys.* **1**, 71 (2010).
- [3] J. Sinova and I Žutić, *Nature Mater.* **11**, 368 (2012).
- [4] K. Ando, S. Takahashi, K. Harii, K. Sasage, J. Ieda, S. Maekawa, and E. Saitoh, *Phys. Rev. Lett.* **101**, 036601 (2008).
- [5] I. M. Miron, K. Garello, G. Gaudin, P.-J. Zermatten, M. V. Costache, S. Auffret, S. Bandiera, B. Rodmacq, A. Schuhl, and P. Gambardella, *Nature* **476**, 189 (2011).
- [6] L. Liu, C. F. Pai, Y. Li, H. W. Tseng, D. C. Ralph, and R. A. Buhrman, *Science* **336**, 555 (2012).
- [7] For a review see: T. Jungwirth, J. Wunderlich, and K. Olejník, *Nature Mater.* **11**, 382 (2012).
- [8] V. M. Edelstein, *Solid State Commun.* **73**, 233 (1990).
- [9] X. Jia, K. Liu, K. Xia, and G. E. W. Bauer, *Europhys. Lett.* **96**, 17005 (2011).
- [10] C. Burrowes, B. Heinrich, B. Kardasz, E. A. Montoya, E. Girt, Y. Sun, Y. Y. Song, and M. Wu, *Appl. Phys. Lett.* **100**, 092403 (2012).
- [11] *Recent Advances in Magnetic Insulators – From Spintronics to Microwave Applications*, M. Wu and A. Hoffmann (eds.), *Solid State Physics* **64**, 1-392 (2013).
- [12] L. Liu, R. A. Buhrman, and D. C. Ralph, arXiv:1111.3702 (cond-mat.mes-hall).
- [13] M. Weiler, M. Althammer, M. Schreier, J. Lotze, M. Pernpeintner, S. Meyer, H. Huebl, R. Gross, A Kamra, J. Xiao, Y.-T. Chen, H. Jiao, G. E. W. Bauer, and S. T. B. Goennenwein, *Phys. Rev. Lett.* **111**, 176601 (2013).
- [14] K. Fuchs, *Proc. Cambridge Philos. Soc.* **34**, 100 (1938).
- [15] E. H. Sondheimer, *Adv. Phys.* **1**, 1 (1952).
- [16] R. E. Camley and J. Barnaś, *Phys. Rev. Lett.* **63**, 664 (1989).
- [17] Th. G. S. M. Rijks, R. Coehoorn, M. J. M. de Jong, and W. J. M. de Jonge, *Phys. Rev. B* **51**, 283 (1995).
- [18] Th. G. S. M. Rijks, S. K. J. Lenczowski, R. Coehoorn, and W. J. M. de Jonge, *Phys. Rev. B* **56**, 362 (1997).

- [19] N. Nagaosa, J. Sinova, S. Onoda, A. H. MacDonald, and N. P. Ong, *Rev. Mod. Phys.* **82**, 1539 (2010).
- [20] H. Nakayama, M. Althammer, Y.-T. Chen, K. Uchida, Y. Kajiwara, D. Kikuchi, T. Ohtani, S. Geprägs, M. Opel, S. Takahashi, R. Gross, G. E. W. Bauer, S. T. B. Goennenwein, and E. Saitoh, *Phys. Rev. Lett.* **110**, 206601 (2013).
- [21] M. Althammer, S. Meyer, H. Nakayama, M. Schreier, S. Altmannshofer, M. Weiler, H. Huebl, S. Geprägs, M. Opel, R. Gross, D. Meier, C. Klewe, T. Kuschel, J.-M. Schmalhorst, G. Reiss, L. Shen, A. Gupta, Y.-T. Chen, G. E. W. Bauer, E. Saitoh, and S. T. B. Goennenwein, *Phys. Rev. B* **87**, 224401 (2013).
- [22] Y.-T. Chen, S. Takahashi, H. Nakayama, M. Althammer, S. T. B. Goennenwein, E. Saitoh, G. E. W. Bauer, *Phys. Rev. B* **87**, 144411 (2013).
- [23] S. Y. Huang, X. Fan, D. Qu, Y. P. Chen, W. G. Wang, J. Wu, T. Y. Chen, J. Q. Xiao, and C. L. Chien, *Phys. Rev. Lett.* **109**, 107204 (2012).
- [24] N. Vlietstra, J. Shan, V. Castel, J. Ben Youssef, G. E. W. Bauer, and B. J. van Wees, *Appl. Phys. Lett.* **103**, 032401 (2013).
- [25] P. M. Haney, H.-W. Lee, K.-J. Lee, A. Manchon, and M. D. Stiles, *Phys. Rev. B* **87**, 174411 (2013).
- [26] S. Takahashi, H. Imamura, and S. Maekawa, in *Concepts in Spin Electronics*, edited by S. Maekawa (Oxford Univ. Press, Oxford, 2006), pp.343-370.
- [27] S. K. Lyo and T. Holstein, *Phys. Rev. Lett.* **7**, 423 (1972).
- [28] H.-A. Engel, B. I. Halperin, and E. I. Rashba, *Phys. Rev. Lett.* **95**, 166605 (2005).

# SUMMARY

In this thesis, we report several effects in spintronics and spin caloritronics related to relativistic spin-orbit coupling.

In Chapter 2, we discuss the relativistic spin caloritronic Hall effects in terms of a semiclassical theory for anomalous thermoelectric effects in ferromagnetic metals due to spin-orbit scattering at impurities, including the anomalous Nernst and Ettingshausen effect, the planar thermal Hall effects, and thermoelectric anisotropic magnetoresistance. The linear response relations between the currents and driving forces are derived for out-of-plane and in-plane magnetizations, respectively. In the out-of-plane configuration, there are anomalous thermoelectric Hall effects linear to the spin-orbit constant, while the thermoelectric anisotropic magnetoresistance and the planar Hall effect in the in-plane configuration are of second order in the spin-orbit coupling. The extrinsic theory systemizes the competing effects/mechanisms from a microscopic point of view and identifies the parameters needed to describe experiments.

We developed a diffusion theory in Chapter 3 for the spin Hall magnetoresistance (SMR) in multilayers made from an insulating magnet F such as yttrium iron garnet (YIG), and a normal metal N with spin-orbit interactions, such as platinum (Pt). In an N|F bilayer system, the SMR requires spin-flip in N and spin-transfer at the N|F interface. Our results explain the SMR both qualitatively and quantitatively with transport parameters that are consistent with other experiments. The degrees of spin accumulation in N that can be controlled by the magnetization direction is found to be very significant. In the presence of an imaginary part of the spin-mixing conductance  $G_i$  we predicted an AHE-like signal (SHAHE), which has been observed experimentally and can be explained with values of  $G_i$  that agree with first principles calculations. We furthermore analyzed F|N|F spin valves for parallel and perpendicular magnetization configurations. The SMR torques under applied currents in N are expected to lead to magnetization dynamics of N|F and F|N|F structures.

In Chapter 4, we generalized the SMR theory in Chapter 3 to a thin-film made of a metallic ferromagnet and take into account the out-of-plane spin currents generated by the spin Hall effect, which were disregarded in Chapter 2. We predict a new contribution to the anisotropic magnetoresistance by the simultaneous action of the anomalous Hall effect and its inverse. By diffusion theory, we compare this

contribution with the conventional anisotropic magnetoresistance, demonstrating that they can be distinguished experimentally by studying its dependence on the film thickness. The extra contribution to the magnetoresistance has a magnetization dependence different from that of the conventional AMR. While the conventional AMR is usually positive, the new contribution is always negative.

In order to analyze the effect of interface and boundary roughness that was disregarded in Chapter 3, we reports in Chapter 5 a Boltzmann study to quantify how the surface/interface scattering affects the spin Hall physics. In a bilayer system made of N and FI, we observe an AHE-like transverse voltage induced by the spin-dependent scattering at the FI|N interface, which is competing with the imaginary SMR predicted in Chapter 3. We further show that the spin diffusion equation on which the SMR in Chapter 3 is based, has to be corrected by the surface/interface roughness in the limit of thin-films. Our model provides an approach to analyze the role of roughness in recent measurements on layered systems.

Even though the theories developed in Chapters 3–5 are not directly related to spin caloritronics, they can be easily generalized for their thermoelectric analogues by the formulation spelt out in Chapter 2, and can be useful for prospective research in spintronics and spin caloritronics.

# SAMENVATTING

In dit proefschrift rapporteren we diverse verschijnselen in spintronica en caloritronica die gerelateerd zijn aan spin-baan koppeling.

In Hoofdstuk 2 bestuderen we relativistische spin caloritronische Hall effecten door het ontwikkelen van een semi-klassieke theorie voor buitengewone thermo-elektrische effecten in ferromagnetische materialen door spin-baan verstrooiing bij imperfecties, waaronder het buitengewone Nernst en Ettinghausen effect, de thermische Hall effecten in een vlak en thermo-elektrische anisotrope magneto-resistiviteit. The lineaire respons relaties tussen de stromen en drijvende krachten zijn afgeleid voor de gevallen van een uit-het-vlak en een in-het-vlak magnetisatie, respectievelijk. In de uit-het-vlak configuratie zijn er buitengewone thermo-elektrische Hall effecten die lineair zijn met de spin-baan constante, terwijl er voor de in-het-vlak configuratie thermo-elektrische anisotrope magneto-resistiviteit en het vlakke Hall effect in the tweede orde spin-baan koppeling optreden. De extrinsieke theorie systematiseert de competerende effecten/mechanismen vanuit een microscopisch gezichtspunt en identificeert de parameters die nodig zijn om experimenten te beschrijven.

We ontwikkelden een diffusie theorie in Hoofdstuk 3 voor de spin Hall magneto-resistiviteit (SMR) in multilagen gemaakt van een isolerende ferromagneet F, zoals yttrium ijzer granaat (YIG), en een normaal metaal N met spin-baan interacties, zoals platinum (Pt). In een N|F dubbele-laag system, vereist SMR zowel spin-flip in N als spin-overdracht op het N|F contactvlak. Onze resultaten verklaren de SMR zowel kwalitatief als kwantitatief met transport parameters die overeenstemmen met andere experimenten. Er is gevonden dat de gradaties van spin accumulatie in N die kunnen worden gestuurd door de magnetisatie richting erg significant zijn. In de aanwezigheid van een imaginair deel van de spin-menging geleiding  $G_i$  voorspellen we een AHE-gelijkend signaal (SHAHE) dat experimenteel kan worden geobserveerd en verklaard kan worden met waarden van  $G_i$  die overeenstemmen met berekeningen volgens eerste beginselen. We analyseerden ook F|N|F spin ventiel voor parallel en loodrecht staande magnetisatie configuraties. De SMR koppels onder toegepaste stromen in N worden verwacht te leiden tot magnetisatie dynamica van of N|F en F|N|F structuren.

In Hoofdstuk 4 generaliseerden we de SMR theorie uit Hoofdstuk 3 voor een dunne film bestaand uit een metallische ferromagneet en nemen uit-het-vlak stro-

men gegenereerd uit het spin Hall effect in beschouwing. Deze waren in Hoofdstuk 2 buiten beschouwing gelaten. We voorspellen een nieuwe bijdrage van anisotrope magnetoresistiviteit, demonstrerend dat deze experimenteel onderscheiden kunnen worden door het besturen van hun afhankelijkheid van de dikte van de film. De extra bijdrage aan de magnetoresistiviteit heeft een magnetisatie afhankelijkheid die verschilt met die van de conventionele AMR. Terwijl de conventionele AMR gebruikelijker wijs positief is, is de nieuwe bijdrage altijd negatief.

Teneinde het ruwheidseffect te analyseren dat buiten beschouwing was gelaten in Hoofdstuk 3, voeren we in Hoofdstuk 5 een Boltzmann onderzoek uit om te kwantificeren hoe de oppervlak/grensvlak verstrooiing van invloed is op de spin Hall fysica. In een dubbele-laag systeem bestaande uit N en FI observeren we een AHE-achtige transversaal voltage geïnduceerd door de spin-afhankelijke verstrooiing aan het FI/N grensvlak dat in competitie is met de imaginaire SMR dat is voorspeld in Hoofdstuk 3. We laten verder zien dat de spin-diffusie vergelijking die de SMR in Hoofdstuk 3 verklaarde, moet worden bijgesteld met de oppervlak/grensvlak ruwheid in de limiet van dunne films. Ons model biedt een aanpak om de rol van ruwheid in recente metingen aan gelaagde systemen te verklaren.

Al zijn de theorieën ontwikkeld in de Hoofdstukken 3–5 niet direct gerelateerd aan spin caloritronica, kunnen ze eenvoudig gegeneraliseerd worden voor hun thermo-elektrische gelijken door de formulering beschreven in Hoofdstuk 2 en kunnen ze nuttig zijn voor toekomstig onderzoek in spintronica en spin caloritronica.

# CURRICULUM VITÆ

**Yan-Ting CHEN**

19-11-1982      Born in Kaohsiung, Taiwan.

## EDUCATION

2001–2005      B. Sc. in Electrophysics  
National Chiao Tung University, Taiwan

2005–2007      M. Sc. in Electrophysics  
National Chiao Tung University, Taiwan

2010–2014      Ph.D. in Theoretical Physics  
Delft University of Technology, the Netherlands  
Promotor: Prof. dr. ir. G. E. W. Bauer



# LIST OF PUBLICATIONS

1. Y. T. Chen, C. C. Chao, S. Y. Huang, C. S. Tang, S. J. Cheng, *Singlet-triplet transitions in highly correlated nanowire quantum dots*, Physica E **42**, 837 (2010).
2. Y. T. Chen, S. J. Cheng, C. S. Tang, *Engineered spin-state transitions of two interacting electrons in semiconductor nanowire quantum dots*, Phys. Rev. B **81**, 245311 (2010).
3. H. Y. Ramirez, C. H. Lin, C. C. Chao, Y. Hsu, W. T. You, S. Y. Huang, Y. T. Chen, H. C. Tseng, W. H. Chang, S. D. Lin, and S. J. Cheng, *Optical fine structures of highly quantized InGaAs/GaAs self-assembled quantum dots*, Phys. Rev. B **81**, 245324 (2010).
4. Y.-T. Chen, S. Takahashi, H. Nakayama, M. Althammer, S. B. T. Goennenwein, E. Saitoh, and G. E. W. Bauer, *Theory of spin Hall magnetoresistance*, Phys. Rev. B **87**, 144411 (2013).
5. H. Nakayama, M. Althammer, Y.-T. Chen, K. Uchida, Y. Kajiwara, D. Kikuchi, T. Ohtani, S. Geprags, M. Opel, S. Takahashi, R. Gross, G. E. W. Bauer, S. T. B. Goennenwein, and E. Saitoh, *Spin Hall Magnetoresistance induced by a Nonequilibrium Proximity Effect*, Phys. Rev. Lett. **110**, 206601 (2013).
6. M. Althammer, S. Meyer, H. Nakayama, M. Schreier, S. Altmannshofer, M. Weiler, H. Huebl, S. Geprags, M. Opel, R. Gross, D. Meier, C. Klewe, T. Kuschel, J.-M. Schmalhorst, G. Reiss, L. Shen, A. Gupta, Y.-T. Chen, G. E. W. Bauer, E. Saitoh, and S. T. B. Goennenwein, *Quantitative study of the spin Hall magnetoresistance in ferromagnetic insulator/normal metal hybrids*, Phys. Rev. B **87**, 224401 (2013).
7. M. Weiler, M. Althammer, M. Schreier, J. Lotze, M. Pernpeintner, S. Meyer, H. Huebl, R. Gross, A. Kamra, J. Xiao, Y.-T. Chen, H. Jiao, G. E. W. Bauer, and S. T. B. Goennenwein, *Experimental test of the spin mixing interface conductivity concept*, Phys. Rev. Lett. **111**, 176601 (2013).

8. Y. Zhou, H. Jiao, Y.-T. Chen, G. E. W. Bauer, and J. Xiao, *Current-induced spin-wave excitation in Pt/YIG bilayer*, Phys. Rev. B **88**, 184403 (2013).
9. Y.-T. Chen, G. E. W. Bauer, and S. Takahashi, *Anomalous thermoelectric effects in ferromagnetic metals*, in preparation.
10. Y.-T. Chen, S. Takahashi, and G. E. W. Bauer, *Size effect in the anisotropic magnetoresistance of ferromagnetic thin-films*, in preparation.
11. Y.-T. Chen, E. Saitoh, S. Takahashi, and G. E. W. Bauer, *Fuchs-Sondheimer theory of the spin Hall effect*, in preparation.